TÉCNICO LISBOA

Structure-scale impact of widespread managed aquifer recharge in Gujarat, India

Gloria Mozzi

Thesis to obtain the Master of Science Degree in

Environmental Engineering

Supervisors:

Prof. Doutora Christina Dornack
Doutor Catalin Stefan (TU Dresden)
Prof. Doutor Luís Filipe Tavares Ribeiro

Examination Committee:

Chairperson: Prof. Doutor Ramiro Joaquim de Jesus Neves
Supervisor: Prof. Doutor Luís Filipe Tavares Ribeiro
Members of the Committee: Dr. Tibor Stigter

September 2019

Structure-scale impact of widespread managed aquifer recharge implementation in Gujarat, India

Master of Science Thesis

by

Gloria Mozzi

Supervisor

Prof. Christina Dornack

Mentors

Dr Catalin Stefan (TU Dresden)
Dr Karen G Villholth (IWMI South Africa)
Dr Paul Pavelic (IWMI Lao PDR)
Mohammad Alam (IWMI India)
Dr. Luís Filipe Tavares Ribeiro

Examination committee

Chairperson: Prof. Doutor Ramiro Joaquim de Jesus Neves
Supervisor: Prof. Doutor Luís Filipe Tavares Ribeiro
Members of the Committee: Dr. Tibor Stigter

This thesis is submitted in partial fulfilment of the requirements for the academic degree of
Master of Science in Water Science and Engineering
IHE Delft Institute for Water Education, Delft, the Netherlands
Master of Science in Environmental Engineering
Instituto Superior Técnico, Universidade de Lisboa, Portugal
Master of Science in Hydro Science and Engineering
Technische Universität Dresden, Germany

MSc research host institution
TU Dresden

September 2019

Acknowledgements

First, I would like to express my sincere gratitude to my thesis mentors Dr Paul Pavelic and Mohammad Faiz Alam from the International Water Management Institute (IWMI), who provided me guidance and precious feedbacks throughout my work. A special thanks goes to Dr Karen Villholth from IWMI, who gave a substantial technical contribution to this work, and is responsible for the arrangement of the partnership with IWMI.

I want to thank my thesis supervisor Dr Catalin Stefan from INOWAS Research Group of TU Dresden, who supported me through the process of researching and writing this thesis.

I truthfully thank Praharsh Patel from IWMI for his dedicated support in translation with local farmers during the field visit in Saurashtra. I would also like to thank Punjan Patel, Dr Shilp Verma and all the colleagues from IWMI Anand office, who kindly supported me during my stay in India.

I sincerely thank Dr Yogita Dashora for providing me with the data from her work "*A simple method using farmers' measurements applied to estimate check dam recharge in Rajasthan, India*" (Dashora et al., 2017). Without this data, the validation of this work would not have been possible.

The last mention goes to my beloved Dresdetians: Karen, Hafsah, Fatima, Jose and Muqeet. Their friendship has been a real support during hard times. I am profoundly grateful for having such amazing colleagues.

I would like to dedicate this work to all the people I encountered during my journey in India. These two months have been not only a moment of work and academic learning, but also of great discovery and cultural exchange. I left a piece of my heart in this amazing country, and I hope I will soon have the chance to go back.

Abstract

The state of Gujarat is located in an arid to semi-arid region in western India. Drinking water and irrigation demands are highly dependent on groundwater resources. In the second half of the last century, the state has witnessed aquifers depletion due to a rapid development of abstraction wells and expansion of irrigated areas. However, different studies reported a significant increase in the water levels occurring from the last decade. There is still a lack of scientific evidence regarding the causes of this groundwater recovery, and different authors have proposed different possible drivers. This work is part of a project which aims to assess the impact of managed aquifer recharge (MAR) on groundwater storage through a multi-scale analysis. This thesis focuses on the development of a tool to study MAR performances at the structure scale for check dams. Based on a field visit and literature review, a conceptual model is developed from analytical equations. This model reveals that check dams are able to store and infiltrate a significant amount of water captured during runoff events. The efficiency of these structures is dependent on their geometry, the hydrogeological setting, maintenance practices, annual precipitation and its distribution during the monsoon season. It is also found that induced recharge by groundwater abstraction from wells located nearby check dams, can enhance their recharge potential up to 20%. In order to validate the model, a simulation is run for a check dam analysed by Dashora et al. (2017) in the years 2014 and 2015. For one of the simulated hydrogeological settings, the fitness with the observations reveals a coefficient of determination R^2 of 0.939 in 2014 and of 0.867 in 2015. It is therefore proved that the tool developed in this work can be used to analyse and predict the hydrological behaviour of check dams in the presence of site-specific data. Also, this tool has the potential to be implemented in a catchment-scale analysis to assess the cumulative effect of the widespread implementation of MAR.

Keywords: MAR, groundwater, rainwater harvesting, multi-scale impact, Gujarat, India

Resumo

O estado de Gujarat está localizado em uma região árida a semi-árida no oeste da Índia. As necessidades de água potável e irrigação são altamente dependentes dos recursos hídricos subterrâneos. Na segunda metade do século passado, o estado testemunhou o esgotamento dos aquíferos devido ao rápido desenvolvimento de poços de extração e expansão de áreas irrigadas. No entanto, diferentes estudos relataram um aumento significativo nos níveis de água ocorridos na última década. Ainda faltam evidências científicas sobre as causas dessa recuperação das águas subterrâneas, e diferentes autores propuseram diferentes fatores possíveis. Este trabalho faz parte de um projeto que tem como objetivo avaliar o impacto da recarga gerenciada de aquíferos (MAR) no armazenamento de águas subterrâneas por meio de uma análise em várias escalas. Esta tese se concentra no desenvolvimento de uma ferramenta para estudar o desempenho do MAR na escala da estrutura de barragens de cheques. Com base em uma visita de campo e revisão da literatura, um modelo conceitual é desenvolvido a partir de equações analíticas. Este modelo revela que as barragens de verificação são capazes de armazenar e se infiltrar em uma quantidade significativa de água capturada durante os eventos de escoamento. A eficiência dessas estruturas depende de sua geometria, ambiente hidrogeológico, práticas de manutenção, precipitação anual e sua distribuição durante a estação das monções. Verificou-se também que a recarga induzida por captação de água subterrânea de poços localizados nas barragens próximas pode aumentar seu potencial de recarga em até 20%. Para validar o modelo, é executada uma simulação para um dique analisado por Dashora et al. (2017) nos anos de 2014 e 2015. Para um dos cenários hidrogeológicos simulados, a adequação às observações revela um coeficiente de determinação R2 de 0,939 em 2014 e de 0,867 em 2015. Portanto, está provado que a ferramenta desenvolvida neste trabalho pode ser usado para analisar e prever o comportamento hidrológico de pequenas barragens na presença de dados específicos do local. Além disso, essa ferramenta tem o potencial de ser implementada em uma análise em escala de captação para avaliar o efeito cumulativo da ampla implementação da MAR.

Table of contents

List of Figures

List of Tables

Abbreviations

AMC	Antecedent Moisture Condition
AMSL	Above Mean Sea Level
BGL	Below Ground Level
CGWB	Central Ground Water Board
DEM	Digital Elevation Model
ERT	Electrical Resistivity Tomography
GSWMA	Gujarat State Watershed Management Agency
IGRAC	International Groundwater Resource Assessment Centre
IMD	India Meteorological Department
IWMI	International Water Management Institute
LULC	Land Use and Land Cover
MAR	Managed Aquifer Recharge
ppm	Part per million
SCS	Soil Conservation Service, US Department of Agriculture
SWDC	State Water Data Centre
VES	Vertical Electrical Sounding

Symbols

α	stream gradient [°]
β	angle of the tail the river[°]
γ	river bank slope [°]
Δ	slope of vapor pressure curve [kPa/°C]
λ	latent heat of vaporization [MJ/kg]
φ	psychrometric constant [kPa/°C]
A	abstraction rate from dug wells [m^3/day]
a	geometric parameter for Bouwer condition A [-]
A_{catch}	catchment area of the check dam [m^2]
A_{cs}	cross section area of the river [m^2]
A_{surf}	surface area of the water in the structure [m^2]
A_{wet}	wetted area [m^2]
CN	runoff curve number [-]
D_w	depth to water table [m]
D_{hr}	depth to hard-rock [m]
D_{well}	drawdown at the well [m]
D_a	drawdown at the structure [m]
E	evaporation volume [m^3]
e	evaporation rate [m/day]
e_s	saturated vapor pressure [kPa]
F_A	geometric check dam parameter for Bouwer condition A' [-]
G	generic losses [m^3]
H_S	height of the check dam [m]
H_w	depth of the water at the check dam [m]
J	Julian day of the year
K	saturated hydraulic conductivity [m/day]
K_p	unsaturated hydraulic conductivity [m/day]
K_{HR}	saturated hydraulic conductivity of the hard rock layer
K_{WZ}	saturated hydraulic conductivity of the weathered zone

k_A	geometric coefficient between wet and surface area
I	infiltration volume [m^3]
i	infiltration rate [m/day]
I_a	initial water abstractions [m]
L	length of the water tail from the structure [m]
L_s	distance of water table characterization from the check dam [m]
Out	outflow [m^3]
P	precipitation volume [m^3]
p	precipitation depth [m/day]
P_{sw}	soil-water pressure [cm]
P_{cr}	Bouwer critic pressure [cm]
p_s	atmospheric surface pressure [kPa]
R	runoff volume [m^3]
r	runoff depth [m/day]
R_a	impendence of the clogging layer [days]
r_s	distance of the structure from the well [m]
r_w	well radius [m]
RH	relative humidity [%]
S	maximum water retention [m]
T	transmissivity of the aquifer [m^2/day]
T_{mean}	mean temperature [°C]
U	wind speed [m/s]
V	water volume in the structure [m^3]
ΔV	daily change in water storage in the check dam [m^3]
V_{MAX}	storage capacity [m^3]
w.p.	wetted perimeter [m]
W_s	width of the check dam [m]
W_b	river bottom width [m]

Chapter 1: Introduction

Over the last half of the century or more, the intense use of groundwater worldwide has resulted in aquifer depletion and the rise of other environmental issues, such as stream depletion, saline intrusion and land subsidence (Konikow and Kendy, 2005). Governments, organisations, scientists and communities are currently focusing on finding alternative solutions to preserve and sustainably manage groundwater resources. Some of these solutions fall into the category of so-called Managed Aquifer Recharge (MAR) practices. These practices consist of water supply based measures aimed to maintain, enhance and secure groundwater bodies (Dillon et al., 2018).

In the last 60 years, there has been a rapid growth of MAR measures of different types and scales worldwide (Dillon et al., 2018). In India, where 75 to 90 % of rainfall is concentrated in the monsoonal months, these techniques were used since ancient times, and some tanks and ponds are believed to be several thousand years old (Mooley and Parthasarathy, 1984; Sakthivadivel, 2007). Due to the rapid expansion of irrigated agriculture and overall economic development, India is currently facing challenges in preserving its groundwater bodies, in terms of quantity and quality (Mukherjee, 2018).

In 2013, the Central Ground Water Board (CGWB) presented a revised Master Plan for Artificial Recharge to Groundwater (another term often used to refer to MAR). As stated in this document, the plan was to construct 11 million structures around the country over a period of 10 years. The national investment amounted as more than US$ 10 Billion, of which US$ 210 Million were designated to the state of Gujarat (CGWB, 2013).

1.1 Background

Situated in the western-most part of India, the state of Gujarat accounts for more than 60 million inhabitants (see Figure 1). Most of the population lives in rural areas, and more than 45% of the inhabitants depend on agriculture for their livelihood. The state is highly diverse in terms of climate: in the extreme south annual precipitation reaches more than 2 000 mm and climate can be classified as humid; in the northern areas climate is arid to semi-arid and, in Kutch precipitation is as low as 300mm/year (CGWB, 2013). Most of the precipitation concentrates in monsoon months (June to September). Annual precipitation is highly variable also among years, with a peak in the coefficient of variation of 80% in the northern Kutch (Shah, 2014). As a result, Gujarat represents one of the most water-stressed states of India (except the humid southern districts).

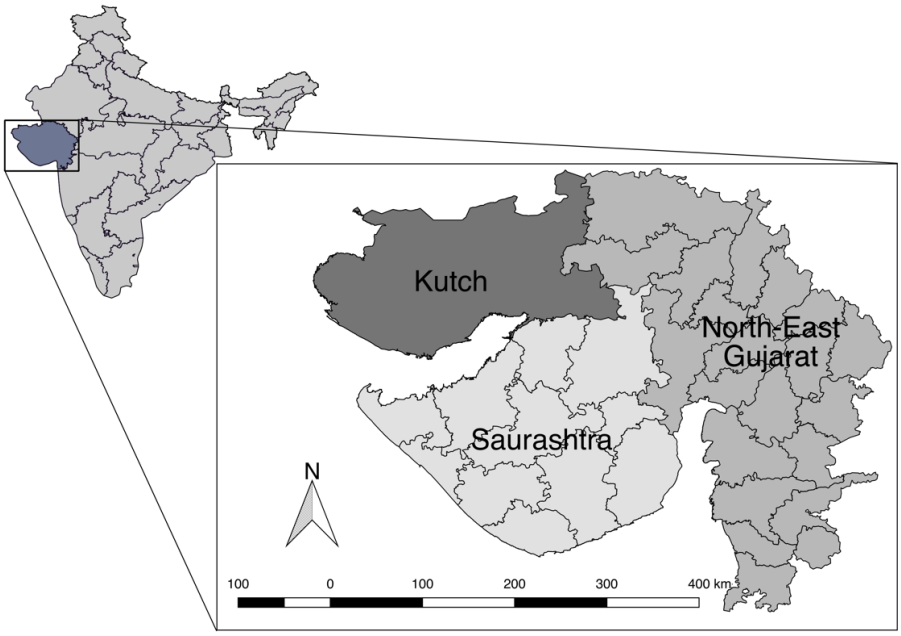

Figure 1: Districts and main regions in Gujarat, India

Throughout history, the region has experienced several droughts. It is reported that in 1900, one-third of the population and most of the livestock died because of a severe famine caused by Chhapaniyo drought (Yagnik and Sheth, 2005). During these times, one of the essential relief measures to cope with starvation and mortality was digging new wells. This is because, at that time groundwater scarcity was not a problem even in times of drought (Bhatia, 1992). At the beginning of the 20th century, diesel pumps for water abstraction started to be imported, and during the second half of the century, the use of more efficient electric submersible pumps has considerably increased (Shah et al. 2008). As a result, water scarcity increasingly emerged as one of the most severe issues of droughts in Gujarat.

From the 1960s onward, water needed to be supplied by tankers and bullock carts in drought times. Wells started to be deepened, borewells were sunk, and village tanks were deepened or repaired. During a drought between 1985-1989, water in Rajkot was supplied by train from sources situated more than 250km away. During these times, state government invested considerable amounts of resources in drinking water supply schemes (Bhatia, 1992).

Even though droughts did no longer cause famines and starvation deaths following the emergence of the Green Revolution in the 1960s, their manifestation started to affect groundwater resources seriously. As a result, great concern from both the government and the scientific community was raised (Gupta, 2002; Kumar et al., 2004; Moench, 1992).

In response to this crisis, the government's actions focused on two main aspects: controlling groundwater use and increasing groundwater recharge. The first target was addressed with new energy policies implemented in 2006 (Jyotigram Yonja scheme), which separated the electric power between domestic and agricultural supply. This scheme provided three-phase power supply 24/7 to domestic users and imposed strict rationing on power supply for agricultural purposes. After the implementation of this initiative, access to high voltage distribution for agricultural purposes is limited to only eight hours a day (Grönwall, 2014).

The second aspect was tackled with the promotion of decentralised managed aquifer recharge (MAR). In the year 2000, the state government supported a mass movement through a participatory program called *Sardar Patel Sahakari Jal Sanchaya Yojana* (Jain 2012). This movement aimed at promoting the implementation of small MAR structures throughout the state and was particularly successful in the regions of Kutch and Saurashtra, the most vulnerable regions of the state in terms of water scarcity (Shah et al. 2009). As a result, an inventory carried out in 2011 Gujarat noted 1,800 percolation tanks, 16 975 check dams and about 25 000 roof-top rainwater harvesting for groundwater and irrigation (plus 475 000 small roof-top containers for domestic use) (CGWB, 2011).

In the last few years, studies have reported some regional aquifer replenishment, with an increasing trend in the groundwater levels starting from years 2002-2004. Asoka et al. (2017) estimated groundwater anomalies between 2013 and 2002 from GRACE data (Gravity Recovery and Climate Experiment). Results showed that groundwater storage has declined in northern India at the rate of 2 cm/year and increased by 1 to 2 cm/year in southern India between 2002 and 2013. Results are shown in Figure 2, where the increasing groundwater storage over most of Gujarat can be seen.

Another study from 2017 analysed the data from CGWB of 19 278 observation wells in the state. This study showed that groundwater storage has been decreasing at the rate of 2.96 ± 0.19 cm/year (5.81 ± 0.38 km^3/year in 1996–2001), and reversed to replenish at the rate of 1.04 ± 0.10 cm/year (2.04 ± 0.20 km^3/year in 2002–2014) (Bhanja et al., 2017).

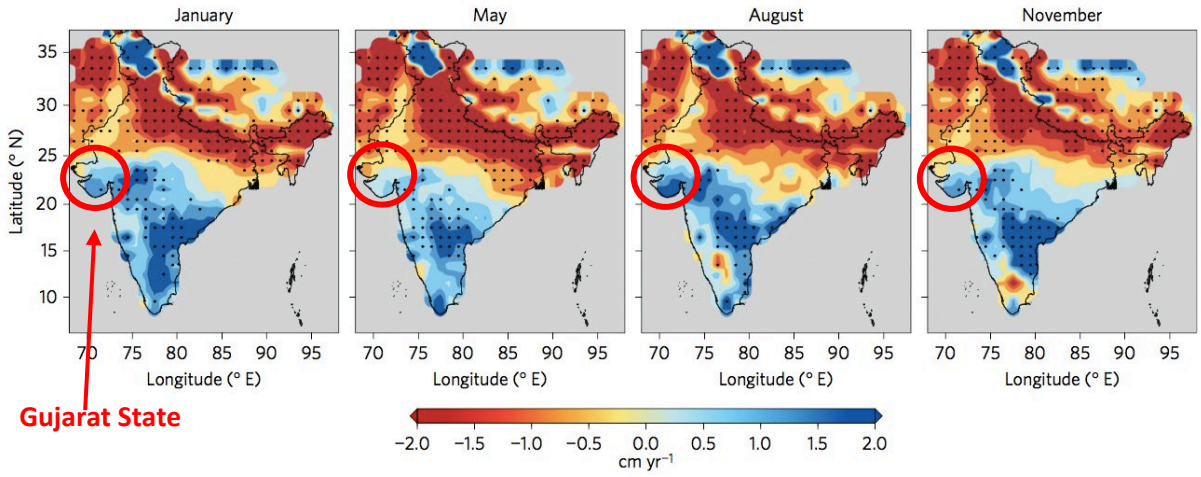

Figure 2: Monthly trends in groundwater anomaly between 2002 and 2013

Data from GRACE data (Asoka et al., 2017)

1.2 Managed Aquifer Recharge

According to Stefan et al. (2018), MAR can have multiple purposes: increasing groundwater storage, improve water quality, restore groundwater levels, prevent saltwater intrusion, manage water distribution systems and enhance ecological benefits. The International Groundwater Resource Centre (IGRAC) identifies five main types of MAR: spreading methods, induced bank infiltration, in-channel modification, rainwater and runoff harvesting and lastly, well, shaft and borehole recharge (IGRAC, 2007).

The vocabulary used for MAR is not yet standardised across countries and regions, and thus, the same type of systems might be referred to in the literature by different names. Figure 3 shows the type of structure analysed in the current study. Throughout this work, the term "*check dam*" will be used to describe this particular configuration, as a common vocabulary for this kind of structures in India.

This system is an in-channel modification type of MAR, and it consists of a physical barrier constructed from earth or masonry material within the channel of ephemeral streams or rivers. This barrier retains water coming from surface runoff and allows more time for infiltration. These structures are particularly suitable in arid or semi-arid regions, where water flows in rivers only for few days per year. In these areas, a large amount of runoff is produced during intense rainfall events, resulting in flooding. This type of MAR structure helps to harvest surface runoff and increase the contact time between water and river bed, hence improving infiltration (Renganayaki and Elango, 2013).

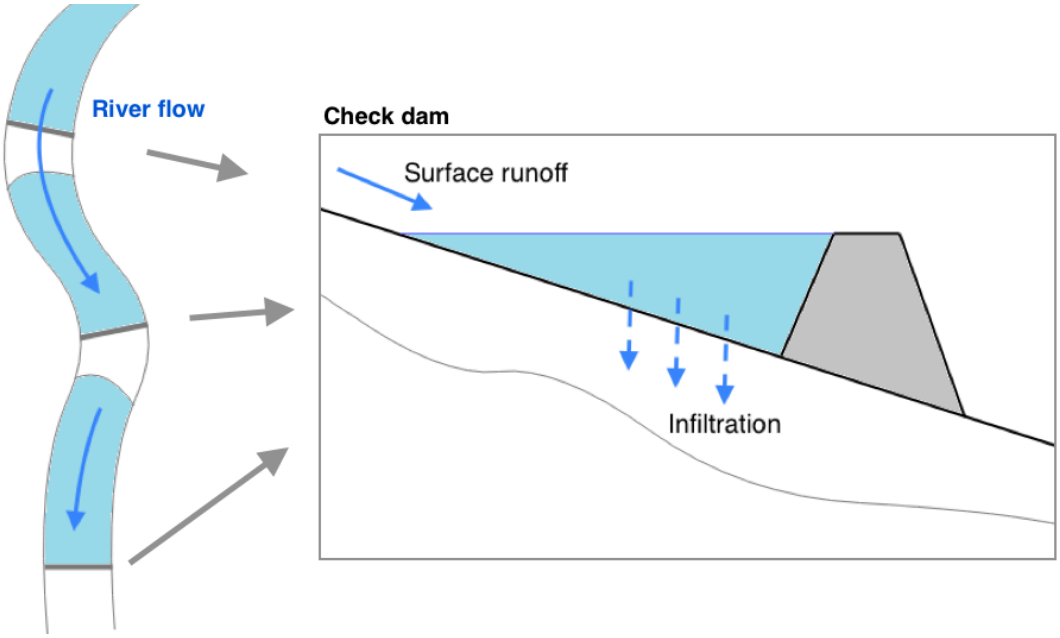

Figure 3: In-channel modification MAR system

1.3 Problem statement and importance

Sustainable management of water resources is a vital and necessary practice, especially in arid and semi-arid regions. However, it is achievable only with a sound scientific understanding of the hydrological impacts of various interventions, including MAR structures implemented in these regions. Despite the broad implementation of MAR structures throughout India, there is limited research combining local and catchment scale hydrological impacts (Glendenning et al. 2012).

Also, there is no unanimity among the scientific community about the causes behind Gujarat's increase in groundwater storage. The main drivers which have been suggested by different authors are: the change in rainfall patterns, the change in energy policies by the government, the import of surface water from the Sardar Sarovar dam and finally the widespread implementation of MAR

systems (Kumar and Perry, 2018, Bhanja et al. 2017, Gupta 2012, Jain 2012). All these hypotheses are further illustrated in Chapter 2.

Because of the lack of clarity and the scale and intensity of MAR implementation, this region offers a unique opportunity to assess the large-scale impact of this technique as well as the effects on local communities.

1.4 Research Objectives

This Master Thesis is part of a project whose purpose is to assess the efficacy of MAR through multi-scalar analysis. The idea is to link the performance of single structures with the aggregate impact of multiple structures on the whole catchment hydrology. The Master Thesis work focuses on analysis at the structure scale for check dams.

The objective is to provide a tool that can be used to analyse the check dam performances in terms of *i)* infiltration, *ii)* evaporation and *iii)* induced recharge by abstraction wells. This tool has two main roles: to be used to quantify recharge capacity of specific structures, and to be integrated into a catchment-scale model to analyse the overall impact of the widespread implementation of check dams.

The study area chosen for this analysis is the Bhawar basin, located on the southwestern part of the Saurashtra peninsula in Gujarat. This area is characterised by hard-rock aquifers (CGWB, 2011) and has witnessed a strong implementation of check dams (Shah, 2014).

1.5 Project description and thesis structure

The project is done in partnership between TU Dresden and the International Water Management Institute (IWMI). The work was divided between Mohammad Alam, IWMI Researcher based in New Delhi and MSc student Gloria Mozzi, Erasmus Mundus fellow of the joint programme in Groundwater and Global Change. As mentioned in the previous section, the thesis focuses on developing a tool to analyse the structure's performance. The integration of this tool in a catchment-scale analysis will be performed by IWMI within the project agenda.

The thesis involved a two-months visit to India (April 2019 – June 2019) followed by modelling and writing up (July to August 2019). The work started with retrieving and analysing data regarding climate, land use, agriculture and hydrogeology. Preliminary GIS mapping of the area was done together with the identification of some of the check dams and potential sites to perform the fieldwork. These sites were then visited, and the work involved both direct measurements and surveys with local farmers. Lastly, a conceptual model for the structure's hydrologic processes was developed based on literature and field results.

Because of the lack of time and equipment, the data collected were not sufficient to calibrate the model on the specific check dams. This model it is based on analytical equations and generic processes, which means this model has the flexibility to be used worldwide for the estimation of

recharge from check dams. The tool has the potential to be calibrated and validated if substantial field measurements are undertaken. Validation was performed with the simulation of a check dam studied by Dashora et al. (2017) in Rajasthan for 2014 and 2015.

This report is divided into six main sections, appendices and references. Chapter 1 introduces the study and illustrates the research objectives. Chapter 2 reviews and summarises the past relevant literature. Chapter 3 describes the study area. Chapter 4 illustrates the methods used to approach the research questions. Chapter 5 presents and analyses the results. Chapter 6 concludes the work with overall insights on the project, as well as suggestions and recommendations for further work.

The five appendices of this work contain additional material describing the study area, the questionnaire used in the field, the pictures taken during the field visit, the code used to develop the tool and additional results of the model.

Chapter 2: Literature review

2.1 Increase in Groundwater levels in Gujarat

Among the scientific community, there is still no unanimity regarding the causes of this recent groundwater replenishment. Bhanja et al. (2017) suggested that the management policies from the government for sustainable water utilisation (so-called Jyotigram Yonja, introduced in 2006) were the main drivers behind this phenomenon. They affirmed that the reduction of agricultural power supply and the separation of agricultural feeder lines from rural domestic supply lines reduced groundwater withdrawals.

However, Kumar and Perry (2018) argued against the actual efficacy of this change of water management policy. They identified instead as primary drivers of the replenishment the increase in annual rainfall and the diversion of water from the Sardar Sarovar dam, located on the Narmada river in the eastern part of Gujarat. To corroborate their hypothesis, they used a study conducted by Dave et al. (2017), who showed a significant (90% confidence level) increasing trend in monsoon rainfall. This study reported an increase of 44.3 mm/decade of annual rainfall in coastal Saurashtra during 1970-2014. Figure 4 in the next page shows the annual rainfall in Rajkot district in Saurashtra from 1971 to 2017. It can be seen that from 2002 annual precipitation has increased: while for the years 1971-2002 the average annual precipitation is 550mm (red line Figure 4), for the rears 2003-2017 the average is 810mm (blue line Figure 4).

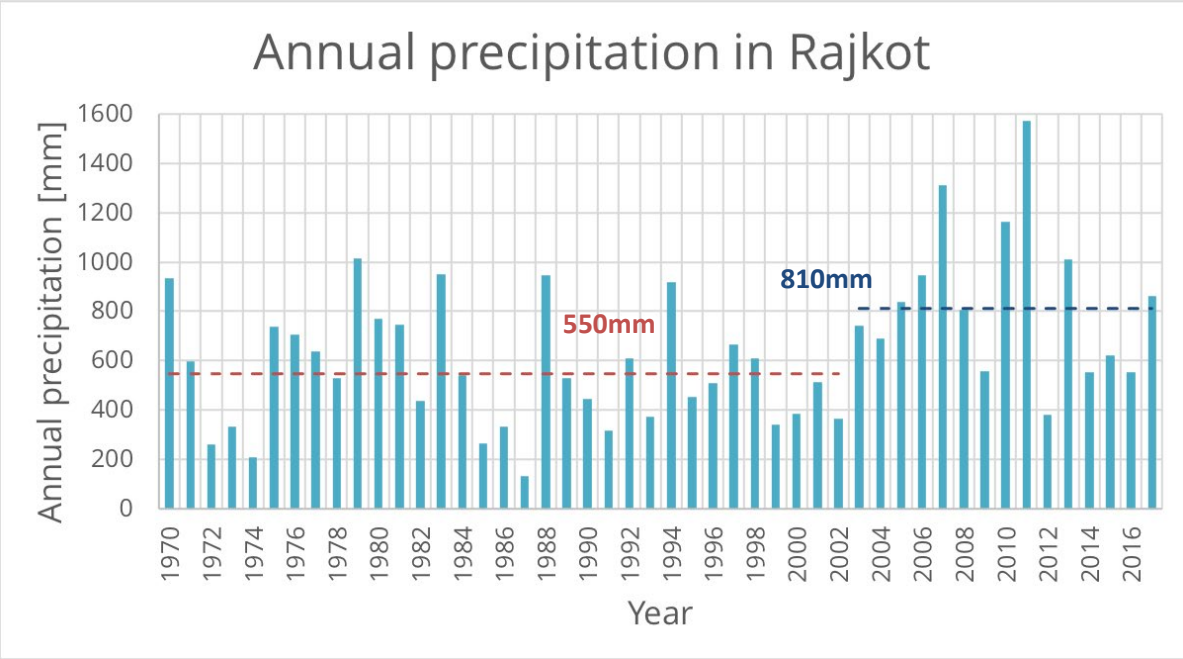

Figure 4: Annual rainfall in Rajkot district[1]

[1] Data from India Meteorological Department (IMD). Red and blue dashed lines are averages for 1971-2002 and 2003-2017 respectively

The last hypothesis is proposed by Gupta (2012) and Jain (2012). Both studies suggested that the implementation of MAR structures such as check dams, and desilting of village tanks are the main reasons behind the rise in the groundwater levels at the end of the monsoon compared to the pre-monsoon conditions. To support this, Jain (2012) performed a simplified water balance in the state of Gujarat. He computed the recharge due to rainfall and recharge by MAR structures with the water fluctuation method. Their main finding was that recharge from check dams and percolation tanks was more than 10% the recharge from the monsoon in Saurashtra region for the years 2002 and 2007. The recharge by MAR was computed as 50% of the total gross storage (therefore considering multiple fillings per year), as indicated in the guidelines by the CGWB (GEC, 1997). This procedure can be suitable for gross regional-scale budgets, but cannot represent the finer dynamic of a catchment, as the specific hydrological processes in the structures are not taken into account.

2.2 Impacts of MAR systems

An integrated assessment of the overall impact of widespread MAR in semi-arid areas is highly critical. By capturing surface runoff, these structures have the potential to lead to inequitable access to water resources, as downstream users can be negatively affected (Batchelor and Singh, 2002). Studies have highlighted some of the limitations of check dams, such as low reliability in dry years and negative hydrological impacts for downstream areas (Kumar et al., 2008). However, the arguments for or against these structures have not been substantiated through integrated and comprehensive large-scale impact assessments (Glendenning et al. 2012). Studies have focused on the estimation of recharge potential of MAR using four different main techniques: water balance (Glendenning and Vervoort, 2010), water table fluctuation (Sharda et al., 2006), remote sensing (Becker 2006, Sharma and Thakur 2007) and tracers (Sharda et al. 2006, Stiefel et al. 2009). Table 1 below summarises the literature found regarding the impacts of MAR structures in India.

Gore et al. (1998) used a catchment-scale groundwater model to estimate the influence of check dams in Wagarwadi watershed, situated in a basaltic formation in the state of Maharashtra, India. Through model calibration from 16 observation wells, they estimated the additional recharge due to MAR structures as 2% of annual average rainfall (leading to an increase of 16% in the total groundwater recharge).

Sharda et al. (2006) conducted a study to estimate potential recharge of different storage structures in a hard-rock aquifer in eastern Gujarat by combining water table fluctuation and chloride mass balance methods. They found that a power function was the best empirical equation to represent the relationship between the structure's depth and potential recharge. They estimated the maximum groundwater recharge of these structures to be between 7.3% and 9.7% of the annual average rainfall.

Sharma and Thakur (2007) applied a combined GIS and water balance based model to estimate the shift in water balance at a watershed level due to the change in land use and implementation of MAR structures in the Kutch district of Gujarat. They estimated a decrease in the runoff of approximately 60% and an increase in recharge of 5%. The amount of actual recharge is limited by the increase of actual evapotranspiration and irrigation demand by a change in land use.

Glendenning and Vervoort (2010) applied a water balance method supported by data collected in a two-year field study in the Arvari hard-rock river basin in Rajasthan, India. They estimated potential recharge as 7% of annual rainfall.

Table 1: Studies on groundwater recharge from MAR structures in India

Study	Location	MAR type	Method	Rainfall [mm]	Estimated recharge*

(Gore et al., 1998)	Parbhani district, Maharashtra	Check dams	Groundwater modelling	990	2%
(Badiger et al., 2002)	Alwar district, Rajasthan	Check dams (*paals*)	Well measurements	652	3% to 8%
(Sharda et al., 2006)	Kheda district, Gujarat	Check dams	Water table fluctuation, Chloride mass balance	845	7.3% to 9.7%
(Sharma et al., 2007)	Kutch district, Gujarat	Check dams and percolation tanks	Water balance and GIS	450	5%
(Stiefel et al., 2009)	Wakal river basin, Rajasthan	Check dams	Environmental tracers	650	0 to 75%
(Glendenning et al., 2010)	Alwar district, Rajasthan	Check dams and ponds	Water balance	449 to 897	7%
(Verma and Krishnan, 2011)	Meghal river basin, Gujarat	Check dams	Lumped basin hydrology model	800	20%
(Massuel et al., 2014)	Gajwel river basin, Andhra Pradesh	Percolation tank	Water balance, Isotope analysis	624	29%
(Dashora et al., 2017)	Dharta river basin, Rajasthan	Check dams	Water balance	573	5 to 12%

*Estimated recharge expressed in % of annual rainfall

2.3 MAR studies in Saurashtra and Bhadar basin

In order to understand the hydrology of the area and to ensure no undue replication of work already done, the existing research on MAR done in Bhadar basin and in general in Saurashtra peninsula was reviewed. IWMI already conducted research on the hydrology and the impacts of MAR in the area, and most of the literature can be found as project reports. The work of Jain (2012) for the whole Saurashtra region is already described above in Section 2.1.

In a 2002 IWMI report, Patel presented a study of the hydrological impacts of groundwater recharge activities in the Saurashtra peninsula. He analysed four ponds, five check dams and four aquifer storage and recovery wells in different basins and different geological settings in Saurashtra. He monitored the water levels of the source area and the observation wells falling under the influenced area. The infiltration rates and infiltration/evaporation ratios were computed for the structures (both regular and desilted in case of ponds and check dams). The average infiltration rate in check dams on weathered basalts was 30mm/day, and the average infiltration/evaporation ratio was 2.5. The average recharge volumes were found to be between 13 000 and 17 000m^3 depending on the check

dam. The radius of influence was 430m upstream and 550m downstream. He also found that siltation reduces both storage capacity as well as the recharge rate (Patel, 2002).

From an IWMI report, Shah (2002) highlighted the socio-economic benefits that MAR brought to farmers and rural communities. In support of his theory, he used the study performed by Joshi (2002), who interviewed 160 farmers in Saurashtra. Farmers reported notably improved productivity of irrigation wells after implementation of check dams. Another study cited by Shah is Trivedi (2002). In this work, 100 farmers were interviewed regarding watershed interventions (five check dams, seven stop dams and four farm ponds). An increase in yield from 180 wells was reported, together with significant income impacts on the nearby households.

In 2011 Verma and Krishnan performed a hydrological study on the Meghal river basin in Saurashtra. The impact of MAR was evaluated based on the total storage volume. They computed the storage volume as the total gross storage of the structures surveyed, considering a value of 2.5 fillings per year for small check dams. They used a lumped Basin Hydrology Model developed in the Matlab simulation package, and they found that the potential artificial recharge is 32% of total recharge in the basin. The infiltration and evaporation from the structures were estimated with constant evaporation and infiltration rates (Verma and Krishnan, 2011).

In 2011 Kamboj et al. analysed the impact of check dams in the Bhadar basin using flow duration curves for selected months and different periods. They modelled the natural runoff, and the calibration and validation were done between the years 1981 and 1996. Once the model was calibrated and validated, they computed the influence of MAR structures implemented after 2000 as the difference between the simulated and observed flows between 2000 and 2001. They found that the river flow reduced at the beginning of the monsoon season (June) and increased the following months. They also found that check dams can store the flow up to five times their combined storage capacity (Kamboj et al., 2011).

Chapter 3: Study Area

The study area is the Bhadar basin, located in Saurashtra peninsula. It lies between 57°9' and 73°56'E longitude and between 23°44' and 24°33'N latitude. Considering the outlet of the Bhadar river at sea in Porbandar, the total area is 7 967 km^2. However, this study considers the major part (83%) of the catchment upstream of the Ganod Gauge station (Figure 5), which has a catchment area of 6 596 km^2. All the characterisations necessary for the catchment-scale modelling of the project will be done over this area.

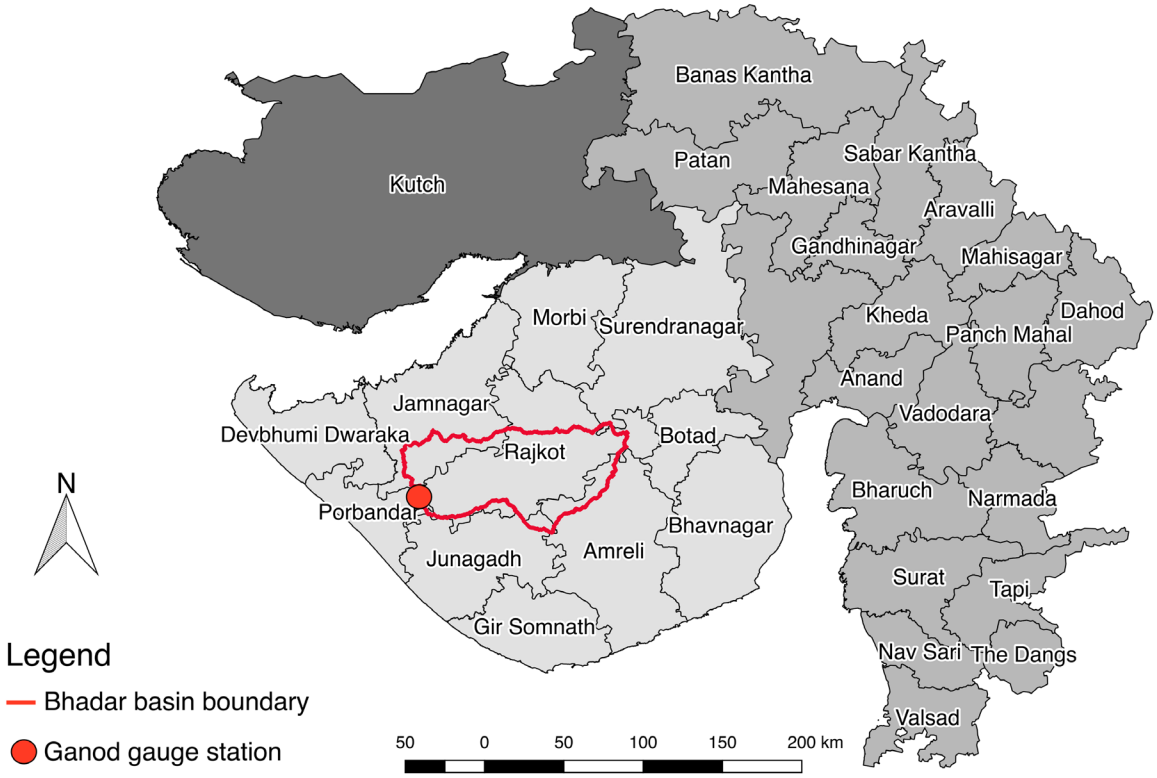

Figure 5: Districts of Gujarat and location of Bhadar basin

The elevation ranges from 35m to 240m AMSL (Figure 6). Geomorphologically, the area is characterized by hilly terrain and low-lying areas (25% of the area lays below 100m AMSL). As indicated in Figure 6, at the centre of the basin there is a dam with a gross storage capacity of 238Mm^3, which was constructed in 1964 for irrigation supply (NWRWS, 2010). The basin falls within the boundary of five Gujarat's districts: Rajkot (72% of Bhadar area), Jamnagar (16%), Amreli (8%), Junagadh (3%) and Surendragar (1%).

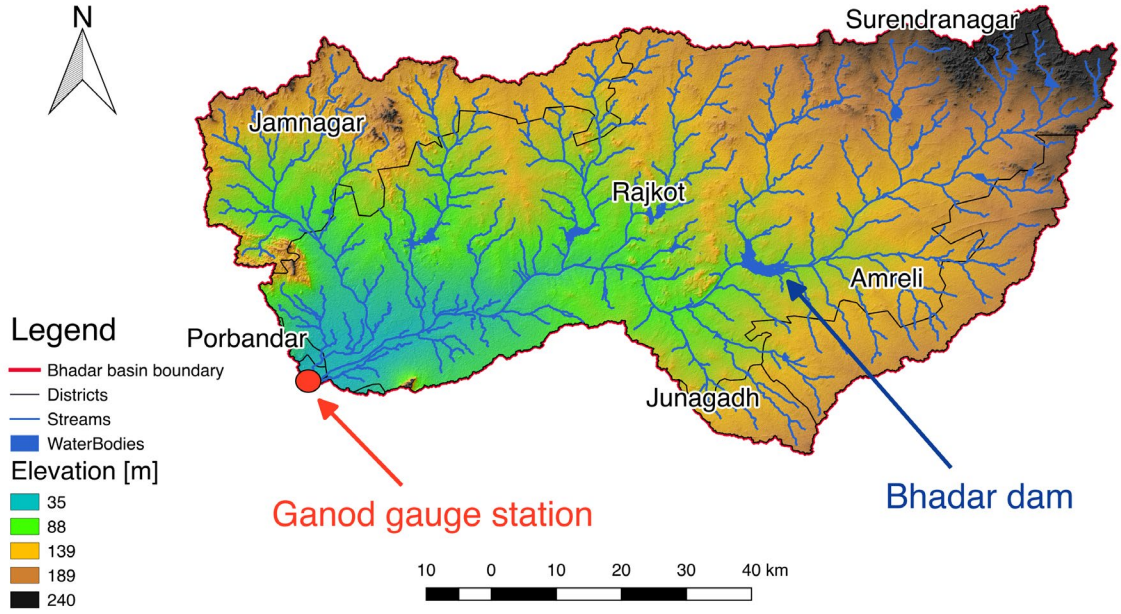

Figure 6: Topography of Bhadar basin[2]

[2] DEM from USGS EROS Archive - Digital Elevation - Shuttle Radar Topography Mission (SRTM) 1 Arc-Second Global (https://earthexplorer.usgs.gov)

3.1 Climate

As mentioned before, the Saurashtra peninsula is characterised by semi-arid climate with most of the rain concentrated in monsoon season. Extreme temperatures, erratic rainfall and high evaporation are the characteristic features of this type of climate. For climatic characterisation of the Bhadar basin, Rajkot district is considered. The general climate of the district is sub-tropical and is characterised by three seasons: summer - from April to June, monsoon - from July to September, and winter - from October to March. Average annual rainfall is 625 mm with more than 90% of the precipitation occurring between June and September during the monsoon season (Figure 7, data from CGWB). It can be noticed that total annual potential evapotranspiration exceeds precipitation by three times, and rainfall is higher than evaporation only for two months per year. This is an indication of the high dependence on water storage for this area.

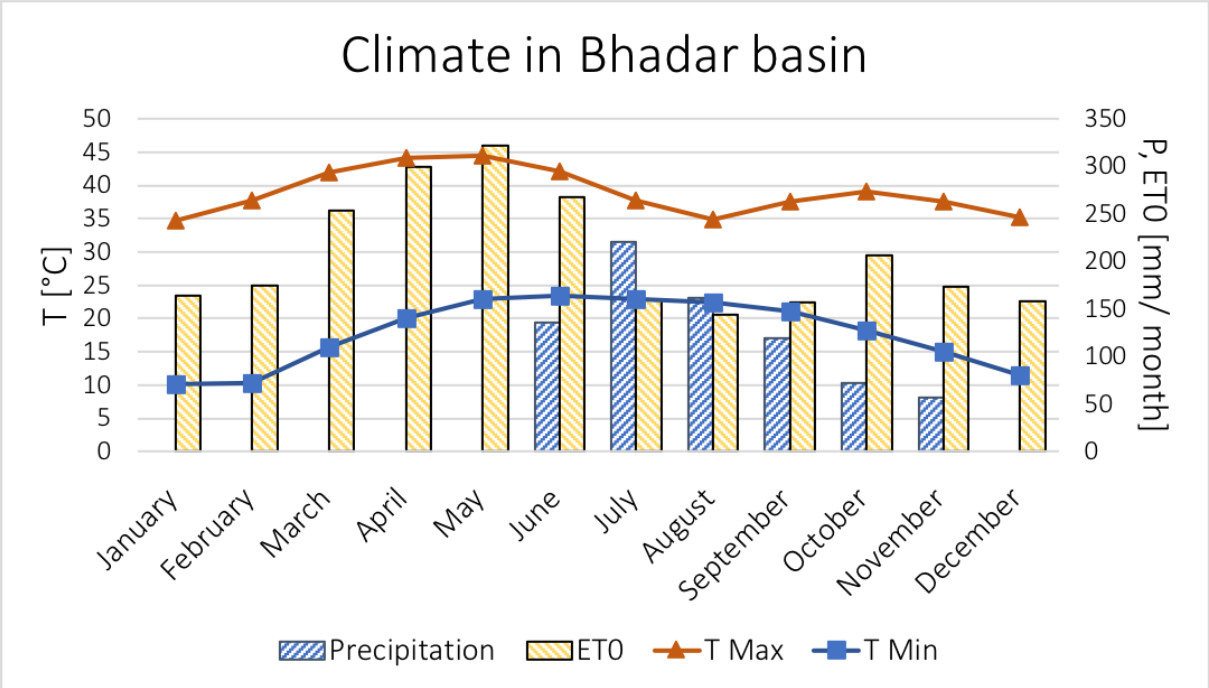

Figure 7: Climate in Bhadar basin[3]

[3] Average monthly precipitation, potential evapotranspiration, maximum and minimum temperatures. Data from State Water Data Centre (SWDC). Values from Upleta station (Data values for P 1983-2017, T and ET0 2001-2017)

3.2 Land Use and Land Cover

Data for Land Use and Land Cover (LULC) are taken from The Oak Ridge National Laboratory Distributed Active Archive Centre (ORNL DAAC). The data set provides LULC classification products at a 100-m resolution for India at decadal intervals for 1985, 1995 and 2005 (Roy et al., 2016). Figure 8 shows the LULC for the Bhadar basin in 2005, while the LULC of 1985 and 1995 can be found in Appendix A (Figure 54 and Figure 55). It can be seen that in 2005, most of the land (85%) is used for agriculture (Cropland). From the analysis of LULC maps, it is noticed that 30% of the area turned from fallow to cropland in the period between 1985 and 2005 (in 1985, fallow land amounted as 35% of the total area of the basin, while in 2005 it was only 5%). This land-use change reflects the intensification of agricultural areas occurred in the whole Saurashtra in those decades, as it is explained in the following Section 3.3.

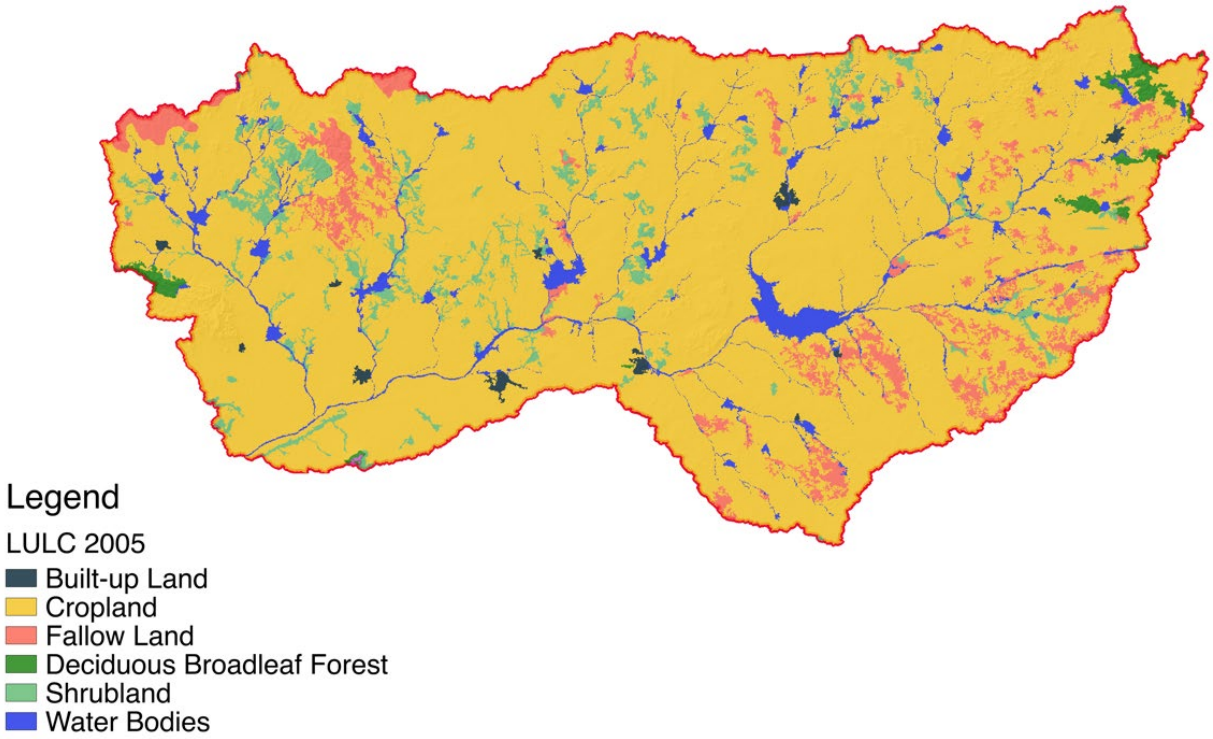

Figure 8: Land Use and Land Cover of Bhadar basin in 2005[4]

[4] Data from ORNL DAAC, one of the NASA data centres managed by the Earth Science Data and Information System (ESDIS) (Roy et al., 2016)

3.3 Agricultural water management in Saurashtra

In the last decades of the 20th century, the agricultural sector of many parts of India showed stagnant or negative growth. For the state of Gujarat however, this decline has been even more pronounced, with a decrease of about 15% of the share of agriculture in state's domestic product (Bagchi et al., 2005). After 2000, however, the state government implemented new policies to promote agricultural development. This was done by energy subsidies, liberalising markets, inviting private capital, reinventing agricultural extension, and improving roads and other infrastructures. As a result, the sector experienced a drastic turnabout (Shah et al., 2009). Cotton, wheat and milk in particular are the products that experienced the highest growth (Shah, 2008). In Saurashtra, cotton irrigated area increased from less than 4 000 Km^2 in 1996, to more than 13 000 Km^2 in 2010 (Shah et al., 2012).

This boost resulted in additional pressure on the groundwater resources, already in critical conditions from the previous decades (Bhatia, 1992). In 2004, India's Central Ground Water Board (CGWB) reported that 14% of sub-districts units assessed (*Talukas*) in the state were overexploited, 5% were critical, and 30% were in semi-critical conditions (CGWB, 2006).

To cope with groundwater depletion, from the 1980s communities and organisations started a mass movement to promote the implementation of small-scale MAR structures across the entire state. In response to a drought in 1999-2000, the state government supported this movement through a participatory program called *Sardar Patel Sahakari Jal Sanchaya Yojana* (Jain, 2012). This action was taken all over the state but had the most success in the regions of Kutch and Saurashtra, which are the driest areas of the state and the most dependent on groundwater for irrigation (Shah et al., 2009).

In 2009, Gujarat State Watershed Management Agency (GSWMA) launched a comprehensive programme (Integrated Watershed Management Programme) which aim was to restore the ecological balance by "harnessing, conserving, and developing degraded natural resources such as soil, vegetation cover, and water through the prevention of soil run-off, regeneration of natural vegetation, rain water harvesting, and recharging of the ground water table".

The number of check dams in the state of Gujarat is reported as 133 732 in 2011, of which 57 090 are located in Saurashtra (ENVIS, 2017). Within the Bhadar river basin, Kamboj et al. (2011) reported a total number of 4 385 check dams in 2010.

3.4 Agricultural management

Cropping seasons in India can be divided in Kharif (June-October), Rabi (October-February) and summer (February-June). Gujarat's main crops are cotton and groundnut, for which the state represents the highest national producer. In the season 2015-2016, the state provided 31% and 35% of the national cotton and groundnut production respectively (Bodh et al., 2017).

Agricultural data are available from the Directorate of Agriculture of the Government of Gujarat at district level (DAG, 2017). The data of the season 2015-2016 for land use, crop area, irrigated area and source of irrigation are processed and presented in Figure 9, Figure 10 and Figure 11 below. The statistics for the Bhadar basin are produced averaging the values of the five districts comprised in the basin, using the fractions of the contributing areas as averaging weights.

Figure 9 shows the main crops in the Bhadar basin, together with their related gross cropped areas. In accordance with the total state statistics, main crops are cotton and groundnut, followed by wheat, spices and condiments, fruits and vegetables, other oilseeds (excluding groundnut), gram, tur and other pulses, bajri and other minor crops. From Figure 10, it can be seen that cotton accounts for more than 70% water requirement in the state. This is because cotton is a more water demanding crop in comparison with groundnut.

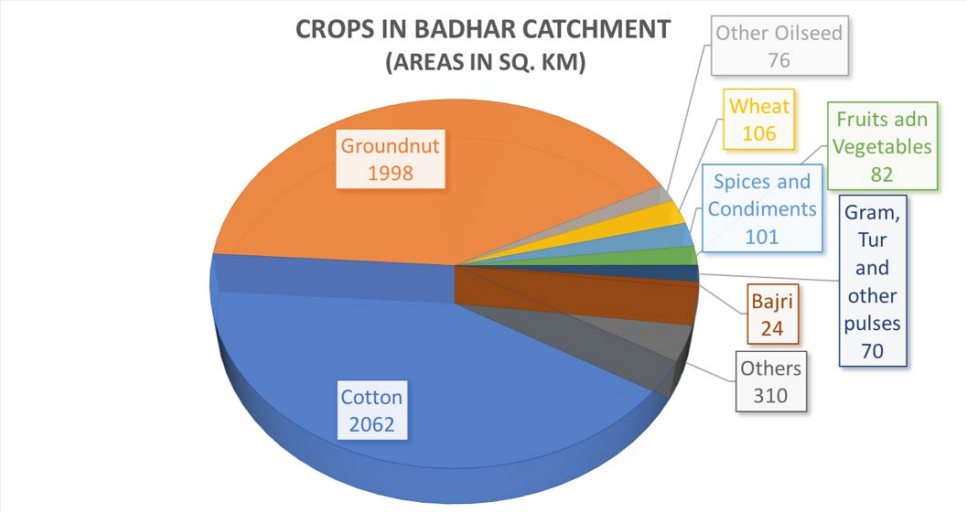

Figure 9: Gross cropped areas in Bhadar basin (gross, areas in sq. Km)[5]

[5] Data from Directorate of Agriculture of the Government of Gujarat (DAG, 2017)

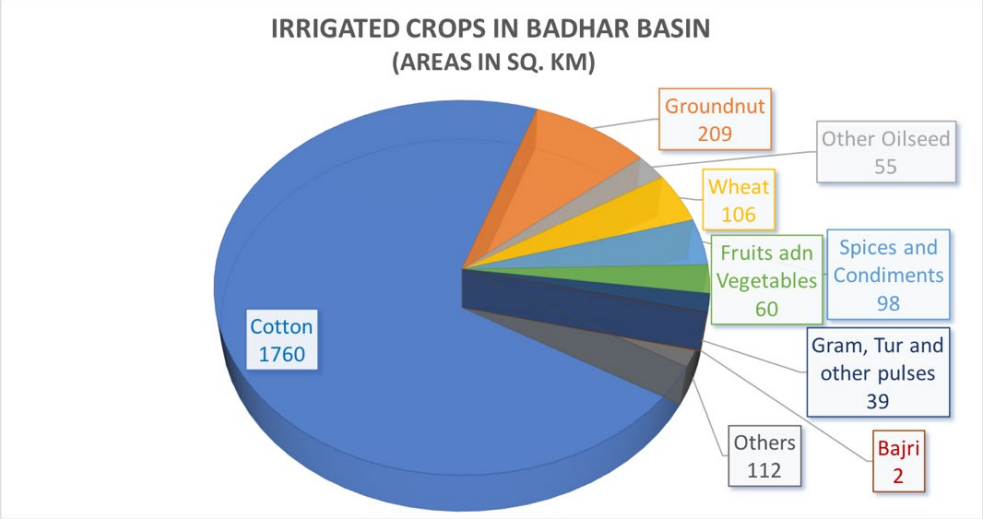

Figure 10: Gross irrigated areas in Bhadar basin (areas in sq. Km)[6]

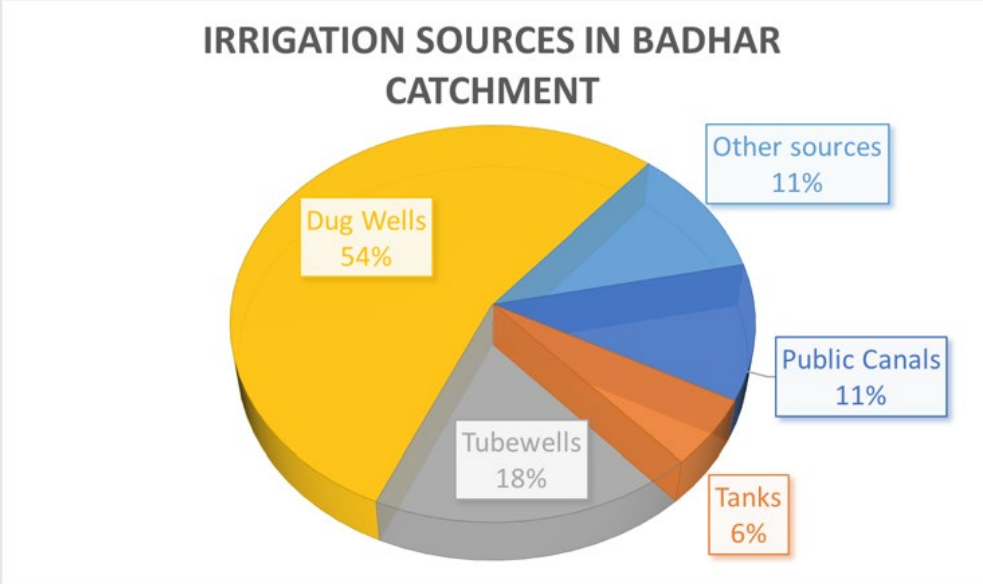

Figure 11: Irrigation sources in Bhadar basin (% from the gross irrigated areas)

Figure 11 shows the sources of irrigation for the gross irrigated areas in Bhadar basin. It can be seen that most of the water comes from large diameter dug wells, and overall groundwater supply serves more than 70% of the irrigation demand. The main surface water resources in the district are from village tanks and canals taking water from the Bhadar dam (which supplies water to a gross area of more 350 Km^2) and other minor dams (NWRWS, 2010).

[6] Data from Directorate of Agriculture of the Government of Gujarat (DAG, 2017)

3.5 Hydrogeology

As it can be seen in Figure 12, the predominant geological formation in the Bhadar basin is the Deccan trap. This setting is a hard-rock formation from the end of the Cretaceous period. This formation is one of the largest volcanic provinces in the world, and it covers about 800,000 km^2 in central India (see Figure 56 in Appendix A) (Watts, 1989).

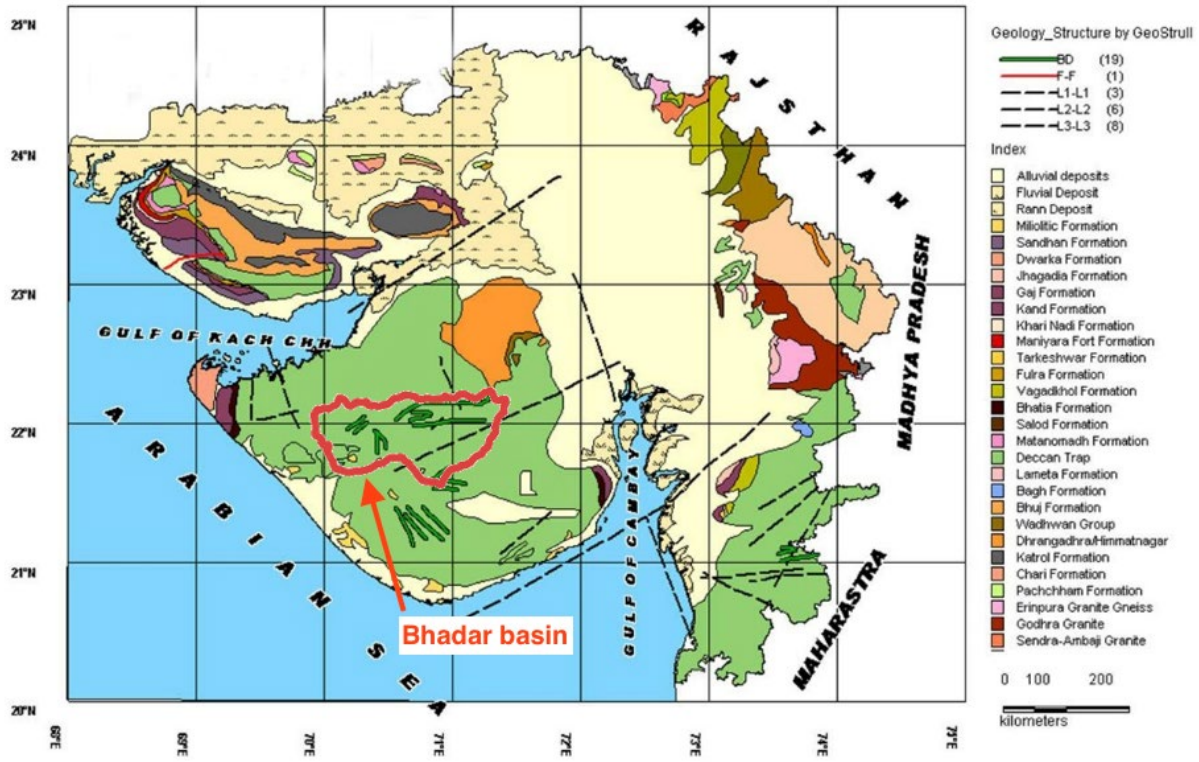

Figure 12: Geology map of Gujarat (Narmada, 2010)

The Deccan trap is a basaltic formation made by multiple lava flows each deposited horizontally to near horizontally. The thickness of each layer sequence represents a single flow event, and it ranges between a few meters to more than 30 m. These flows can be either massive (highly compacted core) or vesicular (characterised by many cavities or “vesicles”, resulting from the escape of gas bubbles during the cooling of the lava) (Singhal, 1997). These vesicles are generally filled with secondary minerals like calcite, zeolites and quartz. Due to the high compactness and the low porosity, this formation results in a poor aquifer with generally low groundwater potential. Primary porosity is derived from vesicles, lava tubes and flow contacts. Secondary porosity is derived from jointing and weathering (CGWB, 2015).

In Bhadar basin, lava flows are generally intruded by different acidic and basic dykes of 2 to 5 m thickness. These features are highly relevant for groundwater movement: in some parts, these dykes are highly weathered and form aquifers themselves; in other places, the dykes are so compacted (non-weathered) that they form a barrier for groundwater movement. Because of the presence of these dykes, hydrogeological conditions for groundwater flow and abstractions can be highly variable within short distances (Kulkarni et al., 2000). The weathered upper layer forms a good aquifer of varying thickness, which in some areas reaches 20 m (Singhal, 1997).

The conceptual model of the hydrogeology in the Deccan trap from a study of Foster et al. (2007) is shown in Figure 13 below.

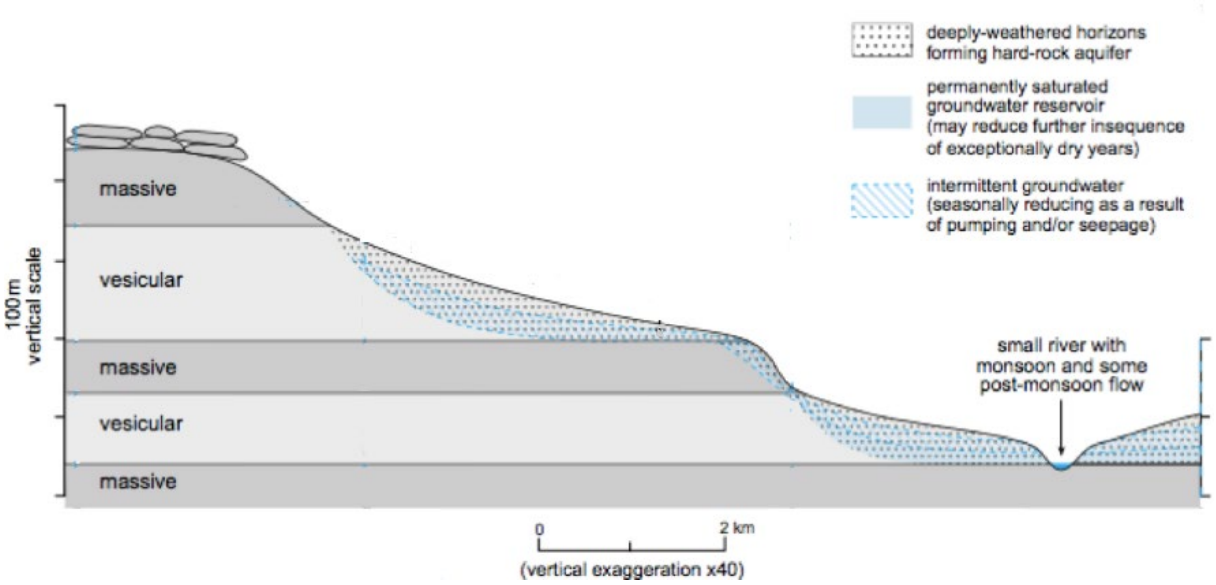

Figure 13: Hydrogeology of a Deccan Trap basin (Foster et al., 2007)

Transmissivity in the Bhadar basin can vary between 0.09 to 1 100m^2/day. Dug wells found in this area tap the basalt with a depth ranging between 5 to 50m. The yield of abstraction is generally comprised between 100 to 500m^3/day. Wells tapping the vesicular horizons can have yields up to 1000m^3/day, while the ones located within the dykes have yields between 15 and 600m^3/day (CGWB, 2015).

With regards of soil deposits, major soil types in Bhadar basin are shallow, medium, black soil characteristic of volcanic settings. Soil textures found in the basin are sandy, loamy sand, clayey and silty type (CGWB, 2015). Soil deposit map can be found in Appendix A (Figure 57).

3.6 Groundwater levels

The groundwater level follows the seasonal behaviour of the monsoon. From the CGWB (2015), it is reported that groundwater levels in the pre-monsoon period (April) can go as low as 40m BGL. Abstraction yields in this period are minimal and most of the dug wells during the summer season are dry.

Groundwater level data from 1996 until 2016 are available from the portal of CGWB[7]. Measurements are both from open wells and piezometers. For each observation wells, four measurements are taken annually: pre-monsoon (April), monsoon (August), post-Kharif (November) and post-Rabi (January). In order to have a general overview of the groundwater level in the area, groundwater level maps are produced in QGIS (Figure 14, Figure 15). These maps are the result of interpolation of 91 observation wells (of which 31 falls within basin boundaries); the values used are all average of the last five years of recordings (2012 to 2016). The depth to water table ranges from 4 to 23m below ground level in the period before monsoon season, while during monsoon it varies between 2 and 15m BGL. These maps are produced to acquire a general idea of groundwater levels of the area and their seasonal behaviour[8].

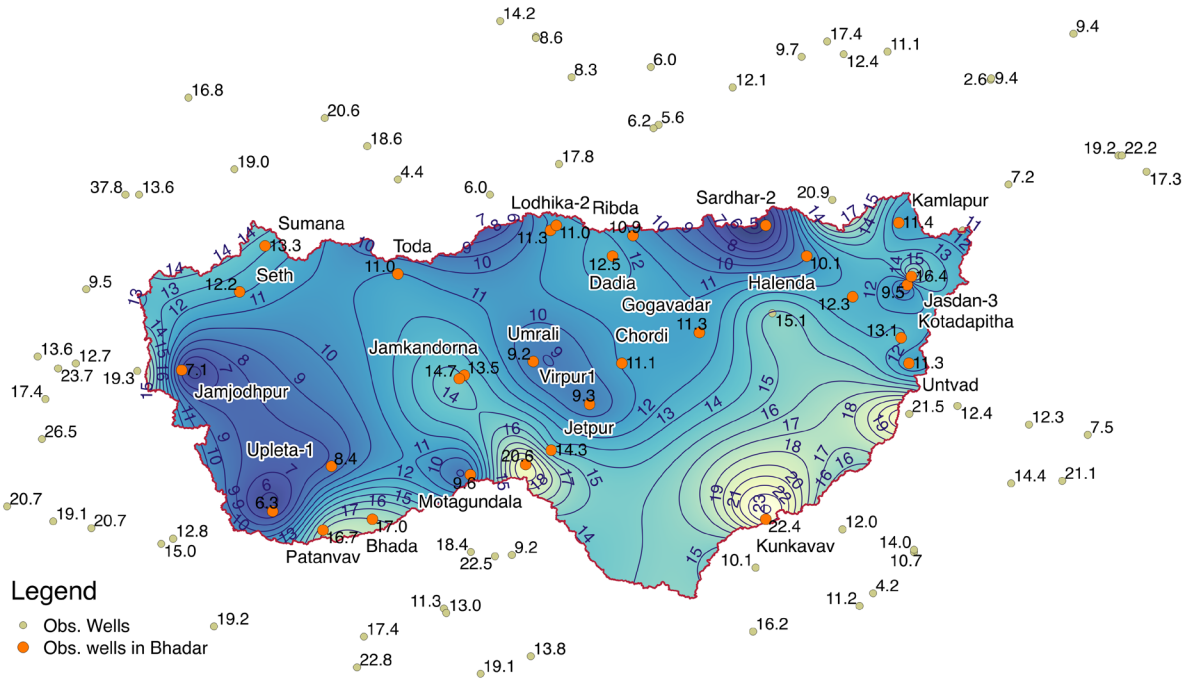

Figure 14: Depth to water table before monsoon season (April) [m BGL][9]

[7] India-WRIS: http://tamcnhp.com/wris/#/waterData

[8] Statistical analysis of the groundwater levels is out of the scope of this work, which focuses only on the structure scale. The study of groundwater trend at the basin scale and their correlation with the presence of check dams is part of the other task of the project, which focuses on the catchment scale.

[9] Values averaged between years 2012 and 2016

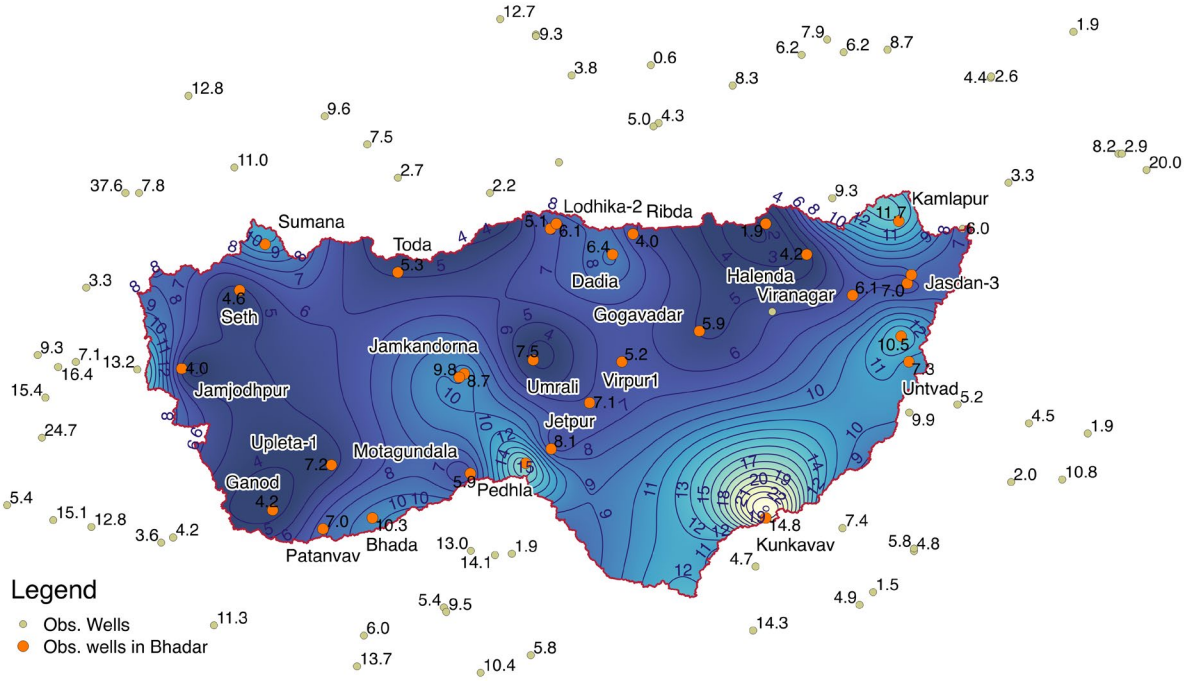

Figure 15: Depth to water table in monsoon season (August) [m BGL][10]

[10] Values averaged between years 2012 and 2016

Chapter 4: Methods

4.1 Field visit

The fieldwork was carried out between the 14th and 16th of May 2019. Being summer, the structures were expected to be empty and the maximum temperature reached peaks of 47°C. Fieldwork activities involved direct check dam measurements as well as surveys with farmers. Because of time and climatic constraints, only three days could be dedicated to the field visit. Based on this time availability, a maximum number of four MAR sites in the basin could be visited.

4.1.1 Site selection

Despite the high intensity of check dams reported in the basin, no spatial data are available regarding their specific locations. The selection of the sites was then based on the location of the observation wells from the CGWB, for which coordinates are available. As mentioned before, a total number of 31 observation wells falls within the basin. Their coordinates were imported in Google Earth Engine, and the area was examined with satellite images. Within the radius of 2km of each well location, check dams that could be visually recognised were mapped.

From satellite images, an overview of the area could be taken. Figure 16, Figure 17, Figure 18 are showed as examples of different configurations. Overall, there is a high density of structures in the ephemeral rivers and check dams are found in series relatively close to each other (for instance in Vrinagar two structures are 150m distant, Figure 18). The structures are highly variable in terms of geometry, dimension and condition. The width of the structures identified varies between 15m to 240m. From the 31 observation well locations, 94 MAR structures could be identified. Their location is shown in Figure 19, together with the sites selected for the field visit.

The criteria for selecting the sites to visit considered the geographical location within the basin, the order of the river, elevation, dimensions of the structures and the distance from the observation well. The idea was to get a diverse sample of sites with respect to these parameters. Some sites with complex configurations (like Bhada Jodiya in Figure 17) were excluded from the selection, as well as the largest structures (like Ganod in Figure 16).

Based on these criteria, three sites were selected to visit and perform check dam assessment and surveys with farmers: Kamlapur, Viranagar and Umrali. Another site selected for visit was Arni, 20km upstream from Upleta observation well (green circle in Figure 19). This site was selected for visit because it was previously studied by Patel (2002). The intention was to potentially use some of his findings, as he performed some measurements and studied the impacts of one check dam in that location. The characteristics of the selected sites that were detectable by remote sensing are displayed in Table 2.

Figure 16: Ganod satellite image

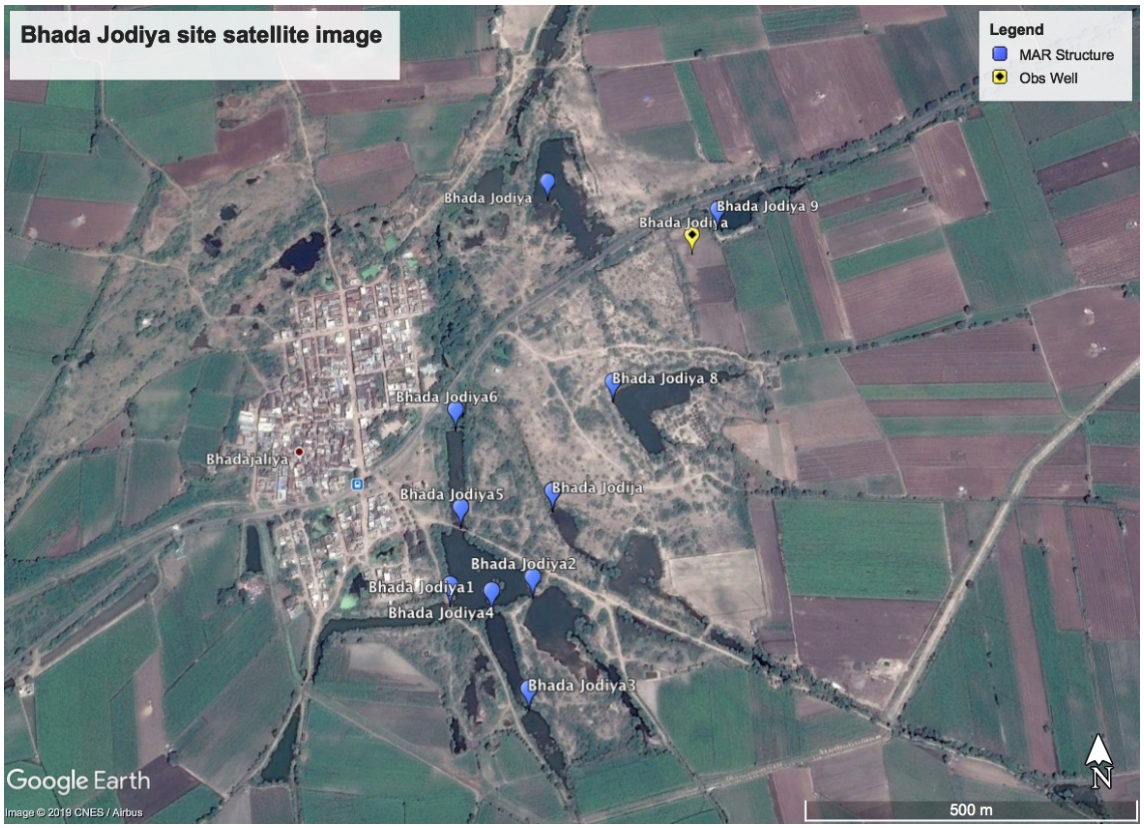

Figure 17: Bhada Jodiya satellite image

Figure 18: Viranagar satellite image

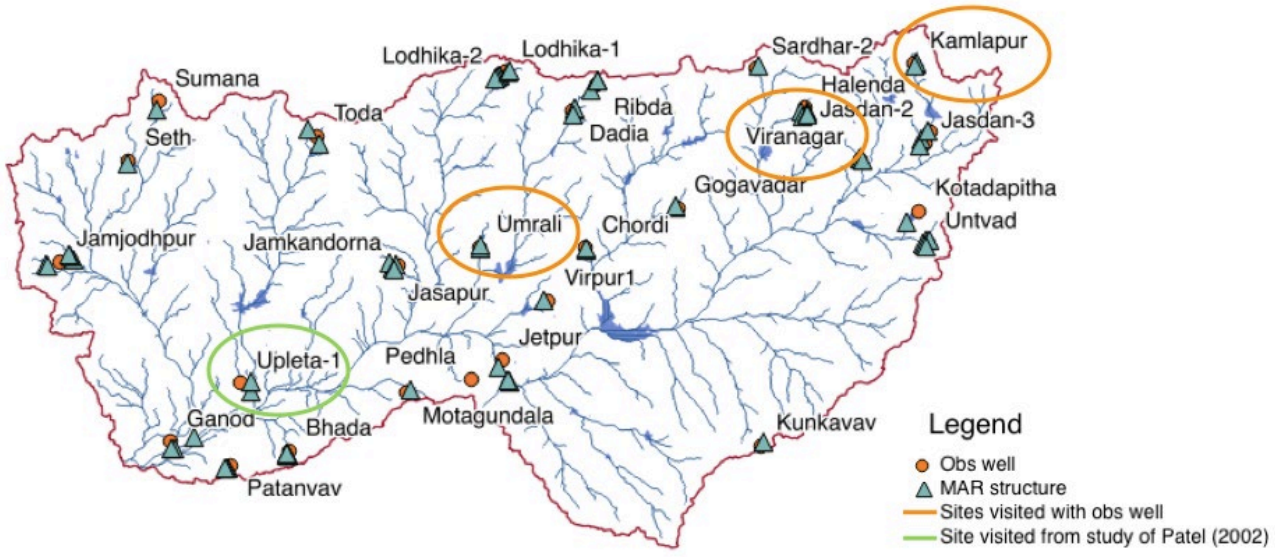

Figure 19: Location of observation wells and corresponding MAR structures

Table 2: Characteristics of the structure that were analysed in the field

Site	Nr check dams	Distance obs. well from MAR [m]	Strahler order	Slope [°]	Elevation [m]	River width [m]	Catchment area [km²]*

Umrali	5	300-340	2	0.7	100	15-50	15.5
Viranagar	5	90-260	2	1.6	180	30-40	24.9
Kamlapur	3	345-410	1	1	240	20-30	14.7
Arni	5	-	1	0.5	100	15-85	12.4

* Upslope area from check dam

4.1.2 Direct measurements

Because check dams were empty at the time of the visit, it was possible to analyse their geometry as well as the river bed. The condition of the structures was assessed, both in terms of integrity and silting. In check dams where desilting occurred and the trace of the removed layer was visible, the depth of the removal was measured. In structures fully covered, it was not possible to assess the depth of the actual silt layer. The width and the height of the structures were measured, together with the river cross-section (width vs depth).

From the large diameter wells found in the vicinity of the structures, some subsurface features could also be assessed. These types of wells have the casing only in the upper part in the weathered zone. Hence, the thickness of the weathered zone (depth to hard-rock) was estimated as the depth of the casing of the well below the ground. Also, diameter and depth to water were measured.

4.1.3 Questionnaires

To cope with the lack of data and feasible measurements, local farmers were interviewed regarding the performance of the check dams. Farmers owning land in the vicinity of the check dams were interviewed. A standardised questionnaire was prepared in advance and can be found in Appendix B. The questions dealt with:

1. Check dams: year of construction, maintenance, hydrological behaviour, water use.
2. Dug wells: water level dynamics, pump installed, abstraction yield.
3. Irrigation practices: cropping areas, crop types, abstraction volumes, irrigation technique, irrigation calendar.

4.2 Conceptual model

4.2.1 Water balance

A daily water balance approach is used to study the hydrological dynamics of the check dam. Figure 20 below shows the volumes considered in the water balance: runoff R, precipitation P, evaporation E, infiltration I, general losses G, and outflow Out.

If during a day, precipitation falls within the catchment area enclosed by the structure, runoff can be produced. This runoff enters the check dam as direct inflow and is then captured. The amount of water entering the check dam as direct precipitation falling upon the impounded area is also considered. From the surface impounded area, evaporation occurs. Water leaving the check dam from the wetted bottom to the subsurface is represented by infiltration. Other types of output, like direct withdrawals from the structure, transpiration by plants, leakages due to seepage or construction mistakes, are considered as general losses. When the structure is at its full capacity, input elements cannot be stored, and water leaves the structure as overflow.

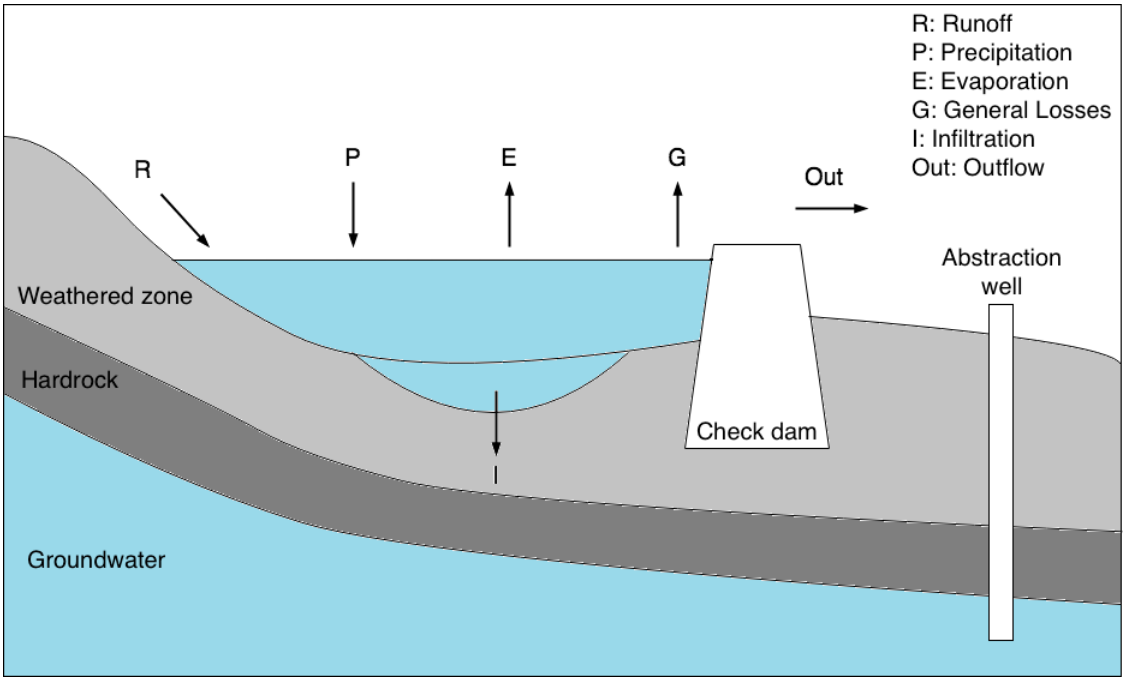

Figure 20: Water balance of the check dam

The change in storage of check dam can be computed as the difference between inputs and outputs (the outflow is calculated afterwards in Equation [3]):

$$\Delta V = R + P - E - I - G \qquad [1]$$

The water volume stored in the structure at the time step t is therefore:

$$V(t) = \min[V(t-1) + \Delta V(t); V_{MAX}] \qquad [2]$$

If the structure has reached its capacity $V_{MAX} > V(t-1) + \Delta V(t)$, the outflow is:

$$Out(t) = V(t-1) + \Delta V(t) - V_{MAX} \qquad [3]$$

In the following sections, the elements of the water budget will be illustrated. Sections 4.2.3 and 4.2.4 explain precipitation and evaporation rate respectively. Runoff is presented in Section 4.2.5, while Section 4.2.6 is dedicated to the estimation of infiltration rate from the check dam.

4.2.2 Check dam geometry

Most of the check dams found in the basin are reservoirs that form a tale along the river (like Vrinagar in Figure 18). Out of the 94 structures mapped, 62 can be considered having a geometry as the one described. Because of this particular shape, the volume can be estimated from the stream gradient and the river cross-section (Figure 21). In this study, the topographic slope calculated from Digital Elevation Model with a resolution of 1 arc-second is taken as an estimate for the stream gradient α. However, this approximation might lead to some errors since stream gradient might differ from the topographic slope, as affirmed by Strahler (1952).

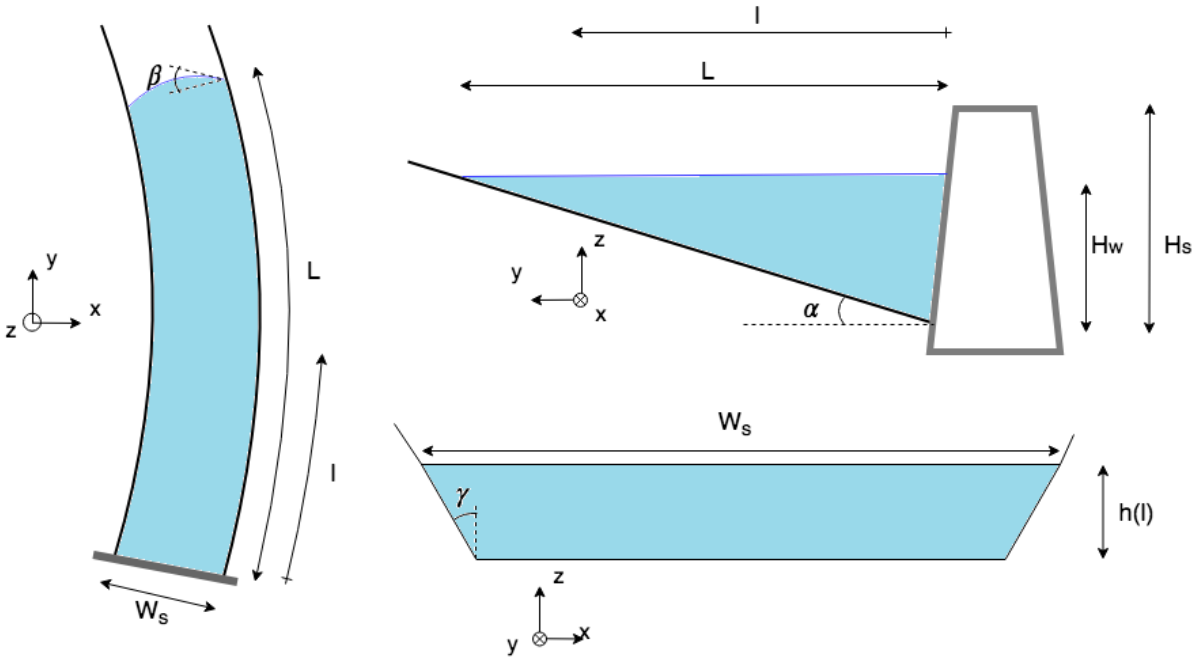

Figure 21: Cross-sections of a check dam and stored water volume

To calculate the length of the tail L, it is assumed that the closest upslope structure is located at a greater distance then L. With this assumption, the tale length can be derived from the water depth at the structure H_W and the stream gradient α (considering $\beta \ll 1$):

$$L = H_W / \tan \alpha \qquad [4]$$

The water depth h at a certain distance l from the structure is:

$$h(l) = \tan \alpha \, (L - l) \qquad [5]$$

In this study, it is assumed that the river width is constant and equal to the structure's width W_s:

$$\partial W_s / \partial l = 0; \; \partial W_s / \partial H_W = 0$$

For trapezoidal river beds, the cross-sectional area A_{cs} can be computed:

$$A_{cs}(l) = h(l)[W_s - h(l)\tan\gamma] \quad [6]$$

Where γ is the river bank slope. For wide and shallow river, the second term in the bracket can be in this case neglected as $h \ll W_s$. In this case, the cross-sectional area can be estimated as:

$$A_{cs}(l) = W_s \tan\alpha\,(L - l) \quad [7]$$

The storage in the structure *V* can be then computed as:

$$V(H_W) = \int_0^L A_{cs}(l)\,dl = \frac{W_s \tan\alpha\, L^2}{2} = \frac{W_s \cdot {H_W}^2}{2\tan\alpha} \quad [8]$$

The storage capacity V_{MAX} of the structure can be therefore approximated with a quadratic relationship with structure's height H_S:

$$V_{MAX} = \frac{W_s \cdot {H_S}^2}{2\tan\alpha} \quad [9]$$

The functions estimating surface and wetted areas (red and blue line in Figure 22) with water depth are then calculated:

$$A_{surf}(H_W) = W_s \cdot L = \frac{W_s \cdot H_W}{\tan\alpha} \quad [10]$$

$$A_{wet}(H_W) \approx k_A \cdot A_{surf} = k_A \cdot \frac{W_s \cdot H_W}{\tan\alpha} \quad [11]$$

Where k_A:

$$k_A = \left[1 + \frac{2H_S}{W_s \cdot \cos\gamma}(1 - \sin\gamma)\right] \quad [12]$$

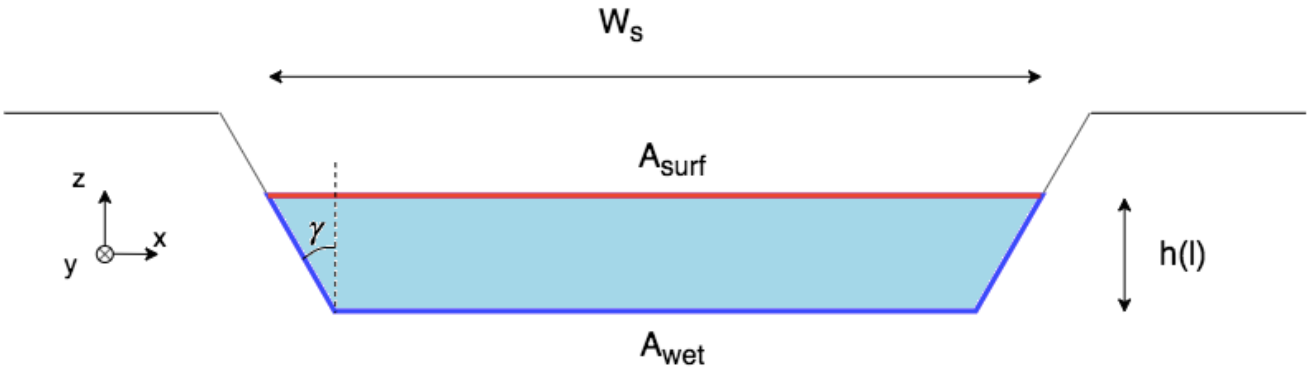

Figure 22: Wetted and surface area

4.2.3 Precipitation

The volume of daily rainfall falling upon the structure can be calculated from precipitation depth p and the surface area A_{surf} (calculated in Equation [10]):

$$P = p \cdot A_{surf} \quad [13]$$

Rainfall data were requested to the State Water Data Centre (SWDC), which provided daily measurements from three meteorological stations located in the Bhadar basin between 1961 and 2017.

4.2.4 Evaporation

As for precipitation, evaporation volume is computed from the evaporation depth e and the surface area calculated in Equation [10]:

$$E = e \cdot A_{surf} \quad [14]$$

Penman equation for evaporation from a free water surface is used as an estimate (Penman, 1948). Evaporation rate e in mm/day is computed with the SI units version of the Penman equation, reformulated by Shuttleworth (1993):

$$e = \frac{\Delta}{\Delta+\gamma}\frac{R_n}{\lambda} + \frac{\gamma}{\Delta+\gamma}\frac{6.43(1+0.536\,U)\cdot e_s(1-RH/100)}{\lambda} \quad [15]$$

With R_n, net incoming radiation in MJ/d/m^2, U wind speed in m/s and RH relative humidity in %. The other parameters of the equations are:

– e_s: saturated vapour pressure (kPa) (being T_{mean} mean daily temperature):

$$e_s = 0.6108 \exp\left(\frac{17.27\,T_{mean}}{237.3+T_{mean}}\right) \quad [16]$$

– Δ: slope of vapor-pressure curve in (kPa /°C):

$$\Delta = \frac{4098\,e_s}{(237.3\,T_{mean})^2} \quad [17]$$

– λ: latent heat of vaporisation (MJ/kg):

$$\lambda = 2.501 - 0.002361\,T_{mean} \quad [18]$$

– φ: psychrometric constant (kPa /°C) (being p_s surface pressure in kPa):

$$\varphi = 0.0016286\frac{p_s}{T_{mean}} \quad [19]$$

Daily climate data were requested to the State Water Data Centre. However, net solar radiation and surface pressure were not among the measured parameters. Because of this, daily values of incoming net solar radiation, wind speed, temperature, surface pressure, relative humidity are all taken from NASA POWER project Data sets (grid resolution of 0.5°)[11].

4.2.5 Runoff

The volume of runoff entering in the check dam is computed from daily runoff depth r and the catchment area A_{catch} of the structure:

$$R = r \cdot A_{catch} \quad [20]$$

[11] NASA Langley Research Center (LaRC) POWER project Data sets: https://power.larc.nasa.gov

The catchment area is computed in QGIS using the Digital Elevation Model of the area and the location of the structure. The Upslope area command was used to contour the catchments from the check dams selected for the field visit.

Surface runoff is estimated with the SCS - Curve Number Method developed by the Soil Conservation Service (SCS, 1972):

$$r = \begin{cases} 0 & if\ p < I_a \\ \dfrac{(p - I_a)^2}{(p - I_a) + S} & if\ p > I_a \end{cases} \quad [21]$$

Where r is the depth of runoff, p is precipitation, I_a initial water abstractions (which account for water stored in small surface depressions, losses due to interception and initial infiltration before runoff occurs) and S is maximum potential storage within the watershed. As indicated by SCS, it is generally assumed $I_a = 0.2S$. The storage parameter S is dependent on the watershed characteristics and antecedent moisture condition (AMC II). In SI units is determined by:

$$S = \frac{25\,400}{CN_{II}} - 254 \quad [22]$$

Where CN_{II} is the runoff curve number for average soil condition (AMC II). Patel et al. (2017) estimated the runoff curve number CN_{II} for the Bhadar basin from land use/ land cover maps and soil maps. The resulting curve number CN_{II} for Bhadar basin is 90.1.

Depending on the soil moisture conditions, runoff curve number must be adjusted. The classification of soil moisture condition is displayed in Table 3.

Table 3: Antecedent soil moisture conditions classification

Soil conditions	**Rainfall in the 5 antecedent days [mm]**	
	Dormant season	Growing season
Dry (AMC I)	< 12.5	< 35
Average (AMC II)	12.5 to 27.5	35 to 52.5
Wet (AMC III)	> 27.5	> 52.5

According to Hawkins et al. (1985), for curve numbers $55 \leq CN_{II} \leq 95$, curve numbers for the other antecedent moisture conditions can be estimated as:

$$CN_I = \frac{CN_{II}}{2.281 - 0.01282\ CN_{II}} \quad [23]$$

$$CN_{III} = \frac{CN_{II}}{0.427 + 0.00573\ CN_{II}} \quad [24]$$

The resulting curve numbers are CN_I =79.9 and CN_{III}=96.5. Applying these numbers into Equation [22] Equation [21], daily runoff is then computed (dormant season is used as criteria to classify AMC).

4.2.6 Infiltration

The infiltrating volume can be computed from infiltration rate i and wetted area A_{wet} (Figure 22, Equation [11]):

$$I = i \cdot A_{wet} = i \cdot k_A \cdot A_{surf} \quad [25]$$

In order to estimate infiltration rate, it is important to consider and understand the factors that affect this process. According to Bouwer (2002), the mechanism of infiltration from a structure depends on *i)* the presence of a clogging layer and *ii)* the depth to the water table.

Figure 23 shows the two types of mechanisms: infiltration controlled by the hydraulic gradient (Figure 23a), and infiltration controlled by gravity (Figure 23b).

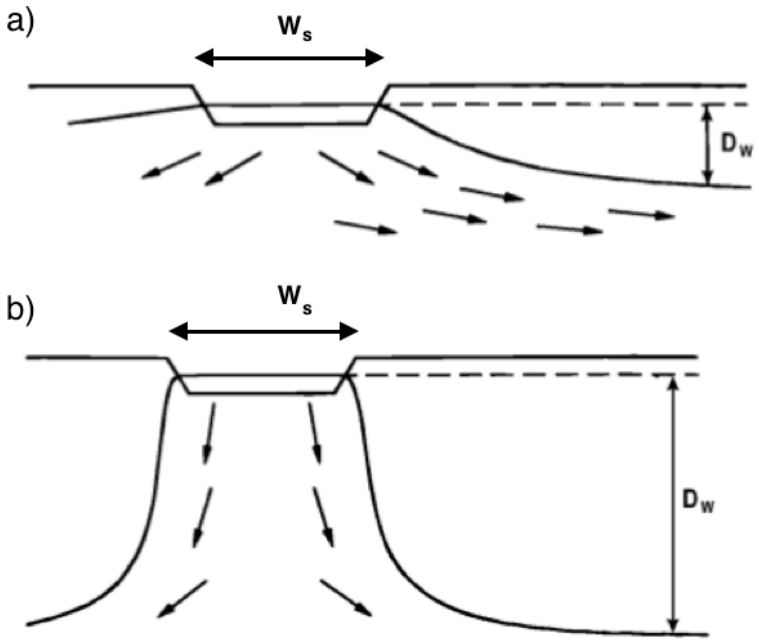

Figure 23: Mechanisms of infiltration (Bouwer, 2002)

Hydraulically controlled infiltration occurs in the absence of a clogging layer, and when the depth to the water table D_W is less than twice the structure width W_S. If the aquifer is relatively deep ($D_W > W_S$) or a layer of low permeability is clogging the basin, the infiltration is controlled by gravity. This behaviour can be seen from Figure 24 below. For shallow aquifers without clogging layer, the infiltration rate goes linearly with depth to the water table. As the water table goes deeper, infiltration rate gradually becomes constant, as controlled by gravity.

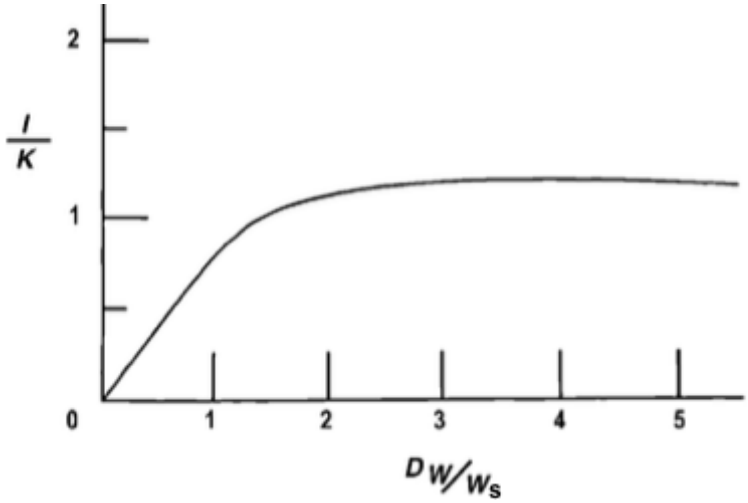

Figure 24: Infiltration without clogging layer (Bouwer, 2002)[12]

Because of the hydrogeological characteristics of the area explained in Section 3.5, both of the aforementioned mechanisms can occur in the basin: at the beginning of the rainy season, when the aquifer is dry and water table is deep, infiltration is controlled by gravity (right horizontal part of the curve in Figure 24); when the groundwater level rises during monsoon season, infiltration is controlled by hydraulic gradient (left linear part of the curve in Figure 24). In fact, groundwater levels showed in Section 3.6, suggest that in the monsoon season, the water level is shallow enough to be hydraulically connected with the water mounding from check dams. In fact, in some part of the basin the level goes as shallow as less than 5 m depth (Figure 15). Being the range of the width of these structures between 15 to 200m, in monsoon season check dams and water table can be considered hydraulically connected.

As a result, a function relating infiltration with water table depth needs to be applied to evaluate infiltration volumes correctly. Moreover, with this relation it is possible to take into account induced recharge by abstractions, as explained further in this section.

The general assumptions for this model can be summarised:

1. Infiltrated water seeps only in lateral and vertical directions, and not in the direction of the stream flow;
2. The soil where infiltration occurs is homogeneous with a uniform hydraulic conductivity;
3. The flow of water infiltrating through the vadose zone is completely saturated (except when a clogging layer is present);
4. The system is considered to be in steady-state;
5. The water table is sufficiently below the surface so that evaporation and water uptake from roots can be neglected;
6. The effect of infiltration from the single check dam on the water table is negligible.

Assumption 1 states that only vertical and lateral flow are considered (x and z directions of Figure 21), and the seepage occurring below the structure in the direction of the stream is neglected (direction y in Figure 21). This flow is highly relevant for the functioning of the structure, as most of

[12] I: infiltration rate [m/day]; K: saturated hydraulic conductivity [m/day]; D_W: depth to the water table; W_S: width of the structure

the water infiltrating is flowing downstream. This has been evidenced in several studies that have reported a skewed radius of influence for observation wells located upstream and downstream of the structures (Patel, 2002; Badiger et al., 2002).

Despite this critical assumption, it is reasonable to assume that the impact on model results are not that grave. In fact, the output of the infiltration model is only a quantitative element to add into the water balance of Equation [1], and the direction and allocation of the infiltrated water are out of the scope of this work. Moreover, the elongated geometry of the stored volumes suggests that seepage in stream direction is quantitatively minor when compared to vertical and lateral flows (for the 62 check dams mapped, the ratio between width and length of the tail is less than 20%)[13].

Assumption 6 neglects the effect of infiltration from the check dam on the water table. Even though this is a relevant hydrogeological process for the performance of the structure, the resulting error can be expected to be relatively small. In fact, it is reasonable to assume that check dams do not affect the water table at a significant distance, as their radius of influence is relatively small (Patel, 2002; Badiger et al., 2002). Because of this, the water table is introduced in the model as an input function (further explained in Section 4.2.8).

If Assumption 1 is counted, the check dam basin can be modelled as an open channel. The relation between infiltration and aquifer properties has been studied by many researchers since the 1930s (Dachler, 1936). Bouwer (1969) summarised most of the research on leakage from open channels and his study is taken here as primary reference for modelling infiltration.

According to Bouwer, there are three main conditions of leakage from an open channel (Figure 25):

- Condition A: Channel embedded in uniform soil underlined by a more permeable material;
- Condition B: Channel embedded in uniform soil underlined by a less permeable material;
- Condition C: The soil in which the channel is embedded is of much lower hydraulic conductivity than the original soil for a relatively short distance (clogging layer).

[13] Check dam's width varies between 15m and 200m, while tail length varies between 150m and 3km

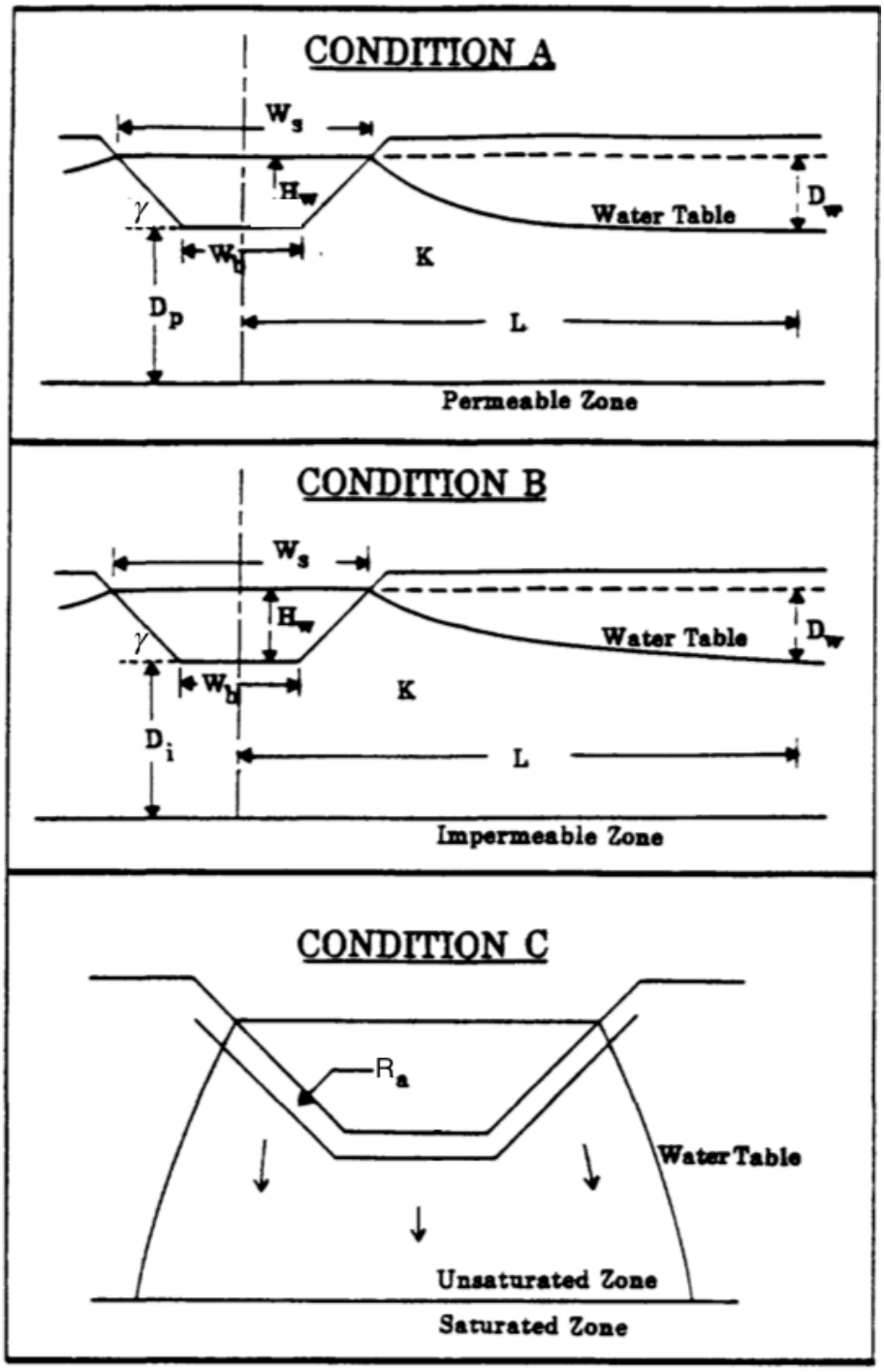

Figure 25: Bouwer's infiltration conditions (Chin, 1990)

As previously explained in Section 3.5 of the previous Chapter, the area is highly heterogeneous and hydrogeological conditions can change within small distances. As a result, it is not possible to generalise which of the three conditions is the most representative. In case of a check dam located on top of a high-permeable dyke, condition A could be the most representative; if the structure is overlaying a highly impermeable layer, condition B might occur; if the bottom of the check dam basin is covered by compacted silt, condition C can be the most representative. All three Bouwer conditions are then simulated and analysed as three case scenarios.

These conditions are illustrated in the following Sections 4.2.6.1, 4.2.6.2 and 4.2.6.3. The effect of abstractions on the infiltration rate is explained in Section 4.2.7. Water table input function is discussed in Section 4.2.8. The flow chart of the overall infiltration model is illustrated below in Figure 26.

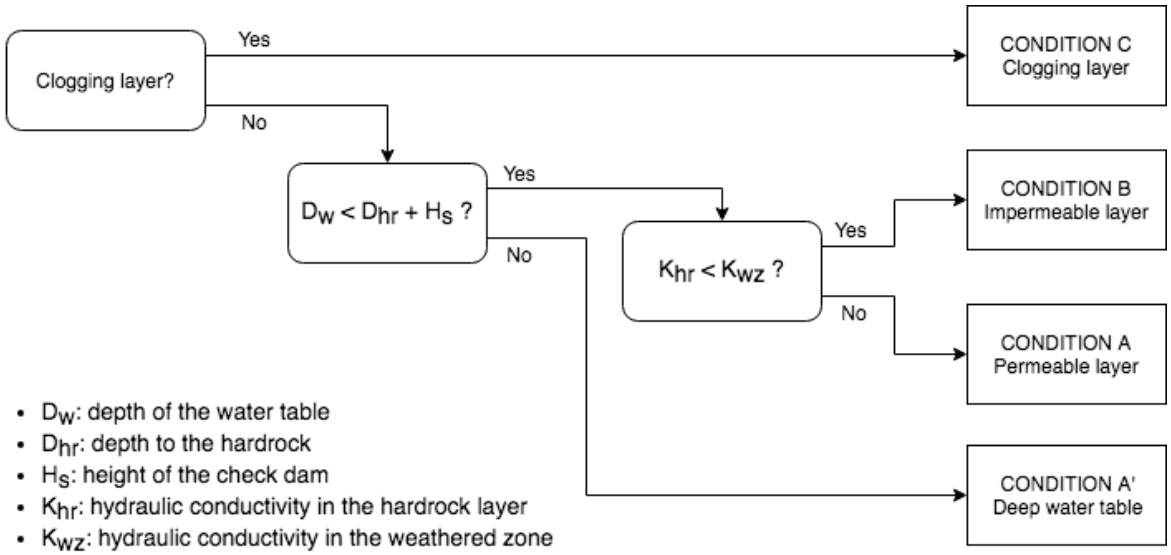

Figure 26: Scheme of the conceptual model

4.2.6.1 Condition A: permeable layer

Condition A occurs when the underlying layer has a higher permeability than the upper one ($K_{HR} > K_{WZ}$). In case of Bhadar area, this might be applicable in areas on the vesicular horizon or highly weathered dykes. This condition assumes a layer of infinite hydraulic conductivity beneath the weathered zone. In this case, water flows both horizontally and vertically through the permeable layer, and the water table approaches a horizontal line with increasing distance from the channel (Figure 27). This means that the point in which water table D_W is assigned, should be at sufficient distance from the structure. In case the water table is below the permeable layer, a subcase A' is considered.

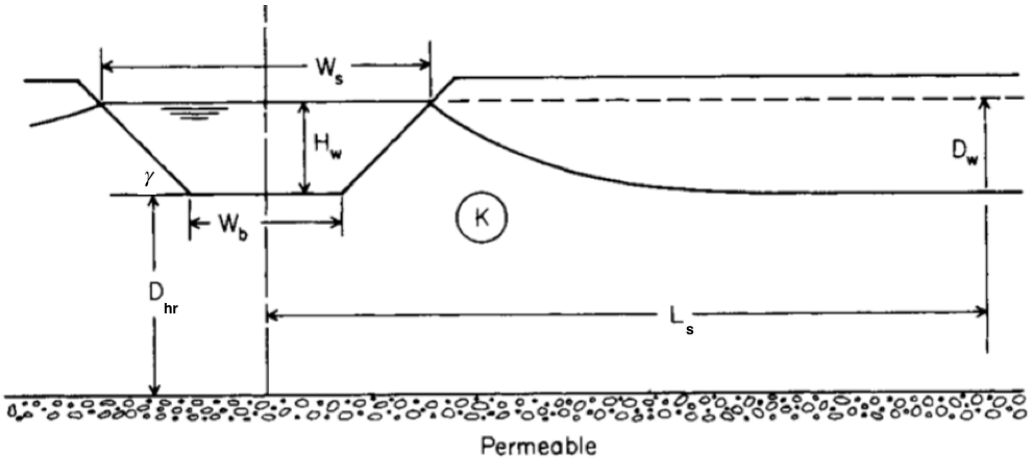

Figure 27: Condition A of infiltration (Bouwer, 1969)

Condition A'

This condition considers the case in which the water table is below the permeable zone ($D_W > D_{hr} + H_s$), with D_{hr} depth to the hard-rock (in m). A solution is obtained by Vedernikov (1934) for $D_{hr} = \infty$. The infiltration rate i_A, (expressed in terms of volume rate per unit length of channel per unit width of the water surface) is:

$$\frac{i_{A'}}{K} = 1 + F_A \frac{H_w}{W_s} \qquad [26]$$

Being F_A a parameter depending on the geometry of the system (Figure 28). No analytical solutions with explicit i_A, for finite D_p are available from literature.

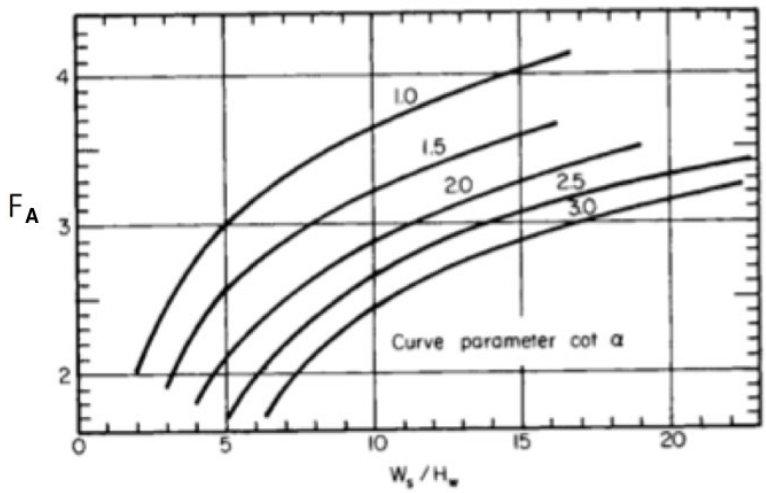

Figure 28: Parameter F_1 in function of W_s/H_w and river bank slope (Bouwer, 1969)

Condition A

If the water table is within the weathered zone ($D_W > D_{hr} + H_S$), the infiltration rate can be estimated with Ernst's solution (Ernst, 1962):

$$\frac{i_A}{K} = \frac{\pi D_w}{W_s \ln[a(D_{hr} + H_w)/w.p.]} \qquad [27]$$

Where $w.p.$ stands for wetted perimeter and a =4,3. As showed by Bouwer, this method is valid for relatively shallow aquifers: $D_w/W_b < 2$. Being W_b the bottom of the channel (see Figure 27).

4.2.6.2 Condition B: impermeable layer

Condition B occurs when the underlying layer has lower permeability than the upper one ($K_{HR} < K_{WZ}$). This might apply to areas in the Bhadar basin over massive and compacted basalt. This condition assumes a lower layer with hydraulic conductivity equal to zero (Figure 29).

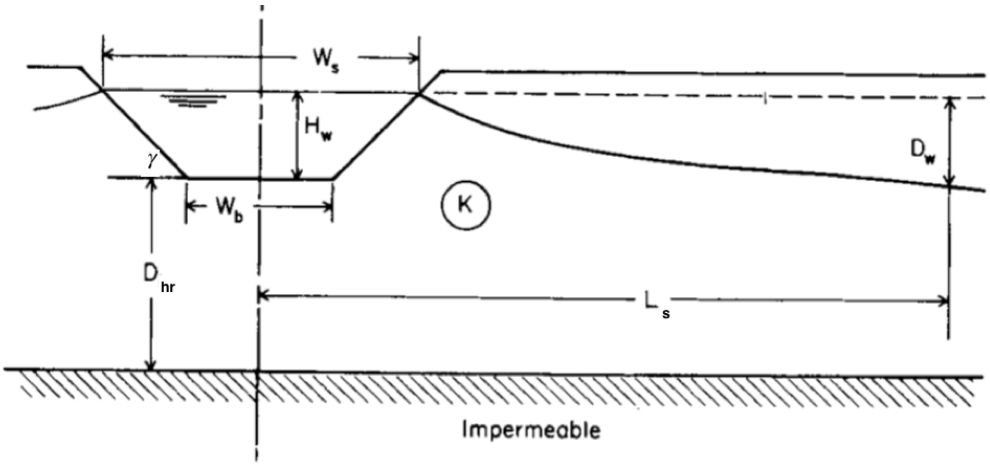

Figure 29: Condition B of infiltration (Bouwer, 1969)

According to Bouwer, if the weathered zone is relatively shallow, the Dupuit-Forchheimer (D-F) assumption can be applied to this condition. This assumption consists of assuming completely horizontal water flow from the channel. This method fails when the depth to the impermeable layer D_p approaches infinity (Bouwer, 1965). In case $D_{hr} < 3W_b$, infiltration rate i_B can be estimated as:

$$\frac{i_B}{K} = \frac{2D_w}{W_s} \frac{H_w + D_{hr} - \frac{1}{2}D_w}{L_s - \frac{1}{4}(W_b + W_s)} \quad [28]$$

$$L_s = \frac{W_s + H_w + D_{hr}}{2} \quad [29]$$

In case of deep aquifers ($D_{hr} > 3W_b$), the solution developed by Ernst can be used (Ernst, 1962). This solution considers head loss due to radial flow and horizontal flow. The infiltration rate resulting from the sum of the two flows is:

$$\frac{i_B}{K} = \frac{D_w/W_s}{(1/\pi)\ln[(D_{hr} + H_w)/w.p.] + \left[\frac{1}{2}L_s/(D_{hr} + H_w - \frac{1}{2}D_w)\right]} \quad [30]$$

Note that if the water table is below the hard-rock layer ($D_W > D_{hr} + H_S$), the check dam and the water table are hydraulically disconnected. In this case, the same behaviour as condition A' is assumed.

4.2.6.3 Condition C: clogging layer

A phenomenon often occurring in dam structures is the accumulation of a silt layer which clogs the basin and reduces infiltration. The presence and amount of silt depend on the characteristics of the area, maintenance practices (de-silting) and the stage of the structure (it might form gradually

throughout the year) (Bouwer, 2002). When the basin is covered with this layer, flow is only due to gravity and the underlying soil is in unsaturated conditions (Figure 30).

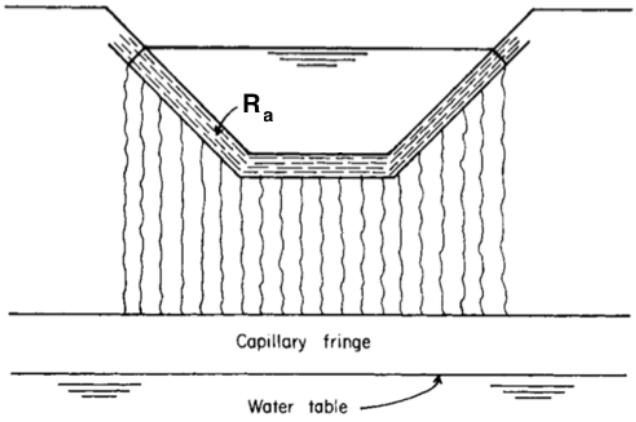

Figure 30: Condition C of infiltration (Bouwer, 1969)

In this case, unsaturated hydraulic conductivity K_p is a function of soil-water pressure head P_{sw}. This relationship is represented by the sigmoid curve displayed in Figure 31. From the figure, it can be seen that most of the reduction of K_p takes place in a relatively small range of P_{sw}. The center of the curve is represented by P_{cr} defined by Bouwer as:

$$P_{cr} = \frac{\int K_p dP_{sw}}{K} \qquad [31]$$

Where K is saturated hydraulic conductivity (K_p at $P_{sw} = 0$).

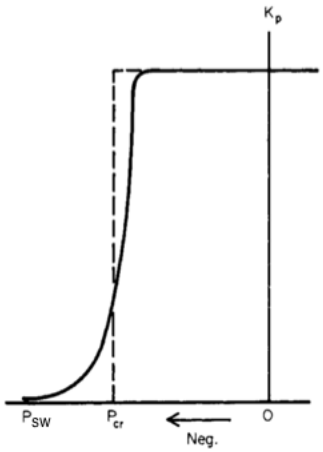

Figure 31: Unsaturated hydraulic conductivity and soil-water pressure (Bouwer, 1969)

For trapezoidal channels, infiltration rate can be then approximated by:

$$i_C = (W_s R_a)^{-1}[(H_w - P_{cr})W_b + (H_w - 2P_{cr})(H_w/\sin\alpha)] \qquad [32]$$

Where R_a is the hydraulic impedance of the clogging layer (in days) and P_{cr} is the critical value of pressure for the change in hydraulic conductivity. This value ranges from approximately -20 cm of water for coarse and medium sands, to -50 to -100 cm water for fine sands and sandy loams, and to -150 cm and less for structureless loams and clays. Note that this estimation is assuming that air has access to the underlaying soil and is valid for a relatively thin layer of low hydraulic conductivity (sufficiently low to cause the downward flow to be less than the saturated hydraulic conductivity K).

According to Bouwer, as long as the water table is more than 1m below the bottom of the infiltration basin, infiltration is controlled by the presence of a clogging layer. This is because the capillary fringe in permeable materials is less than 0.3 m height. It is therefore considered that until the water table $D_w > 1$m, infiltration occurs; when D_w approaches the surface, no infiltration is happening.

4.2.7 Abstractions

Water withdrawals from wells in the proximity of check dams can influence the infiltration rate. This phenomenon is called induced recharge and have been reported by different studies (Chaturvedi and Srivastava, 1979; Butler Jr et al., 2007; Shen and Xu, 2011). Induced recharge by abstractions can be included in the model by integrating the drawdown in the water table D_w that occurs below the structure (Figure 32).

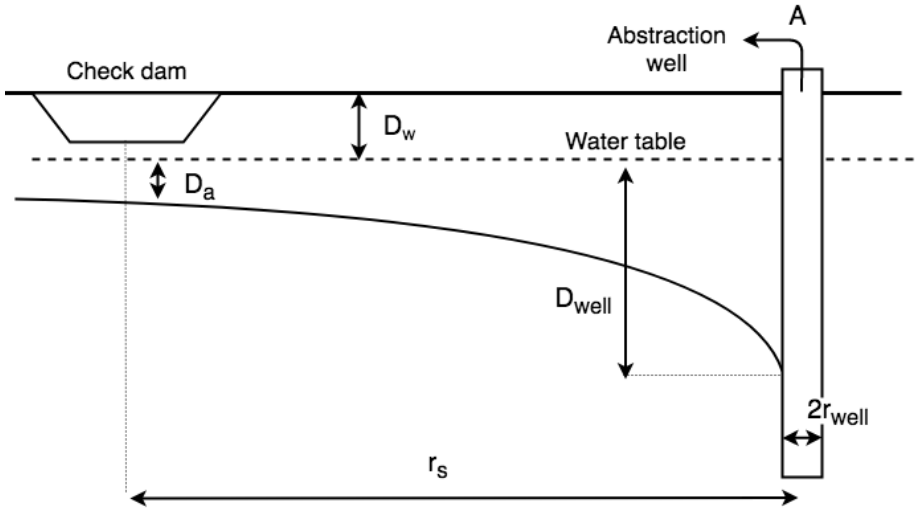

Figure 32: Drawdown from pumping

For this purpose, Thiem equation is used to estimate the decrease in water level D_a at the structure (Thiem, 1906):

$$D_a = -\frac{A}{2\pi T}\ln\left(\frac{r_s}{r_{well}}\right) + D_{well} \qquad [33]$$

Where T is the transmissivity of the aquifer (m^2/day), A is the abstraction rate (m^3/day), r_s is the distance between the check dam and the well, r_{well} is the radius of the well and D_{well} is the decrease in water level in the well (all in m). Note that Thiem equation is valid for porous confined aquifer in steady-state, and it can lead to some inaccuracy if applied to hard-rock aquifers.

Another aspect to consider is that abstractions affect infiltration rate only if the water mound and the water table are hydraulically connected. In case of presence of a clogging layer, water withdrawals will not affect the storage in the structure.

If the perched water from the structure is in contact with the water table, abstractions will enhance infiltration form the structure by increasing water table depth D_w (see Figure 32):

$$D'_w = D_w + D_a \qquad [34]$$

Where D'_w is the new water table depth at the check dam's location that considers the drawdown due to abstractions.

This procedure considers a steady-state system. In fact, it is assumed that abstractions that occur in one day have an effect on the water table only on that particular day. The drawdown is assumed to be completely recovered on the following day. This aspect adds further uncertainty and might enhance the inaccuracy of the model.

It is assumed that water withdrawals from dug wells are due only to irrigation demand. Abstraction volumes, rates and irrigation calendars are estimated from the surveys carried out during field visit and will be presented in the dedicated Results section of this work (Chapter 5).

4.2.8 Water table input function

In order to analyse the water table behaviour in the basin, groundwater level data from the CGWB are used. Measurements from Umrali observation well are taken because of the largest amount of valid data (out of the 21 recorded years between 1996 and 2016, 13 years have complete sets of valid data).

Because water level fluctuation is dependent on precipitation, years are classified based on annual rainfall (measured in Rajkot). *Dry*, *normal* and *wet* categories are defined in Table 4. In Figure 33, the distribution of annual rainfall is displayed for measurements recorded in Rajkot between 1970 and 2017 (48 total measurements). The 13 years of groundwater data are therefore divided into the three categories (six *normal*, five *wet* and two *dry*).

Table 4: Year classification based on annual rainfall

Class	Annual rainfall [mm]
Dry	<400
Normal	600-800
Wet	>800

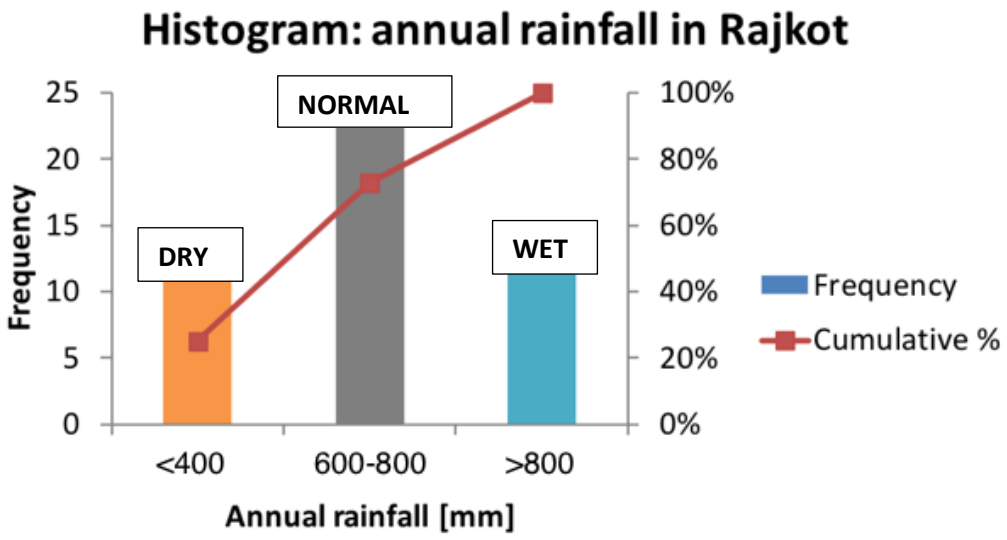

Figure 33: Histogram of the annual rainfall in Rajkot[14]

[14] 48 total measurements from 1970 to 2017

As already mentioned in Section 3.6, for each year four groundwater level measurements are available: post-Rabi (January), pre-monsoon (April), Monsoon (August) and post-Kharif (November). The water table in the area is characterised by an oscillating and periodic behaviour throughout the year, following the seasonal variation of rainfall. A sinusoid is therefore used as an estimation for water level based on the day of the year.

Three functions are therefore developed in order to best fit the sets of measurements available for four months of the year (Equations [35], [36] and [37], where J is the Julian day of the year). The function coefficients are found by graphical qualitative adjustment; results are shown in Figure 34, Figure 35 and Figure 36 in the next page. Note that in *dry* years the function underestimates the water depth in winter months. This is presumably because only two years are available for characterising water table function for dry years.

Normal years: $$D_w = 4\sin\left[\frac{J\cdot\pi}{182{,}4}\right] + 6 \quad [35]$$

Wet years: $$D_w = 5\sin\left[\frac{(J-15{,}2)\cdot\pi}{182{,}4}\right] + 6 \quad [36]$$

Dry years: $$D_w = 2\sin\left[\frac{(J+15{,}2)\cdot\pi}{182{,}4}\right] + 7 \quad [37]$$

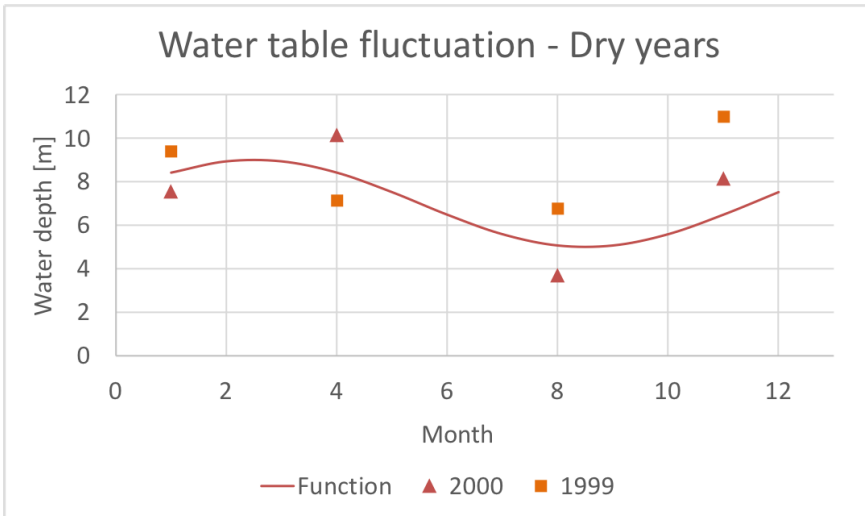

Figure 34: Water table for *dry* years (Annual precipitation less then 400 mm)

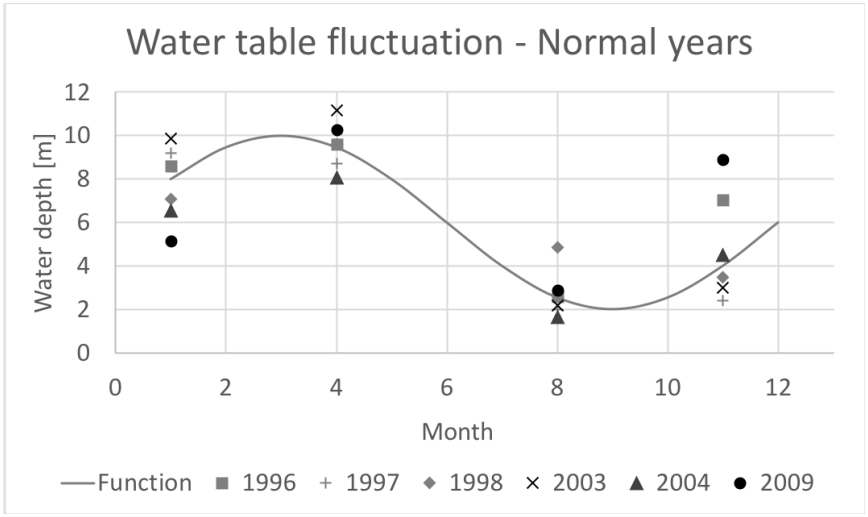

Figure 35: Water table for *normal* years (Annual precipitation between 400 and 800 mm)

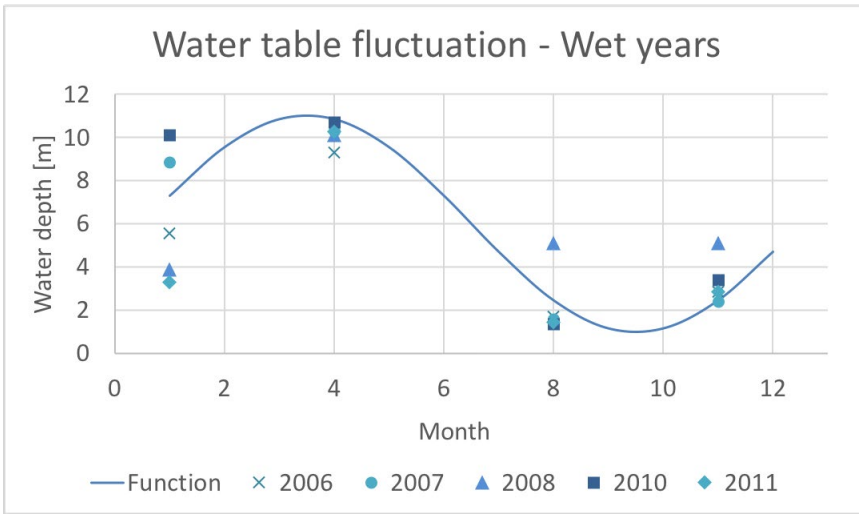

Figure 36:Water table for *wet* years (Annual precipitation higher then 800 mm)

4.2.4 Simulation in R

The conceptual model presented in previous sections is implemented as code in the R environment (R Core Team, 2017). R is a programming language and free software to perform statistical computing. The criteria for which this software was chosen is based on its widespread implementation.

The ambition of this work is to develop a tool that can be easily used and modified by researchers interested in studying check dams behaviour. R language fulfils this objective, as it is widely used and can be coded by users with basic programming skills. Moreover, in contrast with Matlab, it is Open Source.

Figure 37 shows the interface of R studio (RStudio Team, 2018). Check dam's water balance is simulated for eleven years (2000 to 2010). Precipitation, evaporation, runoff and drawdown from abstractions are imported as CSV files. The code computed infiltration volumes for the three different Bouwer conditions. The results of the simulations are presented and discussed further in Chapter 5.

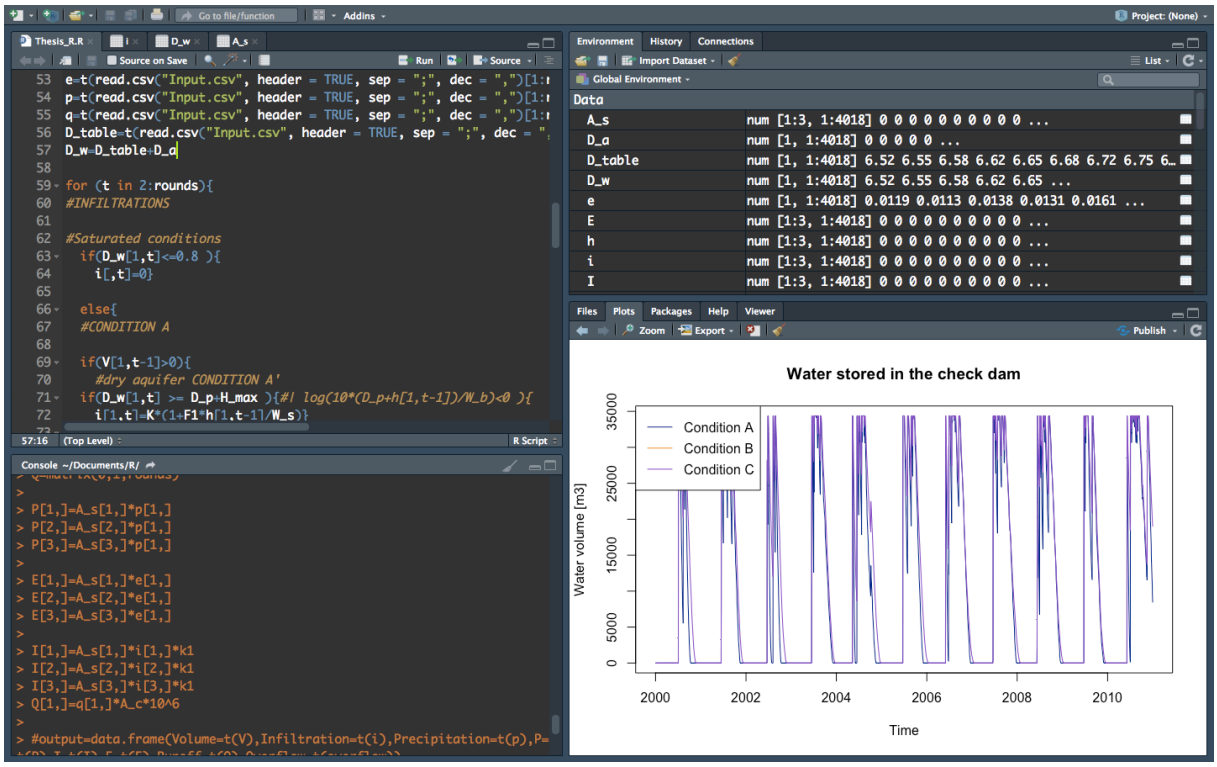

Figure 37: R studio environment

4.2.5 Model validation

In order to validate the model presented, measurements of daily water level would be needed for all the period in which water is present in the check dam. Time constraints did not allow the recording of these measurements for the check dam assessed in the Bhadar basin. Hence, data were requested to Dr Yogita Dashora from the study of Dashora et al. (2017).

This study focused on the estimation groundwater recharge from check dams in Rajasthan. Four different check dams were analysed in the Dharta watershed for the years 2014 and 2015. Measurements involved daily rainfall and water level in the structure for all the monsoon season and the period in which water remained in the check dams. Water level measurements were taken by farmers from a gauge board painted on the upstream side of the structures.

Based on the storage capacity, Badgaon check dam was chosen to perform model validation (average storage capacity 42 000m^3). Before the 2015 monsoon season, the surface of the check dam basin was manually scraped to remove the accumulated silt. The authors reported that the desilting did not have a significant effect on the volume of water storage of the check dam basin. However, average infiltration rates increased by 1.55 times.

Dr Dashora kindly provided data of daily rainfall, evaporation, and water level in Badgaon check dam. Runoff coefficients were also provided: 0.204 and 0.02 for years 2014 and 2015 respectively (2015 was a dry year and did not produce significant runoff). A simulation with the geometry of the Badgaon check dam is run for the years 2014 and 2015. The desilting is taken into account in the model by increasing hydraulic conductivity of 1.55 times for the year 2015. Table 5 below shows the input parameter of the simulation run for the model validation.

Table 5: Simulation input parameter for Badgaon check dam

Width [m]	25
Height [m]	1.7
Stream gradient [°]	0.05
Storage capacity [m^3]	42 000
Catchment area [km^2]	3.38
Hydraulic conductivity [m/day]*	0.1

*for 2014. For 2015, K=0.155m/day

Chapter 5: Results and discussion

5.1 FIeld visit

As described in Chapter 4, field visits took place between the 14th and 16th of May 2019. Four sites were visited, and a total number of 14 check dams was assessed. Pictures of the area can be found in Appendix C of this work.

Overall, the basin is highly developed in terms of MAR. A large number of check dams could be noticed in every stream encountered during the drive. From the field assessment, the width of the check dams ranges between 15 and 50m, height between 1 and 2m. Years of construction are variable as well as the parties involved in the constructions:

- Check dams in Kamlapur were constructed by the government in the early 2000s;
- Check dams in Vrinagar were constructed in 2001 through local aid and support from the BAIF Development and Research Foundation;
- Check dams in Umrali were funded with mixed financed schemes (60% funded by the government, 40% funded by local farmers) in different years (2002, 2009 and 2014);
- Patel (2002) reported that the check dam in Arni was constructed in 1996 by the government; however, all the structures found in the village are not in function anymore (Figure 58 Appendix C).

These findings match what was found in the examined literature. In fact, both studies from Verma and Krishnan (2011) and Shah (2014) reported that multiple NGOs were involved in the construction of check dams as well as different state's department since the 1980s. In the following sections, findings regarding different aspects of the area are summarized.

5.1.1 Conditions and maintenance

The check dams are highly variable in terms of maintenance. Desilting is occurring sporadically, and in some locations, material is removed for construction purposes. In others, silt is taken by farmers and mixed with cow manure as soil for the fields. Many check dams are either broken or fully covered with silt. In Kamlapur, locals intentionally broke the structure because of the risks to the houses in the proximity of the stream (flooding and mosquitoes) (Appendix C, Figure 59). Another check dam in Kamlapur had no storage because it was covered entirely with silt (Appendix C, Figure 60). Local farmers reported that no maintenance occurred in this check dam. In Vrinagar, a considerable amount of both native and deposited soil material (more than 5 m depth) was removed for construction purposes (Appendix C, Figure 62). In Umrali in contrast, farmers owning dug wells in the proximity of one structure financed its first desilting in 2018 (Appendix C, Figure 61). In Arni site, the specific check dam analysed by Patel (2002) seemed to have been structurally damaged over the years due to lack of maintenance. From the other two structures previously identified from satellite images, one was completely silted (Appendix C, Figure 64) and one was not functioning (the river bed had expanded since construction, and the width of the dam does not cover the entire cross-section Appendix C, Figure 58).

5.1.2 Aquifer characteristics

Farmers reported that in summer the dug wells completely dry out, while in wet years during the monsoon season, the aquifer gets almost saturated, with groundwater levels reaching less than 1m BGL. This phenomenon can be explained by the small storage capacity of the upper aquifer (Kumar and Perry, 2018; Verma and Krishnan, 2011). In dry years, it can happen that wells do not get substantially recharged.

Borewells reaching the lower aquifer were confirmed to be 180 to 500m deep (CGWB, 2015). In the area close to Viranagar, few borewells have been drilled up to 150m, but groundwater could not be substantially abstracted. Farmers of different locations reported low groundwater quality from the deeper aquifer, with high salinity levels that sometimes prevents its use for irrigation. The Central Ground Water Board reported that in some part of the districts of the Bhadar basin, groundwater is brackish (EC values between 800 and 6 000 µS/cm) and some areas are affected by high fluoride, up to 4.70 ppm (permissible limit for drinking water supply is 1.5ppm) (CGWB, 2015).

Also in terms of soil cover, the sites are variable. Kamlapur is covered with black soil with many stones (Appendix C, Figure 65). Vrinagar is covered by layers of compacted clay that in some areas assumes a columnar structure (Appendix C, Figure 63). In one of Umrali's check dams, the river bed is hard-rock with no soil cover (Appendix C, Figure 66). Infiltration occurs through fractures in the rocks, and there might be some lower seepage from the structure (water leaking downstream from the bottom of the structure, see Figure 67 in Appendix C).

5.1.3 Hydrology of check dams

As a common practice, water is never directly abstracted from the check dams. In all sites it was reported that in case the check dam has reasonable storage, it stays full throughout all the rainy season. Depending on the rainfall spells, it gets fully recharged multiple times in a year. The period in which the structures empty is dependent on the location and the check dam dimensions. Kamlapur 3 check dam gets dry within 15-20 days from the last rainfall. Umrali 2 gets dry in 1 to 1.5 months after last rainfall, while Umrali 3 (being smaller) gets dry one month earlier. Farmers have reported that the wells influenced by the structures are only the ones in close proximity. However, no radius of influence could specifically be quantified from the information gathered during the field visits.

5.1.4 Wells

Generally, every farmer has at least a dug well and a borewell tapping the deeper confined aquifer. Dug wells analysed have an average diameter of 3,5m and their depth varies between 10 and 30m. Depending on the season and the amount of water in the check dam, if water gets abstracted from the wells, the recovery time can vary between few hours to some days, depending on the local aquifer transmissivity.

One important finding is that as common practice, water is often transferred from the borewells to the dug wells when the last ones get dry. During the visit of Umrali, the artificial refilling of a dug well was witnessed (Appendix C, Figure 68). Dug wells are used in this case as small reservoirs for short irrigations or drinking source for the cattle. All farmers interviewed reported that dug wells have water until the nearby check dam is full. This suggests a hydraulic connection between the two structures. Without the refill from the deeper borewells, dug wells get dry or retain small amounts of ponding water during summer.

Moreover, in Upleta site one dug well was found directly on the river bed. The well has a small hole on the bottom, which supposedly lets water in directly from the water stored by the check dam (Appendix C, Figure 69 and Figure 70). In Arni one dug well was found entirely full of water (level higher than the ground) and with some biological activity (small fishes, Figure 71 in Appendix C). Locals reported that water is monsoon water and ponds in the well without seeping through to the aquifer. As a result, water levels measurements performed from dug wells are not completely representative of the actual water table conditions in the area.

5.1.5 Agriculture and irrigation

The farmers interviewed own between 3 to 12 hectares of land. These values are higher than the national statistics of India, where the average farmland is 1.08 ha in 2015-2016 (GOI, 2018). Farmers in Saurashtra own large crop areas. However, their main income comes from cattle by selling milk.

In accordance with the literature, the main crops are cotton, groundnut and wheat. Cotton is sown in June and is harvested 4 to 8 months later, depending on the crop variety. Groundnut lasts around four months. In Kharif season, generally farmers divide the cropping area between cotton and groundnut simultaneously in order to increase income security. The distribution of the two crops varies according to the market and water availability. This is because cotton is more water demanding then groundnut, as already explained in Section 3.4. If the year has been good in terms of rainfall, farmers grow wheat during winter times. If the year has been particularly dry, they leave the land fallow or they grow other minor crops (like cumin, bajra, castor and fodder crops). Table 6 below summarises the typical cropping calendar.

Table 6: Cropping calendar

June	July	August	September	October	November	December	January	February	March	April	May
Monsoon season											
	Cotton										
	Groundnut										
						Wheat					

Most of the irrigation is done through flooding. Some farmers use sprinkler irrigation in the early stage of the crops. It is reported a small percentage of drip irrigation. Cotton requires between 10 to 15 irrigations depending on the type. Groundnut does not require irrigation in wet years, otherwise it might require one to three irrigation spells. Wheat is highly water demanding, with 10 to 12 irrigations during the growing season. Typical abstraction values for an irrigation event range between 100 and 200m^3/day for a cropping area of 6ha.

Based on this information, a typical irrigation calendar is developed as input for the conceptual model. Table 7 below displays the number of irrigations considered for each crop during the growth. It is assumed that during Kharif the area is equally divided between cotton and groundnut. Assuming 100m^3 abstracted for each irrigation events, groundnut and cotton will require 50m^3 each.

Table 7: Number of irrigations per crop in a year

Crop	Wet year	Normal year	Dry year
Cotton*	10	14	18
Groundnut*	No irrigation	2	5

Wheat	12	12	12

*Abstraction volumes for cotton and groundnut 50m^3/irrigation event, for wheat 100m^3

5.2 Conceptual model results

The data collected during the field are not designed to be sufficient to calibrate the model for each specific site. In Section 5.2.1, the behaviour of the model for a generic check dam is studied. The simulations are run in the R environment. In Section 5.2.2, a sensitivity analysis is performed to assess the effect of each parameter of the model. Results for model validation are illustrated in Section 5.2.3.

5.2.1 Simulations

Based on the check dam assessment from the field visit, it is considered an average check dam of 30m width and 2m height, located on a stream with a gradient of 0.1° and a river bank slope of 20°. The resulting storage volume is 34 400m^3. This value falls within the storage volumes of the check dams reported in different studies in similar areas (Dashora et al., 2017; Glendenning and Vervoort, 2010; Patel, 2002). The catchment area is assumed to be 15km^2, as an average area from the sites selected from the field (See Table 2 of Section 4.1.1). Other input parameters are displayed in Appendix E, Table 13. As assessed from the field visit, direct withdrawals from check dams are not common. Hence, general losses G from the water balance (Equation [1]) can be neglected, as no other relevant outputs could be identified.

A simulation without abstraction is first run for 11 years (2000-2010) for the three Bouwer conditions. The stored water volumes are shown in Figure 38 below and the overall results are summarised in

Table 8 below.

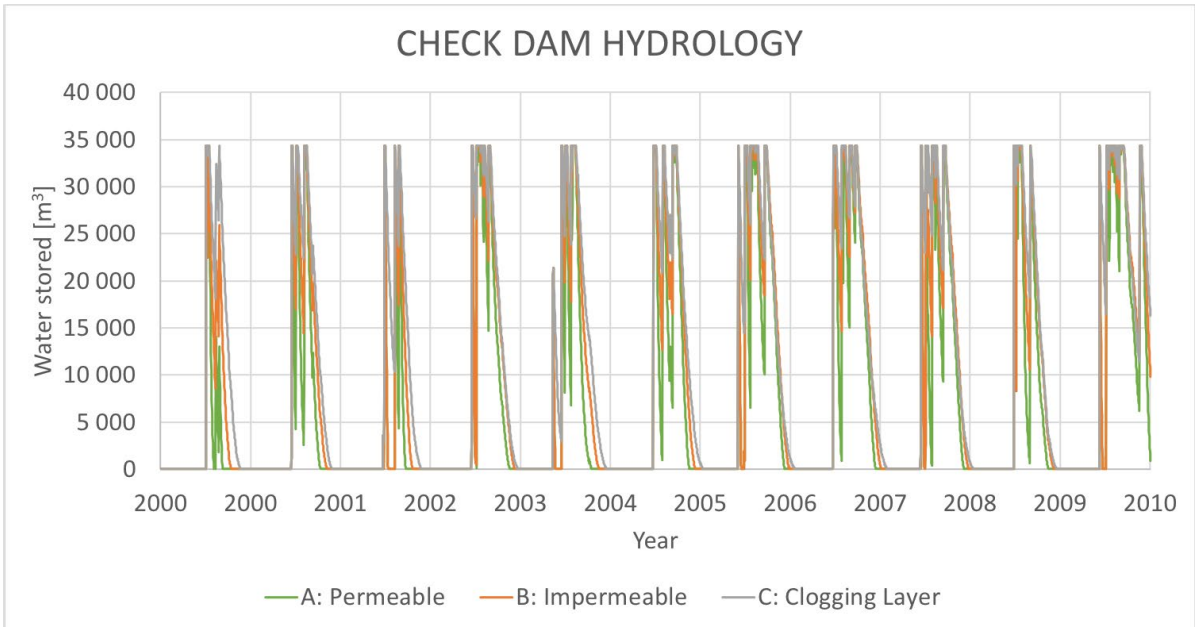

Figure 38: Water volume stored in the check dam, 2000-2010

Table 8: Average values for simulation without groundwater abstraction (years 2000-2010)

	Condition A Permeable layer	**Condition B Impermeable layer**	**Condition C Clogging layer**
Infiltration rates [mm/day]	41.1	23.1	7.8
Infiltrated volume [m^3]	160 000	108 000	39 000
Infiltrated volume [% of Runoff]	2.9	2.0	1.1
Evaporated volume [m^3]	26 000	33 000	60 000
Average annual days of storage	142	164	195

From the storage volumes shown in Figure 38, it can be seen that the check dam gets periodically full and empty every year, as a result of the monsoon season. Water storage varies depending on the Bouwer condition considered, and the difference between the three varies depending on the year. A detailed analysis of water volumes is carried out in Section 0 below.

From the results displayed in

Table 8, the influence of the hydrogeological setting is evident. It can be seen that in sites over a permeable layer (condition A), water infiltrates more quickly compared to sites on an impermeable bedrock. This can be explained by the fact that water stacks more easily over a layer with low permeability. In this case, the water mound forms an obstruction that prevents water to infiltrate. In case of a permeable layer instead, water seeps into the deeper hard-rock, and the flow from the check dam is faster.

Values of infiltration rates match with the ones observed by Patel (2002), which reported an average infiltration rate from Arni check dam of 30.05 mm/day between 1996 and 1999. Infiltration rates are also compatible with the study done by Glendenning and Vervoort (2010) in Rajasthan, where infiltration rates ranged between 12.3 and 55.6 mm/day.

Regarding the presence of a clogging layer, a hydraulic impendence of 200 days is considered. This value corresponds to a 20cm thick layer of silt of hydraulic conductivity of 0.001m/day. From the results, it is demonstrated that the presence of this layer is a great limit for infiltration. In fact, the clogging layer reduces infiltration by almost 70% if compared to condition A and by 55% for condition B. The effect of desilting has also been studied by Patel (2002), where he compared normal and desilted structures in Saurashtra. He found that for percolation tanks, infiltration rates differ of 61% in normal and desilted structures. This value supports the results from the simulation of condition C with clogging layer. However, it is important to note that the amount of clogging depends on the thickness and the hydraulic conductivity of the silt layer. The influence of this parameter is further discussed in the sensitivity analysis in Section 5.2.2.5.

Looking at the infiltrated volumes, it can be seen that the average proportion of infiltration compared to runoff is below 3%. In 2001, condition A records the maximum infiltration with 6.6% of runoff water infiltrated (see Table 15 in Appendix E). This suggests that small-size check dams have a low impact in capturing surface runoff. However, it is presumable that many structures in series would have a considerable effect on river flow.

In fact, the catchment area considered is the one enclosed by the check dam location without considering other structures upstream. This procedure is chosen because the objective of the study is to assess the effects of a single check dam in all the enclosed catchment. The combined effect of

multiple check dam in series should be analysed in the catchment-scale part of this project. As discussed previously, the Bhadar basin has a high-density implementation of MAR. Hence, the effective catchment area should take the effective check dam density into account. For this reason, the influence of the catchment area is analysed further in Section 5.2.2.3.

The values of relative infiltration are particularly low, especially if compared to results by Dashora et al. (2017). The comparison is made with one of the check dams assessed in Rajasthan, which has a similar geometry with the simulated one (storage capacity of 42 000m^3). They found that recharge amounted as 32 and 27% of runoff in 2014 and 2015 respectively.

However, it is important to consider that the relative value of infiltrated water depends on check dam storage capacity, catchment characteristics (like rainfall, slope, land use and so forth), but also on the catchment area. In fact, in the study by Dashora et al. the check dam catchment area is only 3.38km^2, while the one simulated in the present study is 15km^2. This means that the runoff flowing in their check dam is considerably lower, as annual rainfall are similar to the ones typical for the Bhadar basin (505 and 614mm for 2014 and 2015 respectively). If comparing instead the absolute volumes of infiltration, the simulated ones are in accordance with the measurements from Dashora et al., who recorded in 2014 and 2015 annual infiltration volumes of 113 000m^3 and 56 000m^3 respectively.

With regards to the days of storage, there is concurrence with both literature and field visit findings. The days of storage in the check dams assessed by Glendenning and Vervoort (2010) range between 138 and 382 days. Dashora et al. (2017) reported that four different check dams emptied between middle August and middle January. The dates in which the simulated check dam gets empty (Appendix E, Table 14) vary according to the rainfall and the Bouwer condition, but overall they match with what reported by local farmers during the field visit (late September until early January).

5.2.1.1 Water storage

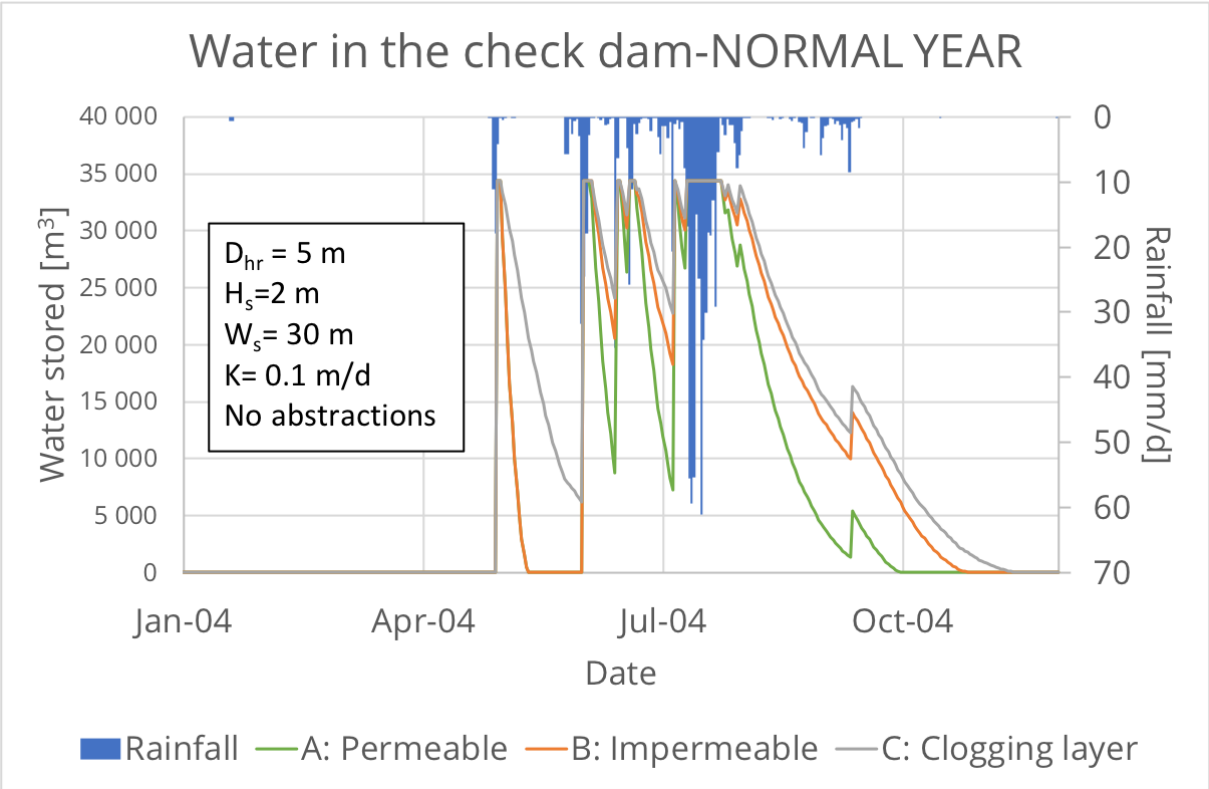

Figure 39: Water volume stored in the check dam – *normal* year (2004)

Figure 39 above shows the water storage in the check dam for the three Bouwer conditions in 2004, which is taken as a representative year (*normal* year with annual precipitation of 784 mm). The graph shows that as soon as runoff starts in middle May, the structure gets at its full capacity. The amount of runoff depends on rainfall intensity as well as the antecedent moisture conditions (AMC), as discussed in Section 4.2.5. Hence, small rainfall events during dry periods are not sufficient to produce surface runoff, which is the main input in the check dam's water balance.

When the structure gets full, infiltration and evaporation start, and the volumes decrease. In condition A and B, the structure gets empty in 13 days, for getting at full capacity again in middle June. It can be seen that the structure gets full multiple times in the year based on rainfall spells.

Condition A with a permeable layer underneath the weathered zone is the one in which the volume decreases the fastest, and the structure gets entirely empty after 173 days (on 31st of October). Condition B and C follow with 197 and 217 days of storage respectively. This is because, as already explained, the permeable layer allows water to infiltrate more compared to a site over an impermeable hard-rock, where water has to flow horizontally.

The case in which a clogging layer covers the storage basin is the one that takes longest to empty. Because of the silt cover, infiltration occurs at the lowest rate. This phenomenon is further illustrated in Section 5.2.1.2. Volumes in case of *dry* and *wet* years can be found in Appendix E (Figure 72 and Figure 74).

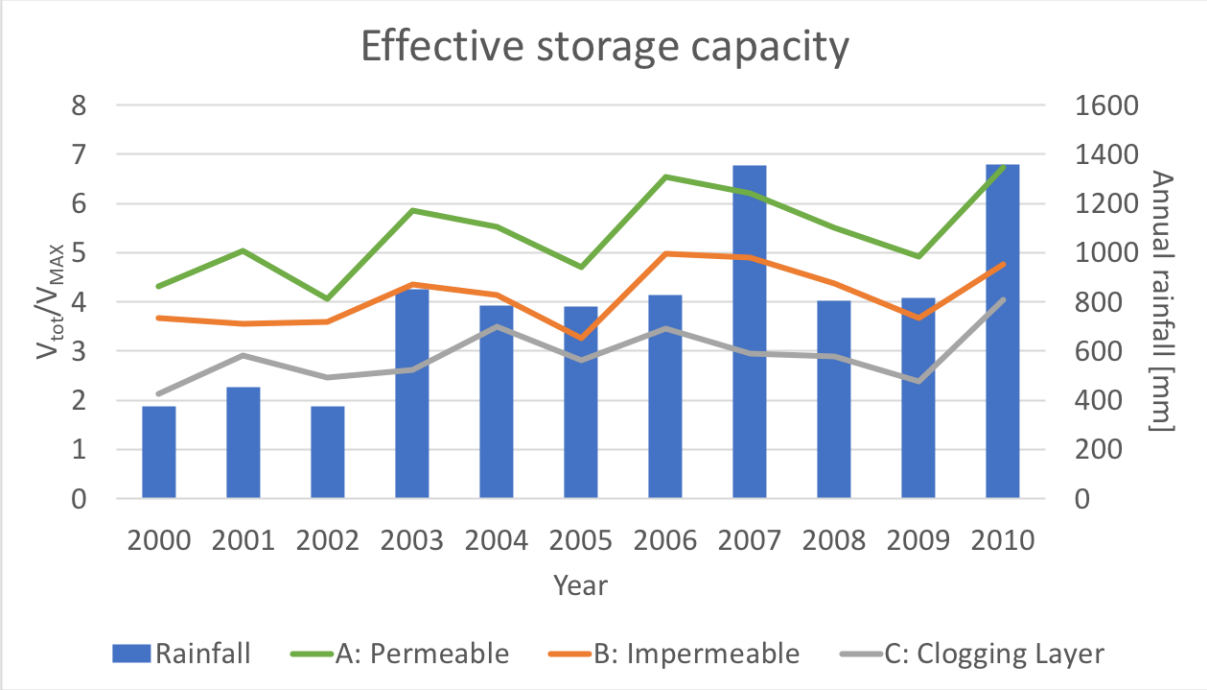

Figure 40: Effective storage capacity[15] of the check dam

Figure 40 above shows the effective capacity of the check dam, together with annual rainfall throughout the simulation period. It is calculated dividing the total volume stored V_{tot} in a year ($V_{tot} = Q + P - Out$), by check dam storage capacity V_{MAX}. This value represents the number of fillings in a year and the effective amount of water stored in the structure.

It can be seen that behaviours of condition A and B fluctuate in similar ways, being condition A generally higher of 1 unit. The case of a clogging layer covering the basin shows a lower and more constant value of this parameter. During the 11 years of simulation, the average effective storage capacity is 4.8, 4.1 and 2.8 for condition A, B and C respectively. These values are in accordance with what found in literature. In fact, results by Kamboj et al. (2011) showed that in Bhadar basin, check dams are able to store more than five times their storage capacity.

The fact that condition A has overall the highest storage efficiency is related to the higher infiltration rate. In fact, check dam in condition A gets empty faster, and this gives a chance to more water to be stored. On the contrary, water in condition C infiltrates slowly, and when surface runoff water enters the structure, more outflow is produced.

From the graph, some correlation between annual precipitation and effective storage capacity can be seen. In fact, for years with high rainfall, the amount of water stored is higher. Table 9 shows the correlation matrix between the effective capacity for the three Bouwer conditions, annual rainfall and number of rainy days in the year. The elements of the matrix are the correlation coefficients between the variables. These coefficients are an indication of the statistical relationship between two variables: the higher the coefficient, the stronger the correlation (Schober et al., 2018). A strong correlation (>0.7) can be seen between effective storage capacity of condition A and B with annual

[15] Effective storage capacity calculated as stored input $V_{tot} = R + P - Out$ divided by the storage capacity V_{MAX}.

rainfall. Also, the number of rainy days in the year is a relevant parameter for the effective capacity, as there is a strong correlation for condition A and C.

This means that the amount of water stored in the check dam depends on the amount of rainfall received by the catchment in a year, but also on the rainfall distribution in the year. In fact, a more distributed precipitation will increase the effective storage: if an intense precipitation event is concentrated in a short period, the effect on the recharge does not increase as the check dam has reached already its full capacity and overflow is produced.

Table 9: Correlation matrix: effective storage capacity with annual rainfall and rainy days

Corr. Coeff.	Rainfall	V_{tot}/V_{MAX} A	V_{tot}/V_{MAX} B	V_{tot}/V_{MAX} C	Days of rain
Rainfall	1				
V_{tot}/V_{MAX} A	0.819	1			
V_{tot}/V_{MAX} B	0.721	0.906	1		
V_{tot}/V_{MAX} C	0.623	0.788	0.617	1	
Days of rain	0.513	0.750	0.605	0.851	1

5.2.1.2 Infiltration

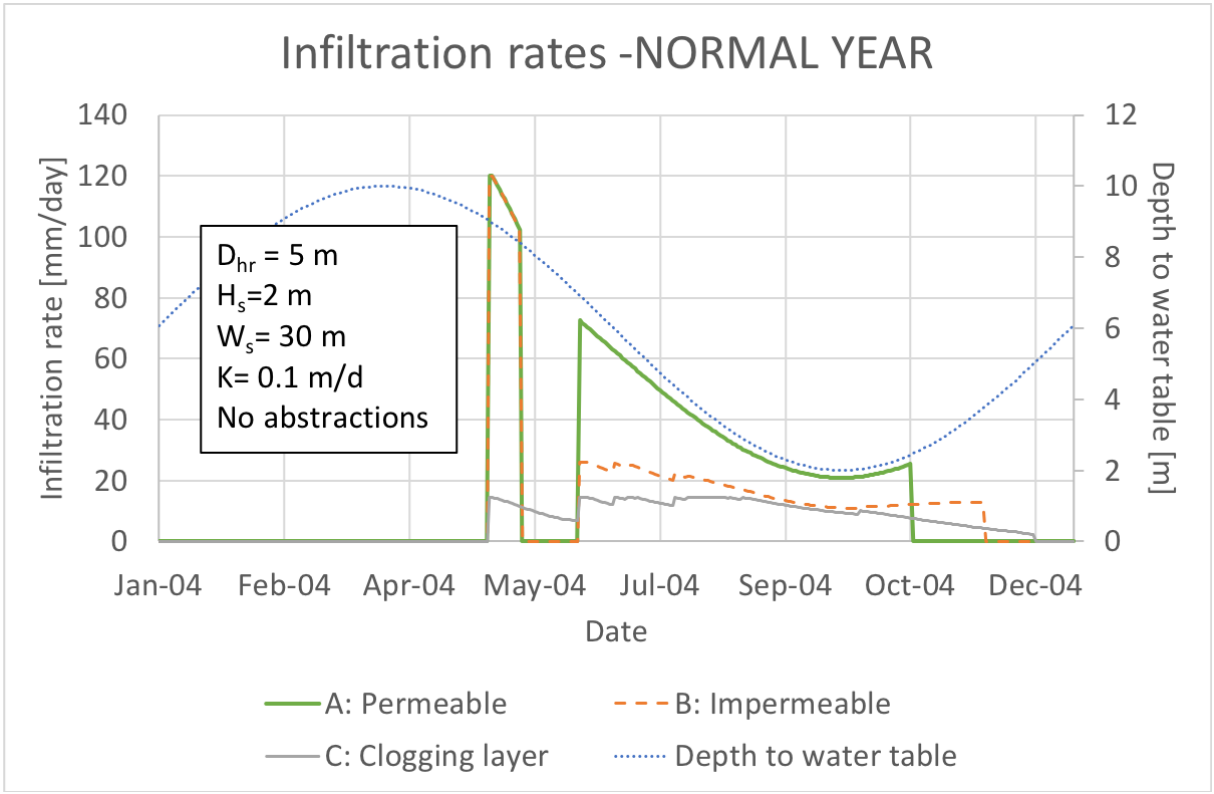

Figure 41: Infiltration rates from check dam – *normal* year (2004)

In Figure 41 shows the infiltration rates for the three Bouwer conditions for the year 2004 (*normal* year). The graph shows condition A and B having an initial infiltration rate of almost 120mm/day in the first phase of filling in the second half of May. Because of this high infiltration rates, the structure gets empty in 13 days for these two settings.

These high infiltration rates are due to the fact that in that period of the year, the water table is below the interface between the weathered zone and the permeable layer. This is visible from the water table function represented in Figure 41. It can be seen that until June, depth to the water table is higher than 7m, which is the depth of the interface with the permeable layer measured from the surface level. In this case, infiltrated water and water table are hydraulically disconnected, and both conditions A and B falls into the sub-case of condition A'. In this phase, infiltration is entirely controlled by gravity and is dependent on the geometry of the check dam as well as the water level in the structure (see Equation [26]). In this case, the ratio between infiltration rate and hydraulic conductivity (I/K) is slightly higher than 1. This is in accordance with what was shown by Bouwer (2002), who studied the model by Dillon and Liggett (1983) regarding the transition between disconnected water table conditions and hydraulic connections for infiltration (see Figure 24 in Chapter 4).

In the second phase of the filling, a difference in infiltration rate between permeable and impermeable layers can be seen. Infiltration rates are much lower than the initial phase (less than 60mm/day for condition A and less than 30mm/day for condition B). It can be seen that infiltration condition A decreases until middle September, where it reaches the minimum of 20mm/day. After this date, infiltration increases again until the structure gets empty.

In contrast with what happened in the first filling stage, in this period the water table is hydraulically connected with the check dam. In fact, the infiltration rate of condition A resembles the water table fluctuation. This can be explained by the fact that infiltration is modelled with a linear function with water table (see Equation [27]). For condition B, similar considerations can be made. As already explained, infiltration rate is generally lower in case of an impermeable layer. In this case, infiltration depends on water table level with a non-linear relationship (Equations [28] and [30]).

If the check dam is covered with a clogging layer, infiltration rate stays below 20mm/day and stays roughly constant until it gets empty (14th December). This Bouwer condition considers the hydraulic disconnection between the water mound and the water table. As a result, infiltration rate does not depend on the fluctuation of the water table, as it is for condition A and B. This mechanism of infiltration is only dependent on the water level in the structure (Equation [32]). This explains the decrease in infiltration rate in the last stage of the storage: when the water level in the check dam decreases, the hydraulic pressure reduces, and infiltration becomes slower (October-December in Figure 41).

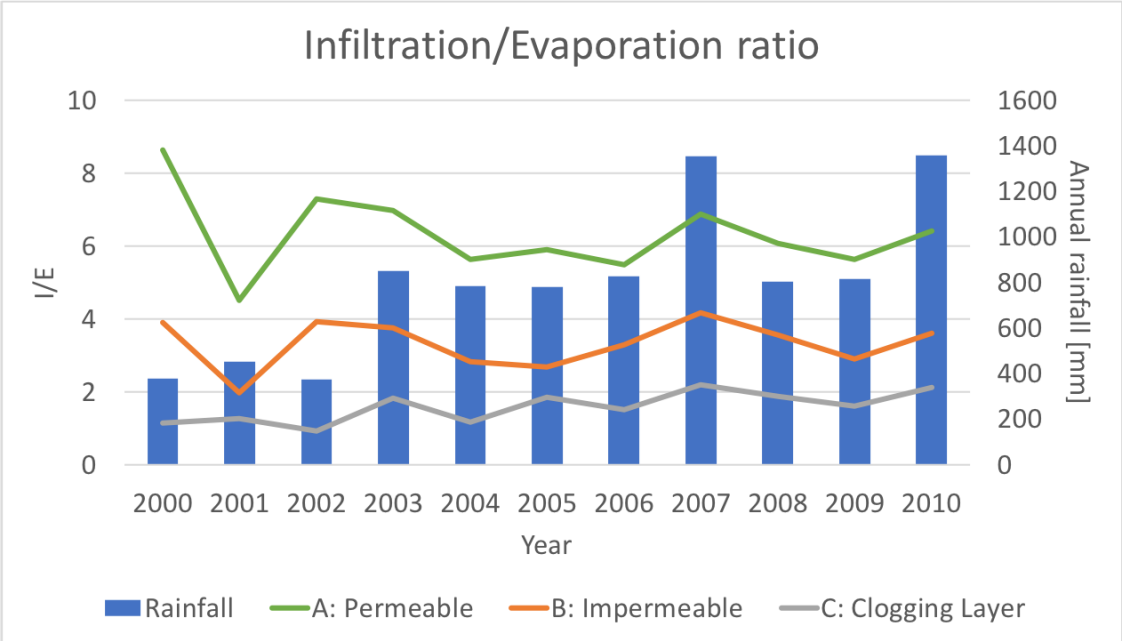

Figure 42: Infiltration-Evaporation ratio

Figure 42 shows the ratio between infiltration and evaporation occurring in the check dam. For dams located in semi-arid areas, losses by evaporation can be a severe limitation in their ability to store and infiltrate water. This value is therefore one of the indicators used to assess the efficiency of the structure (Neumann et al., 2004).

Depending on the year, this ratio ranges between 3.9 and 5.9 for a permeable layer (condition A); between 7.3 and 3.5 for condition B and between 0.9 and 2.2 for condition C. Average values are 5.3, 3.4 and 1.6, which means that 14%, 24% and 40% of the total stored volume V_{tot} is lost by evaporation for A, B and C respectively. These outcomes are in line with the results previously explained: as condition A is the one that infiltrates the most, it is also the more efficient in terms of losses by evaporation. Condition C instead, is the one that implies more loss due to evaporation, which confirms the deterioration that a clogging layer brings to the performances of check dams.

These values are similar to the ones found in the study of Patel (2002) in the Bhadar basin. He estimated infiltration/evaporation ratios occurring in percolation tanks and check dams to range between 1.83 and 8.94 depending on the structure, the maintenance and the hydrogeology of the site. These numbers are also verified by comparing the simulation results with the study done by Dashora et al. (2017). They found a ratio between infiltration and evaporation from four check dams to be comprised between 3.6 and 5.9.

5.2.1.3 Influence of groundwater abstractions

A simulation is run to model the influence of induced recharge from abstractions from nearby wells. It is considered a well located 100m from the check dam from which water is abstracted for irrigation purposes. It is assumed a rate of 100m^3/day for irrigating the total cropping area. Water budgets for this new simulation can be found in Appendix E. Table 10 below summarises the average values of results from this simulation, together with the increase/decrease with respect to the simulation without abstractions. Figure 43 and Figure 44 below show the resulting volumes and infiltration rate for the year 2004 (already used as reference year in Figure 39 and Figure 41 above).

During the 11 years of simulation, the average increase of infiltrated volume is of 7.4% (more than 12 000m^3 per year) for condition A, and of 20.6% (more than 21 000m^3 per year) for condition B. These values confirm the well-known effect of induced recharge by abstraction wells nearby check dams (Moore and Jenkins, 1966).

Table 10: Average values for simulation with abstractions (years 2000-2010)*

	Condition A Permeable layer	**Condition B Impermeable layer**
Infiltration rates [mm/day]	47.9 (+6.8)	31.8 (+8.7)
Infiltrated volume [m^3]	172 000 (+12 000)	129 000 (+21 000)
Infiltrated volume [% of Runoff]	3.1 (+0.2)	2.4 (+0.4)
Evaporated volume [m^3]	23 000 (-3 000)	27 500 (-5 500)
Average annual days of storage	133 (-10)	147 (-18)

*Numbers in brackets indicate the net difference between the condition with abstractions and the one without abstractions (+ increase, - decrease)

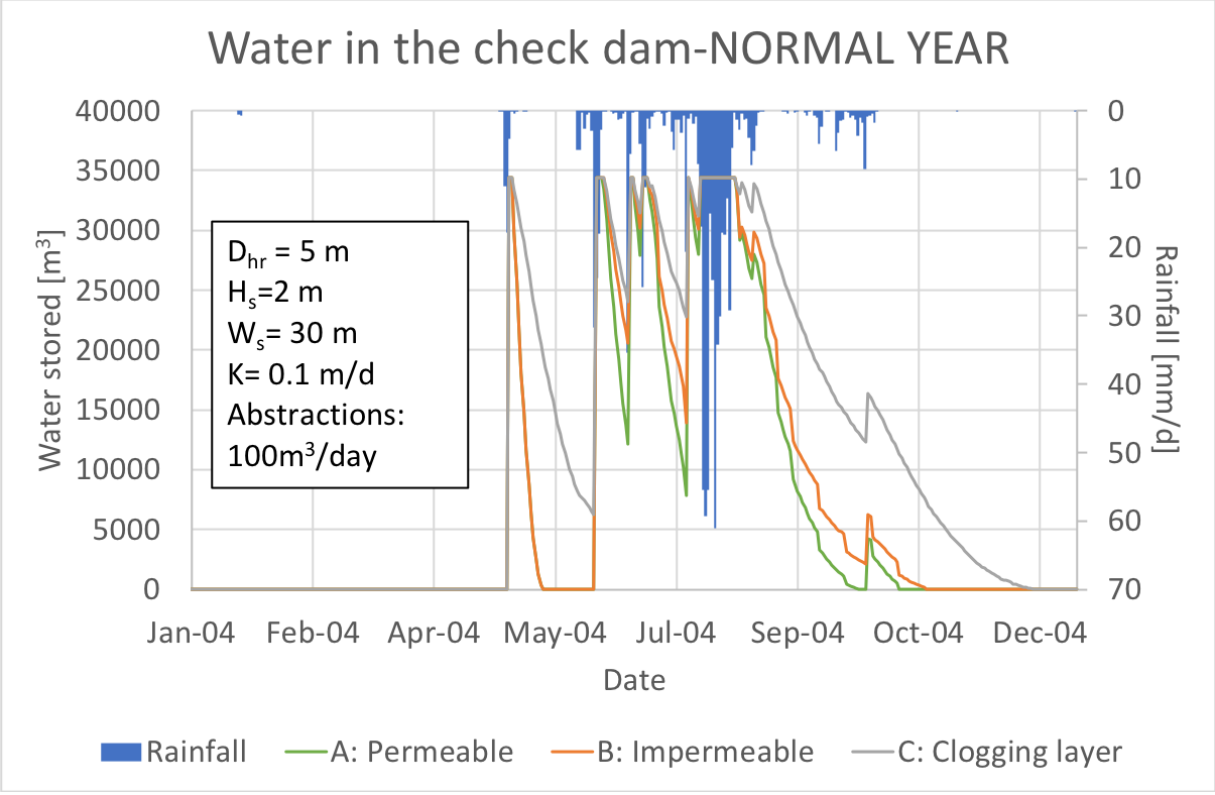

Figure 43: Induced recharge: water stored in the structure – *normal* year (2004)

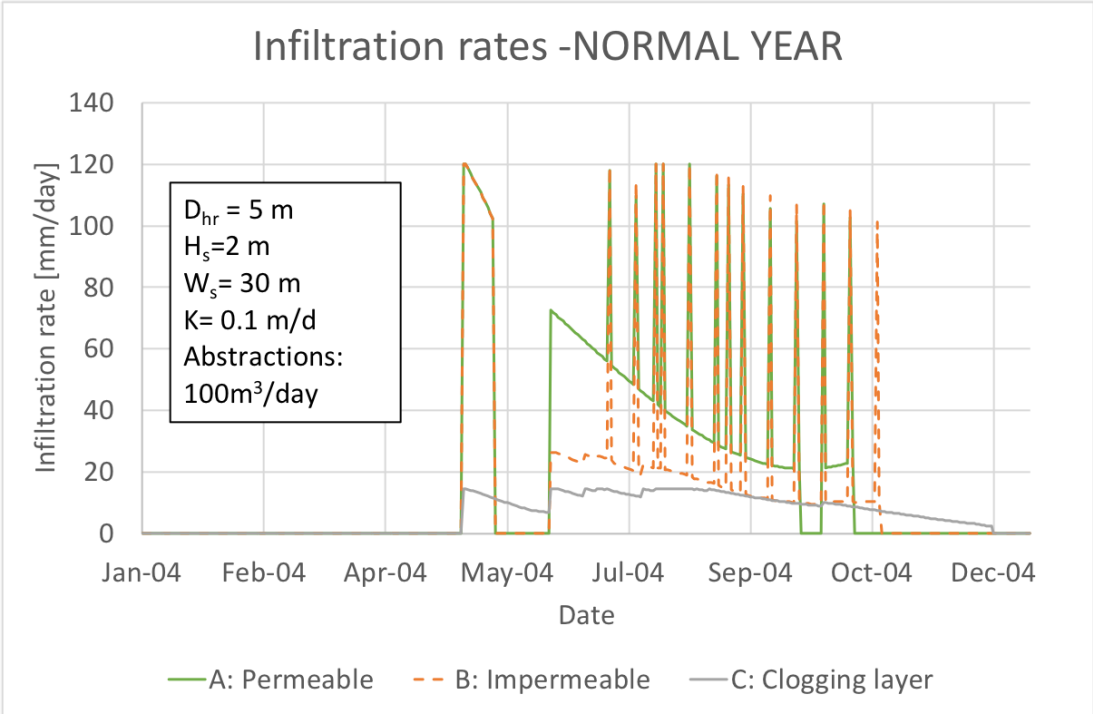

Figure 44: Induced recharge: infiltration rates – *normal* year (2004)

From Table 10 above, the results from the simulation with groundwater abstractions and the differences between the case without abstractions can be seen. Overall, infiltration increases and evaporation decreases.

This difference is due to the induced recharge by abstractions. In fact, the drawdown caused by the pumping decreases the water table at the structure site (see Thiem Equation [33]). As a result, the drop in the water table increases the infiltration rate for the day in which abstractions occurred.

Comparing the water stored in the check dam in 2004 with the simulation without abstractions (Figure 39), no significant difference can be seen. In fact, some additional oscillations are visible, but the overall behaviour is similar. However, the structure gets empty 12 and 26 days before in condition A and B respectively (161 and 171 days of storage).

This can be seen in Figure 44, where some spikes in infiltration rate appear bringing daily infiltration rate to more than 100mm/day for both conditions A and B. A critical limitation of this approach is to consider the effect of the drawdown on the check dam only for the day of abstraction. As a result, the water table decreases for only one day (drawdown at the structure of about 13m with the considered parameters), and it is considered to be entirely recovered the day after.

During the field visit, farmers reported recovering period for wells to be between a few hours and some days. If the season is dry, the recovering period can be up to 15 days. However, if the water table is already low (below the hard-rock layer), infiltration will not be affected by the hydraulic gradient but will be gravity driven (condition A'). Consequently, it is reasonable to assume that the recovery period of the drawdown to be in the order of a day.

As already explained, no effect of induced recharge can be seen in condition C, as in this condition the infiltrating water is disconnected with the water table in an un-saturated downward flow.

5.2.2 Sensitivity analysis

In order to understand the influence of the parameters involved in the conceptual model, a sensitivity analysis is carried out. The impact of each parameter is assessed by varying each one from the original set and comparing the model outputs. The ranges within the parameters are varied, derive from the field visit and literature review. The average infiltrated volume over the simulated 11 years is chosen as the key output variable.

5.2.2.1 Height of the structure (H_s)

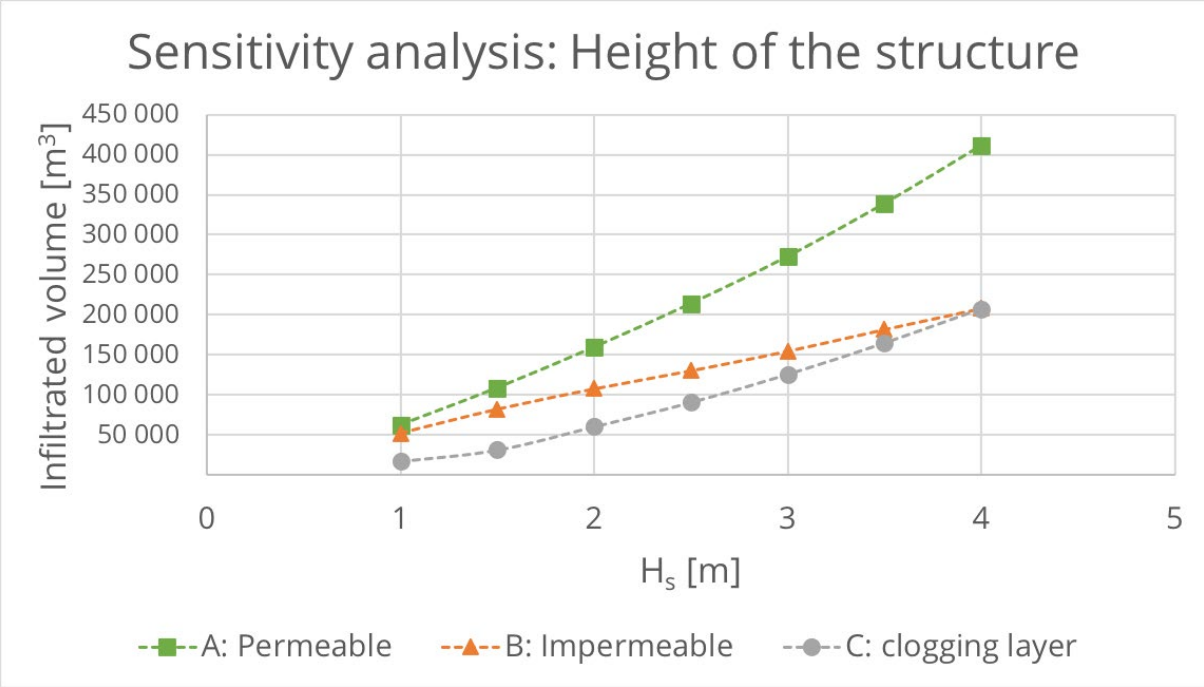

Figure 45: Sensitivity analysis - height of the structure

To analyse the influence of the height of the structure on the check dam performance, simulations are run varying this parameter between 1 and 4m, which is the widest range found in literature (Dashora et al., 2017; Glendenning and Vervoort, 2010; Patel, 2002). Figure 45 shows the results for the three Bouwer conditions.

It can be seen that for all three conditions, the infiltrated volume increases when the height of the check dam increases. This is a consequence of the increased storage capacity V_{MAX}, which follows a quadratic relationship with this parameter (Equation [9]). Condition A with permeable layer is the one that witnesses the highest increase, the increase for condition B is less steep. This is because a permeable layer manages to infiltrate all the additional water resulting from the increase in storage capacity. The water mound resulting from the impermeable layer in condition B, obstruct the water flow and infiltration proceeds at a low rate even with a large amount of storage in the structure.

The average annual infiltration volume also increases in condition C with the increase of height, and in case of 4m structure height, the infiltrated volume is as much as condition B.

5.2.2.2 *Width of the structure (W_s)*

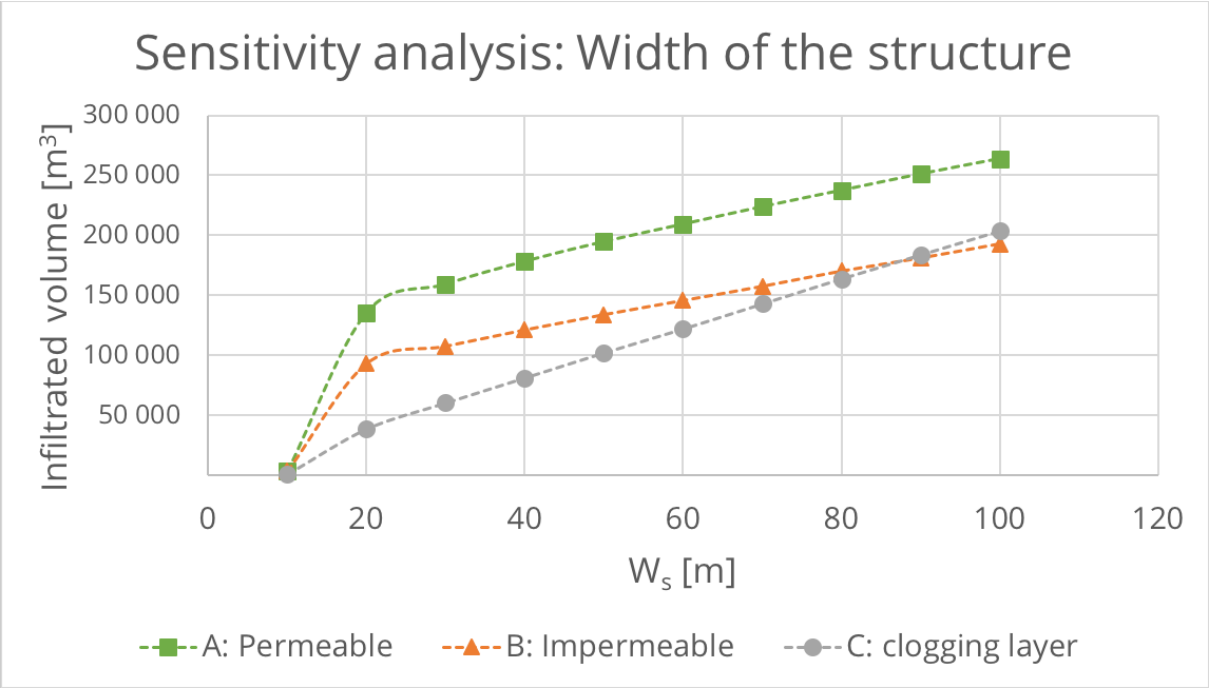

Figure 46: Sensitivity analysis - width of the structure

Regarding the influence of the width of the check dam on average infiltration volumes, similar considerations can be done. The width range used for this analysis is resulting from the check dam assessment from satellite images described in Section 4.1.1.

From Figure 46, it can be seen that infiltration volumes increase with increased width for all the three conditions. If the structure is 10m wide, storage capacity is so low that infiltration volumes are negligible. While increasing the width, a linear relationship can be seen in all three conditions. This is the result of the increased storage capacity, and similar considerations as previously explained for the height of the structure can be made. Note that in this case, the increase is linear and not quadratic because maximum storage volume follows a linear relationship with the width of the structure (Equation [9]).

5.2.2.3 Catchment area (A_{catch})

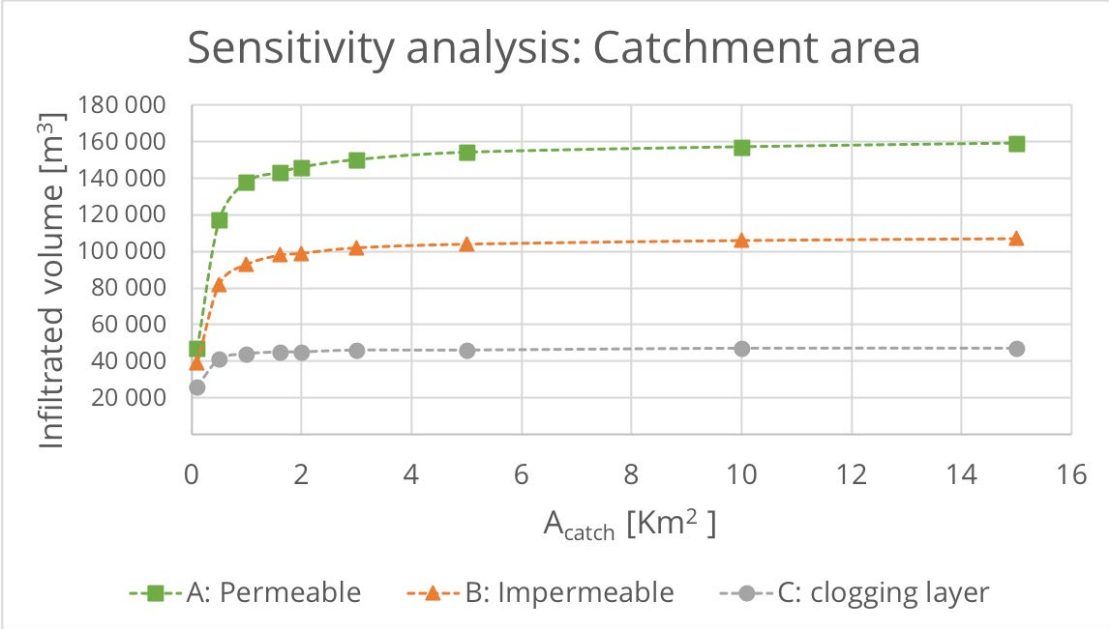

Figure 47: Sensitivity analysis - catchment area

Figure 47 above shows the influence of the catchment area on the infiltration volumes. It can be seen that for areas larger than 2 km^2, the infiltrated volumes for all the Bouwer conditions do not change significantly with an increase in area.

As the catchment area increases, more volume of runoff enters in the check dam. However, if the structure is already at its full capacity, no more water can be stored, and overflow is produced. As a result, no effect is visible in the absolute volumes of infiltration. For areas smaller than 2km^2, infiltration decreases as the effective water stored in the check dam decreases. Note that this threshold value is also associated with the check dam geometry, as it is highly dependent on the storage capacity.

The analysis performed on the check dam hydrology is carried out in order to study the effect of a single check dam in a catchment without any other structures. However, check dam intensity is an important parameter as the effective catchment area can be reduced in the presence of other structures.

For the Bhadar basin, the average density of structures is one check dam every 1.5km^2 (considering the 4385 check dams reported by Kamboj et al. (2011) over an area of 6 596km^2). As a result, the average catchment area considering the effect of other check dams can be reduced to 1.5km^2. This area falls within the region in which infiltration volumes start to decrease because of the less inflow from runoff. This means that if check dams are too close to each other, there might be a negative influence on the infiltration capacity of the structures located downstream.

In case of check dam density of one structure per 1.5km^2, absolute infiltration volumes are 143 000, 98 000 and 45 000m^3 for conditions A, B and C respectively. This values correspond to 19%, 13% and 6% of the incoming runoff, and are closer to the ones found by Dashora et al. (2017).

5.2.2.4 Stream gradient (α)

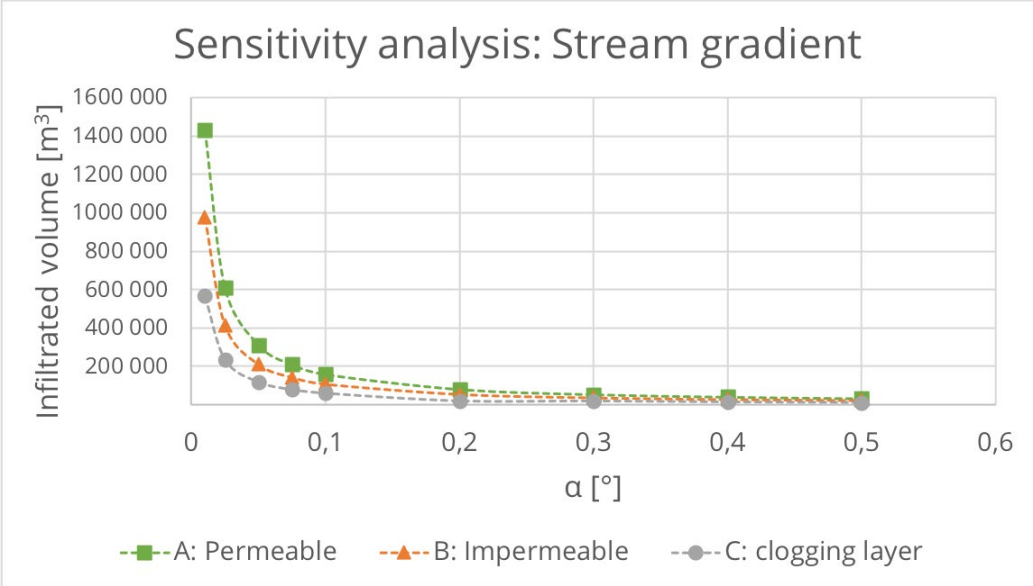

Figure 48: Sensitivity analysis - stream gradient

The impact of the stream gradient α on infiltration volumes is shown in Figure 48. It can be seen that infiltration is highly sensitive to this parameter: a reduction from 0.1° to 0.01° leads to an increase in infiltration of more than nine times for all the conditions. It can also be seen that as stream gradient increases up to 0.5°, infiltrations drop to less than 50 000m^3 for all conditions (average annual infiltration of 33 000m^3, 22 000m^3 and 12 000m^3 for A, B and C respectively).

This high sensitivity is because storage capacity is modelled as inversely proportional to the tangent of the stream gradient (Equation [9]). As a result, infiltration volumes change consistently with small changes of this parameter, especially for low values of α.

The procedure to estimate the geometry of the check dam is one of the most significant limitations of this model. In fact, the stream gradient is difficult to measure on the site, and it might differ from the slope in the topography (Strahler, 1952). Moreover, from the field visit it could be seen that stream beds are highly heterogeneous, and the storage capacity is more related to the micro-topography, especially in sites where a large amount of soil material was removed.

The best way to overcome this limitation would be to measure on the site the area-volume-elevation relationship. This function describes the dependence of the impoundment area with the depth of water in the structure. This curves can be often described as a power function (Sharda et al., 2006). The parameters of these functions can be estimated on the field with the use of specific equipment (dumpy level or theodolite) which was not available for this study.

5.2.2.5 Hydraulic conductivity (K) and impendence (R_a)

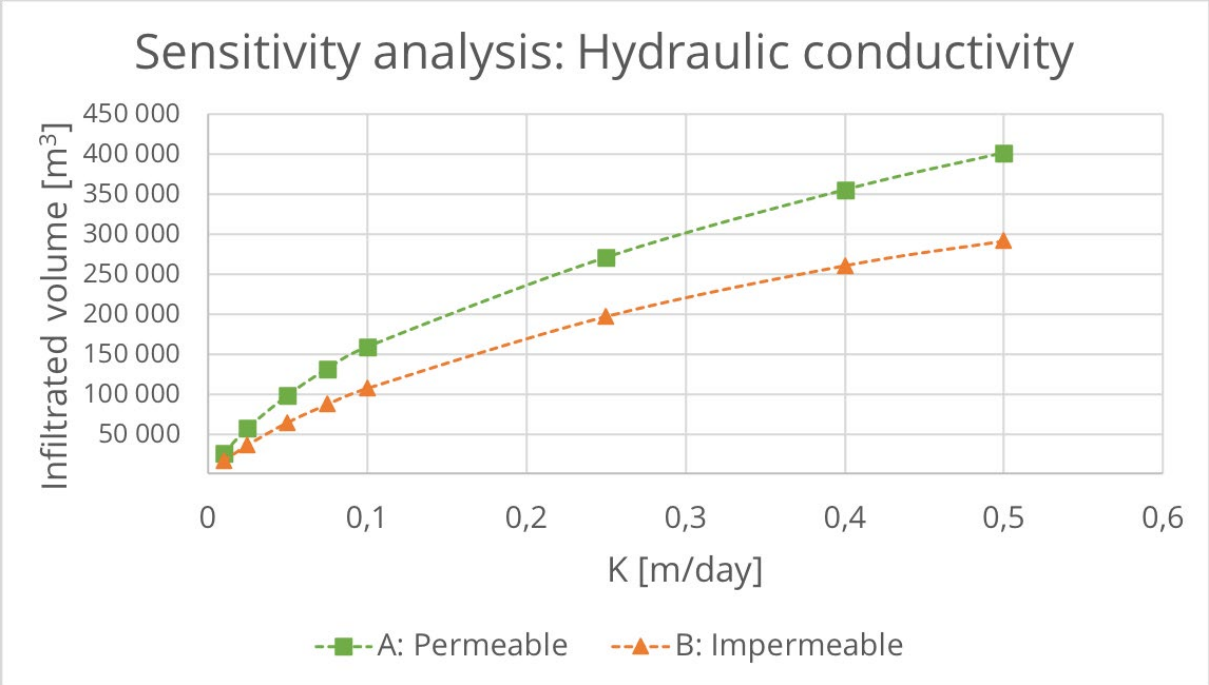

Figure 49: Sensitivity analysis - hydraulic conductivity of the weathered zone

In Figure 49, the influence of the hydraulic conductivity of the weathered zone on the average infiltration volumes can be seen. Only conditions A and B are displayed, as condition C is dependent on the hydraulic impendence of the clogging layer and it is then analysed further in this section.

It can be seen that for both conditions with permeable and impermeable layer, infiltration volumes increase with hydraulic conductivity. By increasing hydraulic conductivity from 0.01 to 0.1m/day, infiltrated volume increases 5.25 times; if increasing K from 0.1 to 0.5, infiltrated volumes increase of 1.5 times. This result could be expected, as hydraulic conductivity resembles the flow velocity in a porous media.

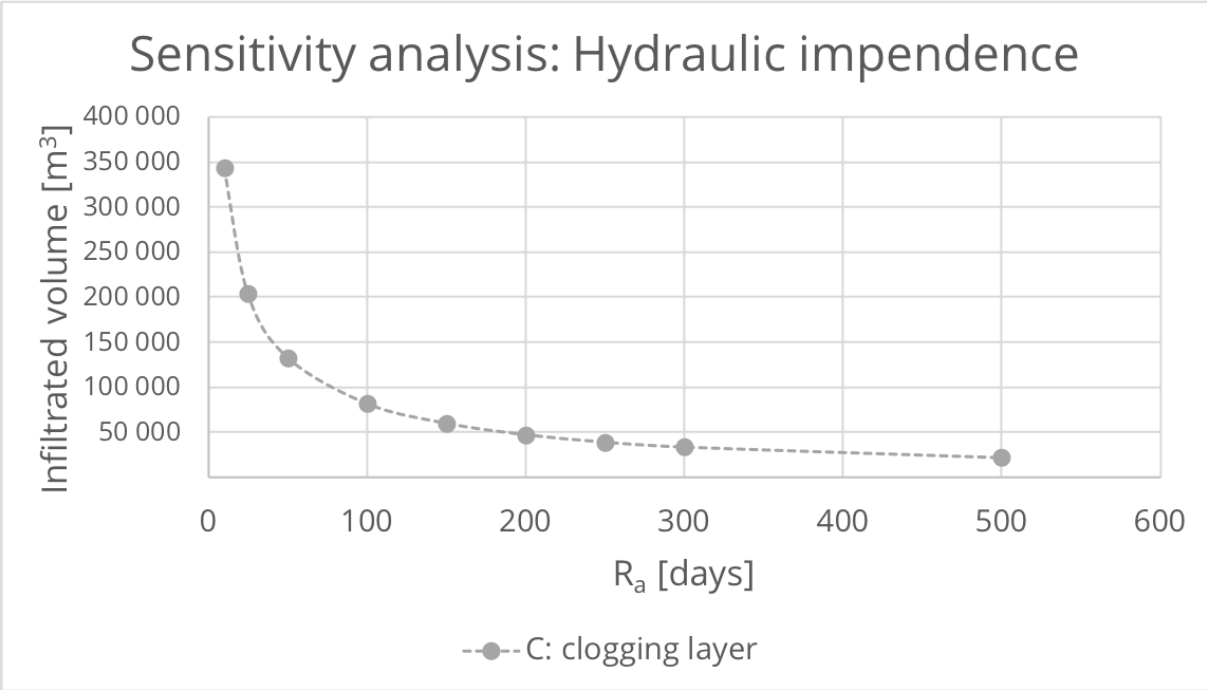

Figure 50: Sensitivity analysis - hydraulic impendence of the clogging layer

Figure 50 shows the variation of infiltrated volume with the hydraulic impendence of the clogging layer for condition C. It can be seen that infiltration drastically decreases by increasing the impendence of the layer. This parameter in fact, is an indication of the ability of water to penetrate the layer and infiltrate in the weathered zone in an unsaturated flow. By increasing the impendence, the clogging layer becomes more difficult to be penetrated.

When this parameter approaches zero, infiltration radically increase. This is because the model assumes this mechanism of infiltration as only influenced by gravity. If the impendence of the clogging layer approaches zero, one of the other two Bouwer condition would be more representative. Note that in reality, the change between a behaviour with and without clogging layer is not discrete, but instead is a gradual transition.

In fact, the accumulation of silt is a natural process that occurs in most of the check dams. It is the amount of silt (expressed by the thickness of the layer) and its characteristics (as hydraulic conductivity) that influence the infiltration behaviour. When this layer is thick and compacted (high hydraulic impendence), the infiltration mechanism can be represented by condition C. If this layer is relatively thin, and therefore the hydraulic impendence is low, infiltration mechanism can be represented by conditions A or B.

5.2.2.6 Depth to hard-rock (D_{hr})

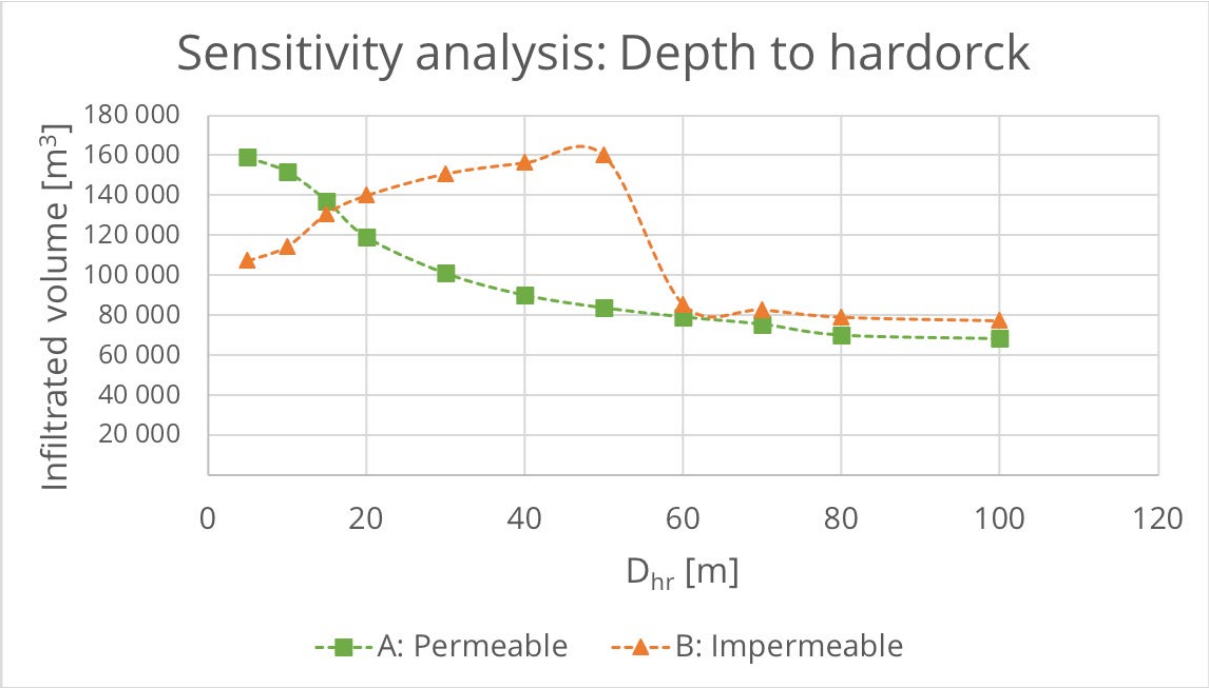

Figure 51: Sensitivity analysis - depth to hard-rock

The influence of the depth of the hard-rock layer on infiltration volumes is displayed in Figure 51 above. Only conditions A and B are considered in this analysis as infiltration with a clogging layer is only driven by gravity and not influenced on the underneath layer (see Equation [32]).

Infiltration in condition A decreases as depth to hard-rock increases. This is because of the assumption of a layer with infinite permeability considered for this condition: as this layer gets deeper, the interface in which water drain gets further away from the basin and water mounding in the weathered zone inhibits the process of infiltration. Note that in this analysis, the depth of the water table D_w is not changed, and therefore the hydraulic gradient in the weathered zone stays constant.

Figure 51 shows also that in the case of condition B, infiltration volumes witness an initial increase with the increase in hard-rock depth. When this depth reaches 60m, infiltration suddenly decreases and assumes values similar to the ones for the condition with a permeable layer.

This threshold corresponds to the one indicated by Bouwer for the validity of D-F assumption: $D_{hr} \gtrapprox 3W_b$ (see Section 4.2.6.2, Chapter 4). For shallow aquifers in fact, the flow is considered purely horizontal and the increase in depth of the impermeable interface decreases the obstructive effect of the water mound. However, when this depth reaches higher values and the aquifer becomes relatively deep, the influence of the boundary between the layers dissipate and the limiting factor becomes the hydraulic gradient in the weathered zone given by the water table D_w, likewise in condition A. The transition between these two conditions deserves attention and should be taken into account when modelling an impermeable layer with D-F and Ernst's equations.

5.2.2.7 Depth to water table (D_w)

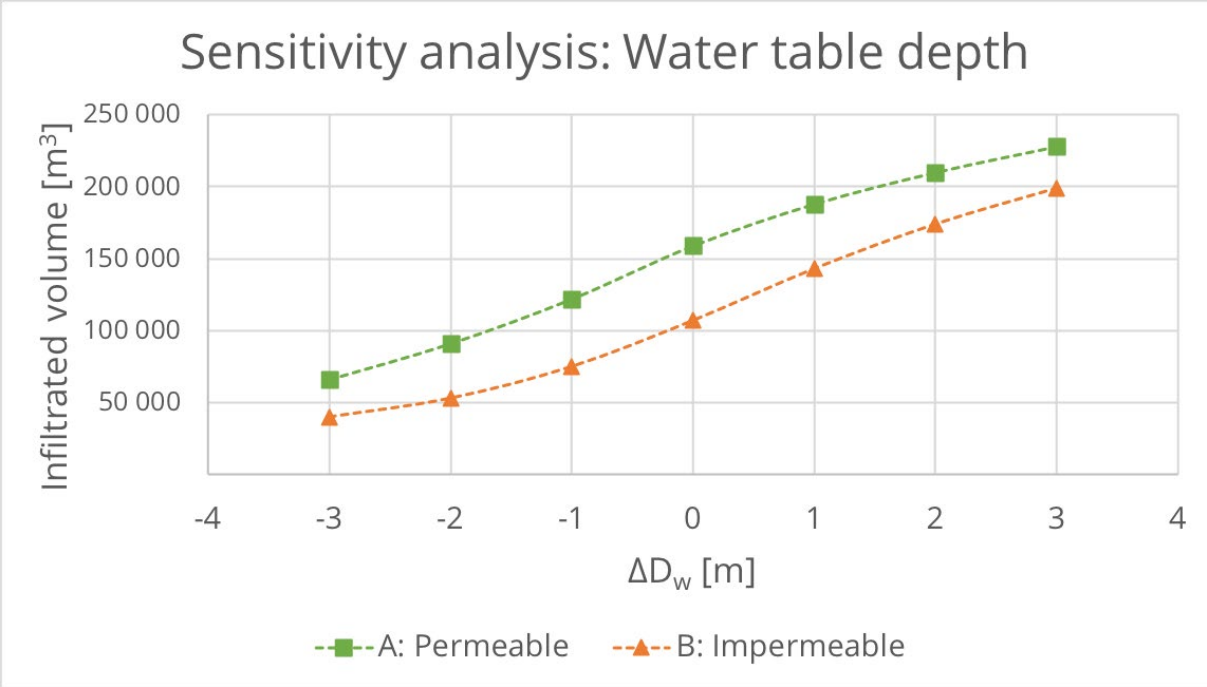

Figure 52: Sensitivity analysis - depth to the water table

Figure 52 shows the influence of the depth to the water table on infiltration volumes. For this, the sinusoids input functions (Equations [35], [36] and [37] in Section 4.2.8 of Chapter 4) are shifted by ±3m. Only conditions A and B are displayed, as condition C with clogging layer is not influenced by the water table. The right side of the graph represents deeper water table, while negative values stand for shallower groundwater.

As water depth increases, infiltration volumes increase for both conditions. This is because as the hydraulic gradient increases, more infiltration can occur.

5.2.3 Model validation

A simulation for the three Bouwer condition is run with meteorological data and geometry of Badgaon check dam for the years 2014-2015. Table 11 displays the overall results of the simulation, together with the ones by (Dashora et al., 2017). Figure 53 shows instead, the water level observed in the check dam together with the ones simulated by the model.

Table 11: Badgaon check dam – simulation results and measurements

	Dashora et al. (2017)		**Condition A (permeable layer)**		**Condition B (impermeable layer)**		**Condition C (clogging layer)**	
	2014	2015	2014	2015	2014	2015	2014	2015
Infiltrated volume [m³]	113 000	56 000	116 000	48 000	97 000	47 000	62 000	38 000
Evaporated volume [m³]	19 000	4 700	20 500	3 600	22 500	6 500	27 500	21 500
Date of empty	Nov 11	Aug 28	Nov 09	Aug 25	Nov 26	Sept 14	Jan 30	Dec 27

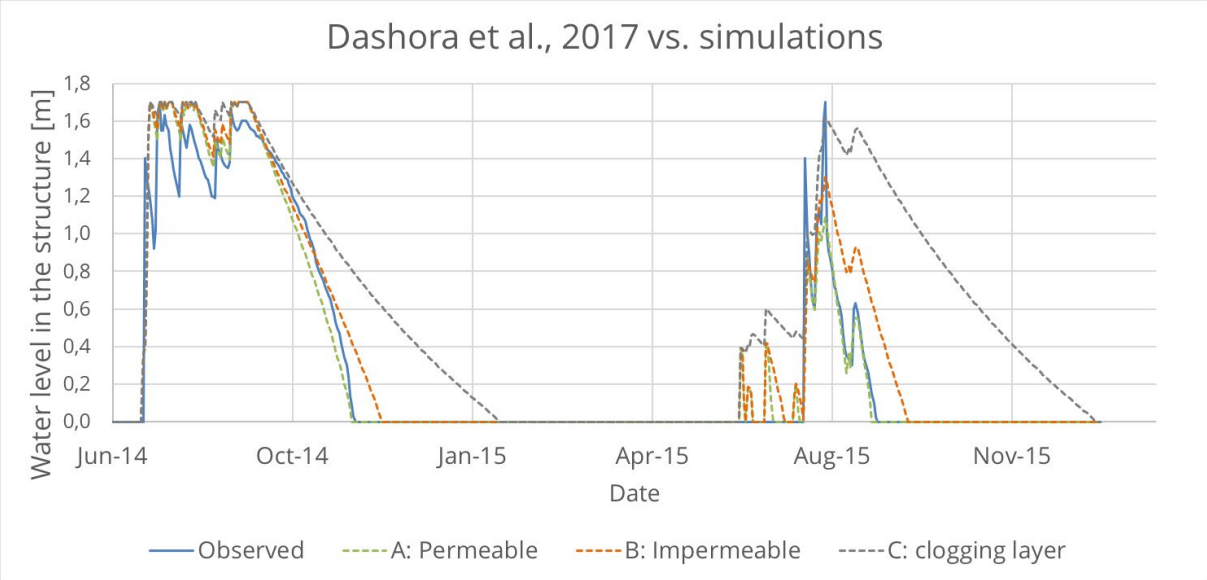

Figure 53: Water levels - simulation and measurements from Dashora et al. (2017)

From Table 11, it can be seen that the error of the model in estimating the infiltration volumes for condition A is less than 3% in 2014 and about 15% for 2015. For this condition with a permeable layer, the model is able to predict the date in which the structure gets empty with an error of two days in 2014 and three days in 2015.

Regarding conditions B and C, it can be seen that the discrepancy with the observed values is higher. In fact, the error in the infiltration volumes is about 5% in 2014 and 16% in 2015 in case of condition B, while for condition C it is 45% in 2014 and 32% in 2015. These results suggest that the Bouwer condition A with a permeable layer underneath the weathered zone is the one most representative for the Badgaon check dam assessed by Dashora et al. (2017).

This can also be seen by Figure 53, where the water levels are visible for the simulation together with the field measurements. In the year 2014, all Bouwer condition follow relatively close to the

measurements. There is a general overestimation of the water level from the model, but the difference is generally lower than 0.2m. When the structure starts to get empty, it can be seen that condition A follow closely the measurements recorded by farmers.

In 2015, it can be seen that in June the model simulates some water in the check dam while no recording of this occurred. This discrepancy can be explained by the fact that during this period, there were few days of precipitation with around 30mm/day falling upon the catchment. These days of precipitation were not enough to produce surface runoff because of the dry conditions of the basin before the monsoon season. The model, however, computes runoff by multiplying the precipitation depth by a runoff coefficient (0.02 in 2015) and does not take into consideration the antecedent moisture condition of the basin.

After the structure gets full and water is measured in the check dam at the end of July, condition A fairly replicates the observations, and it predicts the day of empty with only three days discrepancy.

The statistics of the validation are presented in Table 12 below. The table displays the coefficient of determination R^2 between the model and the observed water depth values for the years 2014 and 2015. This coefficient is comprised between 0 and 1, and it is an indication of the goodness-of-fit measure for linear regression models (Cameron and Windmeijer, 1997). When computing this coefficient, the days in which both the model and the observations are zero are excluded.

Table 12: Validation results

R^2 of water levels	**2014**	**2015**
Condition A	0.939	0.867
Condition B	0.934	0.731
Condition C	0.885	0.331

In concordance with the previous results, it can be seen that condition A is the most representative for the Badgaon check dam for both years 2014 and 2015, with an R^2 of 0.939 and 0.867 respectively. Condition B has a lower fitness with the observations, with R^2 of 0.934 in 2014 and of 0.731 in 2015. The case of clogging layer (condition C), is the least representative of the three Bouwer conditions, with a coefficient of determination of 0.885 in 2014 and 0.331 2015. These results can be explained by the fact that the Badgaon check dam did not have a thick layer of silt; especially in 2015, when the surface was manually scraped. The fact that R^2 is generally lower for all Bouwer conditions in 2015 can be explained by the discrepancy in surface runoff previously illustrated.

The validation of the model using the measurements from Dashora et al. (2017) indicates that the tool developed in this work can be successfully applied to check dams in other semi-arid areas. However, the performance of the model is directly linked with the method used to estimate surface runoff and its accuracy compared to measurement data.

Chapter 6: Conclusions

In this study, a tool is developed in R to analyse and simulate the water balance of check dams to understand the impact of local hydrology and hydrogeology in hard-rock region of Gujarat. The tool is used to simulate the check dam behaviour under different hydrogeological settings and parameters.

The studies found in past literature have focused on analysis based on field measurements for specific structures, or on developing models at catchment-scale. This tool is instead based on analytical equations and can be applied for different generic structures in semi-arid regions.

The model was validated by implementing measurements from a check dam studied by Dashora et al. (2017) in Rajasthan in 2014-2015. The coefficient of determination R^r from the validation was found to be 0.939 in 2014 and 0.867 in 2015.

The main findings regarding some focal points are here listed:

- **Stored Volume:** It is demonstrated that check dams get full multiple times per year, being able to store up to six times their storage capacity in wet years and as little as two times their capacity in dry years. The amount of captured water varies in years according to the annual precipitation and the distribution of rainfall events.
- **Runoff:** For check dams with dimensions similar to the ones assessed in the field, the impact of a single structure on surface runoff is relatively low: on average the volume stored is less than 4% of runoff. However, it is presumable that the cumulative effect of multiple structures in series would lead to a significant impact on river flow for downstream areas.
- **Infiltration:** For a check dam with a storage capacity of 34 000m^3, the model showed infiltration volumes ranging between 40 000 and 2 000 m^3. Results show that the hydrogeological setting is an essential parameter for the amount of water infiltrated from the structure. If the structure is on a site in which the underlying hard-rock has a high permeability, infiltration rates can go above 40mm/day. In the hard-rock beneath the weathered zone is compacted and impermeable, infiltration decreases because of the water mound created and rates can decrease of about 50% compared to a site over a permeable layer. The presence of a clogging layer can reduce infiltration volumes up to 70%, depending on the impendence of the silt cover.
- **Evaporation:** The fraction of water volume stored by the check dam and lost by evaporation ranges between 10 and 50%. This volume varies among year depending on the precipitation and meteorological conditions. Losses by evaporation are mainly influenced by the hydrogeological setting, maintenance practices and catchment characteristics.
- **Effect of abstractions:** It is found that induced recharge from nearby abstraction wells can increase the recharge volumes up to 20%, but only if the basin is not covered with a clogging layer. The influence of abstractions is dependent on the characteristics of the aquifer, the distance of the well and the irrigation calendars.

The main factors influencing check dam behaviour are structure geometry, characteristics of the setting, catchment area and depth to the water table.

Geometry plays an important role in the infiltration capacity of these structures. The main parameters that characterize check dam geometry in this model are width, height and stream gradient. These parameters are relevant for infiltration because they affect the storage capacity of the check dam: by increasing the storage capacity, the structure's ability to capture more runoff increases. The most sensitive parameter for this set is the stream gradient: varying from 0.01° to 0.1° infiltration decreases by nine times.

Meteorological parameters influence the amount of incoming water in the structure, as well as the volumes lost by evaporation. Hydrogeological conditions, such as soil properties, the permeability and the depth of the lower layer, influence the downward hydraulic flow and therefore, the amount of water infiltrating from the structure.

Another aspect to consider it that check dam intensity affects the effective catchment area covered by the structures, and therefore the volume of water inflow. If this density reaches a threshold limit, structures concentrated in a small area can negatively influence their infiltration capacity. For the geometry simulated, this threshold was found to be around one check dam every 2km^2. However, this value is dependent on the storage capacity of the structures.

The depth to the water table is an important feature for recharge, as it regulates the degree of hydraulic connection between water mound from the structure and groundwater. This connection is fundamental to determine the mechanism and the quantity of infiltration of ponding water from the check dam into the sub-surface.

Recommendations and future development

As previously explained, check dam geometry has a significant influence on their hydrological behaviour. In order to improve the accuracy of the model in predicting water budgets, it is suggested to measure area-volume-elevation curves on the field. This should be done during the summer season, when the structures are dry, with the use of dumpy levels or theodolites. Infiltration tests are also suggested to estimate hydraulic conductivity in the weathered upper zone. Geophysical surveys - like Vertical Electrical Sounding (VES) or Electrical Resistivity Tomography (ERT) - could be performed to understand the hydrogeological setting underneath the weathered upper layer. Because the model is dependent on the water table dynamics, it is also suggested to measure groundwater depth at different distances from the structure. By doing so, it is possible to determine a more accurate and site-specific water table functions over time.

In the presence of measurements from the field, the developed model has great potential to predict check dam behaviour. Complete calibration and validation would require measurements of precipitation, evaporation, and runoff. The daily water level in the structure should also be measured with a high temporal resolution water level data logger (e.g. diver) or with daily measurements performed by locals.

The study of individual structures can be incorporated into a catchment-scale model, as is the intention of the larger project that enables this study. This would allow studying the cumulative impact of small-scale decentralised MAR implementation, on both groundwater resources and surface runoff.

Finally, it is remarked that this tool has the potential to be used in different semi-arid locations. Because it is based on analytical equations, it can be applied in different hydrogeological settings (also on alluvial aquifers) with adequate site-specific data.

REFERENCES

ASOKA, A., GLEESON, T., WADA, Y., MISHRA, V., 2017. RELATIVE CONTRIBUTION OF MONSOON PRECIPITATION AND PUMPING TO CHANGES IN GROUNDWATER STORAGE IN INDIA. NAT. GEOSCI. 10, 109–117. HTTPS://DOI.ORG/10.1038/NGEO2869

BADIGER, S., SAKTHIVADIVEL, R., ALOYSIUS, N., SALLY, H., 2002. PRELIMINARY ASSESSMENT OF A TRADITIONAL APPROACH TO RAINWATER HARVESTING AND ARTIFICIAL RECHARGING OF GROUNDWATER IN ALWAR DISTRICT, IWMI-TATA WATER POLICY PROGRAM: WATER POLICY RESEARCH HIGHLIGHT, ANNUAL PARTNERS MEET 2002.

BAGCHI, A.K., DAS, P., CHATTOPADHYAY, S.K., 2005. GROWTH AND STRUCTURAL CHANGE IN THE ECONOMY OF GUJARAT, 1970-2000. ECON. POLIT. WKLY. 40, 3039–3047.

BATCHELOR, C., SINGH, A., 2002. MITIGATING THE POTENTIAL UNINTENDED IMPACTS OF WATER HARVESTING, IN: IWRA INTERNATIONAL REGIONAL SYMPOSIUM 'WATER FOR HUMAN SURVIVAL', 26-29TH NOVEMBER, 2002. NEW DELHI, INDIA, PP. 26–29.

BECKER, M.W., 2006. POTENTIAL FOR SATELLITE REMOTE SENSING OF GROUND WATER. GROUND WATER 44, 306–318. HTTPS://DOI.ORG/10.1111/J.1745-6584.2005.00123.X

BHANJA, S.N., MUKHERJEE, A., RODELL, M., WADA, Y., CHATTOPADHYAY, S., VELICOGNA, I., PANGALURU, K., FAMIGLIETTI, J.S., 2017. GROUNDWATER REJUVENATION IN PARTS OF INDIA INFLUENCED BY WATER-POLICY CHANGE IMPLEMENTATION. SCI. REP. 7, 1–7. HTTPS://DOI.ORG/10.1038/S41598-017-07058-2

BHATIA, B., 1992. LUSH FIELDS AND PARCHED THROATS: POLITICAL ECONOMY OF GROUNDWATER IN GUJARAT. ECON. POLIT. WKLY. A142–A170.

BODH, P.C., SINGLA, S., SHARMA, A., 2017. AGRICULTURAL STATISTICS AT A GLANCE 2017. NEW DELHI, INDIA.

BOUWER, H., 2002. ARTIFICIAL RECHARGE OF GROUNDWATER: HYDROGEOLOGY AND ENGINEERING. HYDROGEOL. J. 121–142. HTTPS://DOI.ORG/10.1007/S10040-001-0182-4

BOUWER, H., 1969. THEORY OF SEEPAGE FROM OPEN CHANNELS, ADVANCES IN HYDROSCIENCE. ACADEMIC PRESS, INC. HTTPS://DOI.ORG/10.1016/B978-1-4831-9936-8.50008-8

BOUWER, H., 1965. LIMITATION OF THE DUPUIT-FORCHHEIMER ASSUMPTION IN RECHARGE AND SEEPAGE. TRANS. ASAE 8, 512–515.

BUTLER JR, J.J., ZHAN, X., ZLOTNIK, V.A., 2007. PUMPING-INDUCED DRAWDOWN AND STREAM DEPLETION IN A LEAKY AQUIFER SYSTEM. GROUNDWATER 45, 178–186.

CAMERON, A.C., WINDMEIJER, F.A.G., 1997. AN R-SQUARED MEASURE OF GOODNESS OF FIT FOR SOME COMMON NONLINEAR REGRESSION MODELS. J. ECONOM. 77, 329–342.

CGWB, 2015. DISTRICTS GROUND WATER BROCHURES [WWW DOCUMENT]. CENT. GR. WATER BOARD (CGWB), MINIST. WATER RESOUR. INDIA. URL HTTP://CGWB.GOV.IN/DISTRICT-GW-BROCHURES.HTML (ACCESSED 4.26.19).

CGWB, 2013. MASTER PLAN FOR ARTIFICIAL RECHARGE TO GROUND WATER IN INDIA [WWW DOCUMENT]. URL HTTP://CGWB.GOV.IN/DOCUMENTS/MASTERPLAN-2013.PDF (ACCESSED 4.1.19).

CGWB, 2011. STATE PROFILE - GROUNDWATER SCENARIO OF GUJARAT [WWW DOCUMENT]. URL HTTP://CGWB.GOV.IN/STATE-PROFILES/GUJARAT.PDF (ACCESSED 4.1.19).

CGWB, 2006. DYNAMIC GROUNDWATER RESOURCES OF INIDA (AS ON MARCH, 2004). CENTRAL GROUND WATER BOARD (CGWB), MINISTRY OF WATER RESOURCES,GOVERNMENT OF INDIA. FARIBADAD.

CHATURVEDI, M.C., SRIVASTAVA, V.K., 1979. INDUCED GROUNDWATER RECHARGE IN THE GANGES BASIN. WATER RESOUR. RES. 15, 1156–1166.

CHIN, D.A., 1990. A METHOD TO ESTIMATE CANAL LEAKAGE TO THE BISCAYNE AQUIFER , DADE COUNTY , FLORIDA. TALLAHASSEE, FLORIDA.

DACHLER, R., 1936. GRUNDWASSERSTROMUNG (FLOW OF GROUNDWATER). JUL. SPRINGER, WIEN 141.

DAG, 2017. SEASON AND CROP REPORTS (2015-2016) [WWW DOCUMENT]. DIR. AGRIC. GOV. GUJARAT. URL HTTPS://DAG.GUJARAT.GOV.IN/SCR-INFO.HTM (ACCESSED 4.14.19).

DASHORA, Y., DILLON, P., MAHESHWARI, B., SONI, P., DASHORA, R., DAVANDE, S., PUROHIT, R.C., MITTAL, H.K., 2017. A SIMPLE METHOD USING FARMERS' MEASUREMENTS APPLIED TO ESTIMATE CHECK DAM RECHARGE IN RAJASTHAN, INDIA. SUSTAIN. WATER RESOUR. MANAG. 4, 301–316. HTTPS://DOI.ORG/10.1007/S40899-017-0185-5

DAVE, H., JAMES, M.E., RAY, K., 2017. TRENDS IN INTENSE RAINFALL EVENTS OVER GUJARAT STATE (INDIA) IN THE WARMING ENVIRONMENT USING GRIDDED AND CONVENTIONAL DATA 12, 977–998.

DILLON, P., STUYFZAND, P., GRISCHEK, T., LLURIA, M., PYNE, R.D.G., JAIN, R.C., BEAR, J., SCHWARZ, J., WANG, W., FERNANDEZ, E., STEFAN, C., PETTENATI, M., VAN DER GUN, J., SPRENGER, C., MASSMANN, G., SCANLON, B.R., XANKE, J., JOKELA, P., ZHENG, Y., ROSSETTO, R., SHAMRUKH, M., PAVELIC, P., MURRAY, E., ROSS, A., BONILLA VALVERDE, J.P., PALMA NAVA, A., ANSEMS, N., POSAVEC, K., HA, K., MARTIN, R., SAPIANO, M., 2018. SIXTY YEARS OF GLOBAL PROGRESS IN MANAGED AQUIFER RECHARGE. HYDROGEOL. J. 1–30. HTTPS://DOI.ORG/10.1007/S10040-018-1841-Z

DILLON, P.J., LIGGETT, J.A., 1983. AN EPHEMERAL STREAM-AQUIFER INTERACTION MODEL. WATER RESOUR. RES. 19, 621–626.

ENVIS, 2017. STATUS OF ENVIRONMENT AND RELATED ISSUES - WATER.

ERNST, L.F., 1962. GRONDWATERSTROMINGEN IN DE VERZADIGDE ZONE EN HUN BEREKENING BIJ AANWEZIGHEID VAN HORINZONTALE EVENWIJDIGE OPEN LEIDINGEN. CENTRUM VOOR LANDBOUWPUBLIKATIES EN LANDBOUWDOCUMENTATIE.

FOSTER, S., GARDUÑO, H., TUINHOF, A., 2007. CONFRONTING THE GROUNDWATER MANAGEMENT CHALLENGE IN THE DECCAN TRAPS COUNTRY OF MAHARASHTRA – INDIA, GW MATE. WORLD BANK, WASHINGTON D.C.

GEC, 1997. GROUND WATER ESTIMATION METHODOLOGY.

GLENDENNING, C.J., VAN OGTROP, F.F., MISHRA, A.K., VERVOORT, R.W., 2012. BALANCING WATERSHED AND LOCAL SCALE IMPACTS OF RAIN WATER HARVESTING IN INDIA-A REVIEW. AGRIC. WATER MANAG. 107, 1–13. HTTPS://DOI.ORG/10.1016/J.AGWAT.2012.01.011

GLENDENNING, C.J., VERVOORT, R.W., 2010. HYDROLOGICAL IMPACTS OF RAINWATER HARVESTING (RWH) IN A CASE STUDY CATCHMENT: THE ARVARI RIVER, RAJASTHAN, INDIA. PART 1. FIELD-SCALE IMPACTS. AGRIC. WATER MANAG. 98, 331–342. HTTPS://DOI.ORG/10.1016/J.AGWAT.2010.11.010

GOI, 2018. AGRICULTURE CENSUS 2015-16.

GORE, K.P., PENDKE, M.S., GURUNADHA RAO, V.V.S., GUPTA, C.P., 1998. GROUNDWATER MODELLING TO QUANTIFY THE EFFECT OF WATER HARVESTING STRUCTURES IN WAGARWADI WATERSHED, PARBHANI DISTRICT, MAHARASHTRA, INDIA. HYDROL. PROCESS. 12, 1043–1052. HTTPS://DOI.ORG/10.1002/(SICI)1099-1085(19980615)12:7<1043::AID-HYP638>3.0.CO;2-I

GRÖNWALL, J., 2014. POWER TO SEGREGATE: IMPROVING ELECTRICITY ACCESS AND REDUCING DEMAND IN RURAL INDIA. SIWI PAPER 23. STOCKHOLM: SIWI.

GUPTA, R.K., 2012. THE ROLE OF WATER TECHNOLOGY IN DEVELOPMENT: A CASE STUDY IN GUJARAT, INDIA, IN: WATER AND THE GREEN ECONOMY - CAPACITY DEVELOPMENT ASPECTS. UN-WATER DECADE PROGRAMME ON CAPACITY DEVELOPMENT (UNW-DPC), BONN, GERMANY, P. 208.

GUPTA, R.K., 2002. WATER AND ENERGY LINKAGES FOR GROUNDWATER EXPLOITATION: A CASE STUDY OF GUJARAT STATE, INDIA. INT. J. WATER RESOUR. DEV. 18, 25–45. HTTPS://DOI.ORG/10.1080/07900620220121639

HAWKINS, R.H., HJELMFELT, A.T., ZEVENBERGEN, A.W., 1985. RUNOFF PROBABILITY, STORM DEPTH, AND CURVE NUMBERS. J. IRRIG. DRAIN. ENG. 111, 330–340. HTTPS://DOI.ORG/10.1061/(ASCE)0733-9437(1985)111:4(330)

IGRAC, 2007. ARTIFICIAL RECHARGE OF GROUNDWATER IN THE WORLD.

JAIN, R.C., 2012. ROLE OF DECENTRALIZED RAINWATER HARVESTING AND ARTIFICIAL RECHARGE IN REVERSAL OF GROUNDWATER DEPLETION IN THE ARID AND SEMI-ARID REGIONS OF GUJARAT, INDIA, IWMI-TATA WATER POLICY PROGRAM: WATER POLICY RESEARCH HIGHLIGHT.

JOSHI, M. V, 2002. WATER CRISIS AND WATER CONSERVATION IN SAURASHTRA. SAURASHTRA UNIVERSITY, RAJKOT.

KAMBOJ, S., MUL, M., VAN DER ZAAG, P., VERMA, S., 2011. SMALL RESERVOIR BIG IMPACT: IMPACT OF RAINWATER HARVESTING STRUCTURES ON RIVER FLOW REGIME. IHE - DELFT INSTITUTE FOR WATER EDUCATION.

KONIKOW, L.F., KENDY, E., 2005. GROUNDWATER DEPLETION: A GLOBAL PROBLEM. HYDROGEOL. J. 13, 317–320. HTTPS://DOI.ORG/10.1007/S10040-004-0411-8

KULKARNI, H., DEOLANKAR, S.B., LALWANI, A., JOSEPH, B., PAWAR, S., 2000. HYDROGEOLOGICAL FRAMEWORK OF THE DECCAN BASALT GROUNDWATER SYSTEMS, WEST-CENTRAL INDIA. HYDROGEOL. J. 8, 368–378.

KUMAR, M.D., PATEL, A., RAVINDRANATH, R., SINGH, O.. P., 2008. CHASING A MIRAGE: WATER HARVESTING AND ARTIFICIAL RECHARGE IN NATURALLY WATER-SCARCE REGIONS. ECON. POLIT. WKLY. 43, 61–71.

KUMAR, M.D., PERRY, C.J., 2018. WHAT CAN EXPLAIN GROUNDWATER REJUVENATION IN GUJARAT IN RECENT YEARS? INT. J. WATER RESOUR. DEV. 00, 1–16. HTTPS://DOI.ORG/10.1080/07900627.2018.1501350

KUMAR, M.D., SINGHAL, L., RATH, P., 2004. VALUE OF GROUNDWATER CASE STUDIES IN BANASKANTHA. ECON. POLIT. WKLY. 3498–3503.

MASSUEL, S., PERRIN, J., MASCRE, C., MOHAMED, W., BOISSON, A., AHMED, S., 2014. MANAGED AQUIFER RECHARGE IN SOUTH INDIA: WHAT TO EXPECT FROM SMALL PERCOLATION TANKS IN HARD ROCK? J. HYDROL. 512, 157–167. HTTPS://DOI.ORG/10.1016/J.JHYDROL.2014.02.062

MOENCH, M.H., 1992. CHASING THE WATERTABLE EQUITY AND SUSTAINABILITY IN GROUNDWATER MANAGEMENT. QUALITY 27, A171–A177.

MOOLEY, D.A., PARTHASARATHY, B., 1984. D. A. MOOLEY AND B. PARTHASARATHY INDIAN INSTITUTE O F TROPICAL METEOROLOGY, PUNE-5, INDIA 6, 287–301.

MOORE, J.E., JENKINS, C.T., 1966. AN EVALUATION OF THE EFFECT OF GROUNDWATER PUMPAGE ON THE INFILTRATION RATE OF A SEMIPERVIOUS STREAMBED. WATER RESOUR. RES. 2, 691–696. HTTPS://DOI.ORG/10.1029/WR002I004P00691

MUKHERJEE, A., 2018. GROUNDWATER OF SOUTH ASIA. SPRINGER.

NEUMANN, I., BARKER, J., MACDONALD, D., GALE, I., 2004. NUMERICAL APPROACHES FOR APPROXIMATING TECHNICAL EFFECTIVESSNESS OF ARTIFICIAL RECHARGE STRUCTURES 46.

NWRWS, 2010. BHADAR WATER RESOURCES PROJECT, NARMADA WATER RESOURCES WATER SUPPLY AND KALPSAR DEPARTMENT [WWW DOCUMENT]. URL HTTPS://GUJ-NWRWS.GUJARAT.GOV.IN/SHOWPAGE.ASPX?CONTENTID=1643&LANG=ENGLISH (ACCESSED 4.15.19).

OLESON, T., 2016. IMPACT OR ERUPTIONS : ARE BOTH TO BLAME IN THE GREAT END-CRETACEOUS WHODUNIT? [WWW DOCUMENT]. EARTH. URL HTTPS://WWW.EARTHMAGAZINE.ORG/ARTICLE/IMPACT-OR-ERUPTIONS-ARE-BOTH-BLAME-GREAT-END-CRETACEOUS-WHODUNIT (ACCESSED 4.1.19).

PATEL, A.S., 2002. IMPACT OF GROUNDWATER RECHARGE ACTIVITIES IN SAURASHTRA, IWMI-TATA WATER POLICY PROGRAM: WATER POLICY RESEARCH HIGHLIGHT.

PATEL, J., SINGH, N.P., PRAKASH, I., MEHMOOD, K., 2017. SURFACE RUNOFF ESTIMATION USING SCS- CN METHOD-A CASE STUDY ON BHADAR. IMP. J. INTERDISCIP. RES. 3.

PENMAN, H.L., 1948. NATURAL EVAPORATION FROM OPEN WATER, BARE SOIL AND GRASS. PROC. R. SOC. LONDON. SER. A. MATH. PHYS. SCI. 193, 120–145.

R CORE TEAM, 2017. R: A LANGUAGE AND ENVIRONMENT FOR STATISTICAL COMPUTING.

RENGANAYAKI, S.P., ELANGO, L., 2013. A REVIEW ON MANAGED AQUIFER RECHARGE BY CHECK DAMS: A CASE STUDY NEAR CHENNAI, INDIA. INT J RES ENG TECHNOL 2, 416–423.

ROY, P.S., MYIYAPPAN, P., JOSHI, P.K., KALE, M.P., SRIVASTAV, V.K., SRIVASATAVA, S.K., BEHERA, M.D., ROY, A., SHARMA, Y., RAMACHANDRAN, R.M., BHAVANI, P., JAIN, A.K., KRISHNAMUTHY, Y.V.N., 2016. DECADAL LAND USE AND LAND COVER CLASSIFICATIONS ACROSS INDIA, 1985, 1995, 2005. HTTPS://DOI.ORG/10.3334/ORNLDAAC/1336

RSTUDIO TEAM, 2018. RSTUDIO: INTEGRATED DEVELOPMENT ENVIRONMENT FOR R.

SAKTHIVADIVEL, R., 2007. THE GROUNDWATER RECHARGE MOVEMENT IN INDIA. AGRIC. GROUNDW. REVOLUT. OPPOR. THREAT. TO DEV. 195–210.

SCHOBER, P., BOER, C., SCHWARTE, L.A., 2018. CORRELATION COEFFICIENTS: APPROPRIATE USE AND INTERPRETATION. ANESTH. ANALG. 126, 1763–1768.

SCS, 1972. SECTION 4: HYDROLOGY, IN: NATIONAL ENGINEERING HANDBOOK. USDA SOIL CONSERVATION SERVICE, WASHINGTON, DC.

SHAH, T., 2014. TOWARDS A MANAGED AQUIFER RECHARGE STRATEGY FOR GUJARAT, INDIA: AN ECONOMIST'S DIALOGUE WITH HYDRO-GEOLOGISTS. J. HYDROL. 518, 94–107. HTTPS://DOI.ORG/10.1016/J.JHYDROL.2013.12.022

SHAH, T., 2008. TAMING THE ANARCHY: GROUNDWATER GOVERNANCE IN SOUTH ASIA, 1ST EDITIO. ED. RESOURCES FOR THE FUTURE, WASHINGTON DC. HTTPS://DOI.ORG/HTTPS://DOI.ORG/10.4324/9781936331598

SHAH, T., 2002. DECENTRALIZED WATER HARVESTING AND GROUNDWATER RECHARGE, IWMI-TATA WATER POLICY PROGRAM: WATER POLICY RESEARCH HIGHLIGHT. IWMI - TATA WATER POLICY PROGRAM.

SHAH, T., BHATT, S., SHAH, R.K., TALATI, J., 2008. GROUNDWATER GOVERNANCE THROUGH ELECTRICITY SUPPLY MANAGEMENT : ASSESSING AN INNOVATIVE INTERVENTION IN GUJARAT , WESTERN INDIA 95, 1233–1242. HTTPS://DOI.ORG/10.1016/J.AGWAT.2008.04.006

SHAH, T., GULATI, A., P., H., SHREEDHAR, G., JAIN, R.C., 2009. SECRET OF GUJARAT'S AGRARIAN MIRACLE AFTER 2000. ECON. POLIT. WKLY. 44, 45–55. HTTPS://DOI.ORG/10.2307/25663939

SHAH, T., MEHTA, Y., KHER, V., 2012. AGRICULTURAL GROWTH AND RURAL DYNAMISM. IWMI-TATA WATER POLICY PROGR. WATER POLICY RES. HIGHLIGHT.

SHARDA, V.N., KUROTHE, R.S., SENA, D.R., PANDE, V.C., TIWARI, S.P., 2006. ESTIMATION OF GROUNDWATER RECHARGE FROM WATER STORAGE STRUCTURES IN A SEMI-ARID CLIMATE OF INDIA. J. HYDROL. 329, 224–243. HTTPS://DOI.ORG/10.1016/J.JHYDROL.2006.02.015

SHARMA, A.K., THAKUR, P.K., 2007. QUANTITATIVE ASSESSMENT OF SUSTAINABILITY OF PROPOSED WATERSHED DEVELOPMENT PLANS FOR KHAROD WATERSHED, WESTERN INDIA. J. INDIAN SOC. REMOTE SENS. 35.

SHEN, S.-L., XU, Y.-S., 2011. NUMERICAL EVALUATION OF LAND SUBSIDENCE INDUCED BY GROUNDWATER PUMPING IN SHANGHAI. CAN. GEOTECH. J. 48, 1378–1392.

SHUTTLEWORTH, W.J., 1993. EVAPORATION IN: MAIDMENT, DR HANDBOOK OF HYDROLOGY.

SINGHAL, B.B.S., 1997. HYDROGEOLOGICAL CHARACTERISTICS OF DECCAN TRAP FORMATIONS OF INDIA, IN: HARD ROCK HYDROSYSTEMS. IAHS, PP. 75–80.

STEFAN, C., ANSEMS, N., 2018. WEB-BASED GLOBAL INVENTORY OF MANAGED AQUIFER RECHARGE APPLICATIONS. SUSTAIN. WATER RESOUR. MANAG. 4, 153–162. HTTPS://DOI.ORG/10.1007/S40899-017-0212-6

STIEFEL, J.M., MELESSE, A.M., MCCLAIN, M.E., PRICE, R.M., ANDERSON, E.P., CHAUHAN, N.K., 2009. EFFECTS OF RAINWATER-HARVESTING-INDUCED ARTIFICIAL RECHARGE ON THE GROUNDWATER OF WELLS IN RAJASTHAN, INDIA. HYDROGEOL. J. 17, 2061–2073. HTTPS://DOI.ORG/10.1007/S10040-009-0491-6

STRAHLER, A.N., 1952. HYPSOMETRIC (AREA-ALTITUDE) ANALYSIS OF EROSIONAL TOPOGRAPHY. GEOL. SOC. AM. BULL. 63, 1117–1142.

THIEM, G., 1906. HYDROLOGISCHE METHODEN: DISSERTATION ZUR ERLANGUNG DER WÜRDE EINES DOKTOR-INGENIEURS DURCH DIE KÖNIGLICHE TECHNISCHE HOCHSCHULE ZU STUTTGART.

TRIVEDI, A.B., 2002. THE IMPACT OF WATERSHED DEVELOPMENT PROGRAM ON AGRICULTURE AND RURAL DEVELOPMENT WITH REFERENCE TO SAURASHTRA. VIVEKANAND RESEARCH AND TRAINING INSTITUTE.

VEDERNIKOV, V. V, 1934. VERSICKERUNGEN AUS KANALEN. WASSERKRAFT WASSERWIRTSCH 11, 13.

VERMA, S., KRISHNAN, S., 2011. MEGHAL RIVER BASIN RESEARCH PROJECT. INDIA NATURAL RESOURCE ECONOMICS AND MANAGEMENT (INREM), INTERNATIONAL WATER MANAGEMENT INSTITUTE (IWMI),.

WATTS, A.B., COX, K.G., 1989. THE DECCAN TRAPS: AN INTERPRETATION IN TERMS OF PROGRESSIVE LITHOSPHERIC FLEXURE IN RESPONSE TO A MIGRATING LOAD. EARTH PLANET. SCI. LETT. 93, 85–97. HTTPS://DOI.ORG/10.1016/0012-821X(89)90186-6

YAGNIK, A., SHETH, S., 2005. THE SHAPING OF MODERN GUJARAT: PLURALITY. HINDUTVA BEYOND, NEW DELHI.

APPENDICES

Appendix A

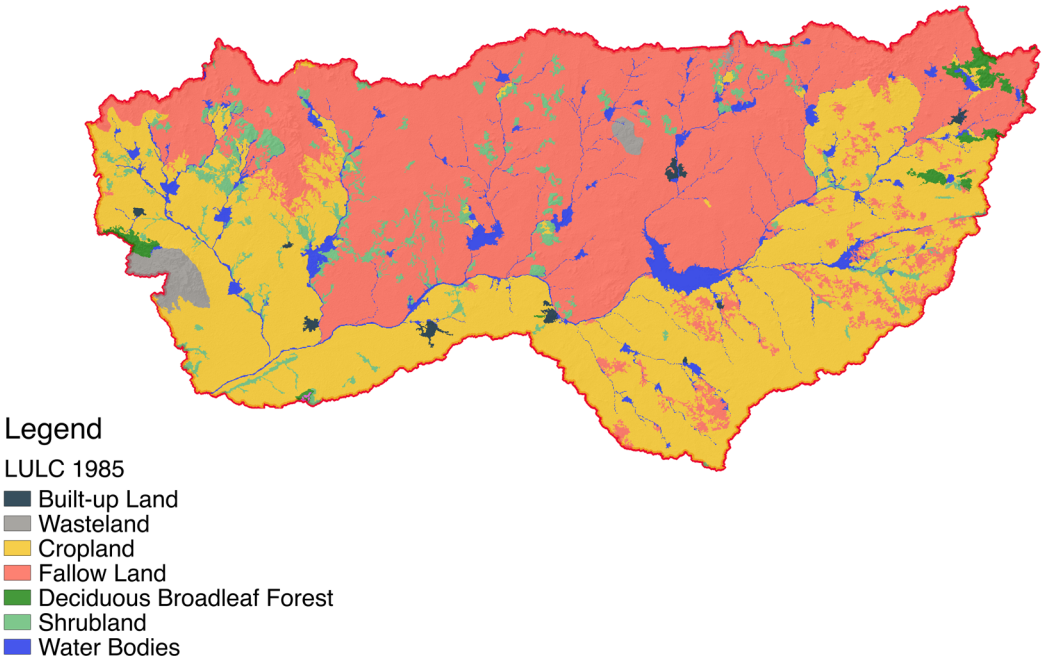

Figure 54: Land Use and Land Cover in Bhadar basin – 1985

Data from ORNL DAAC (Roy et al., 2016)

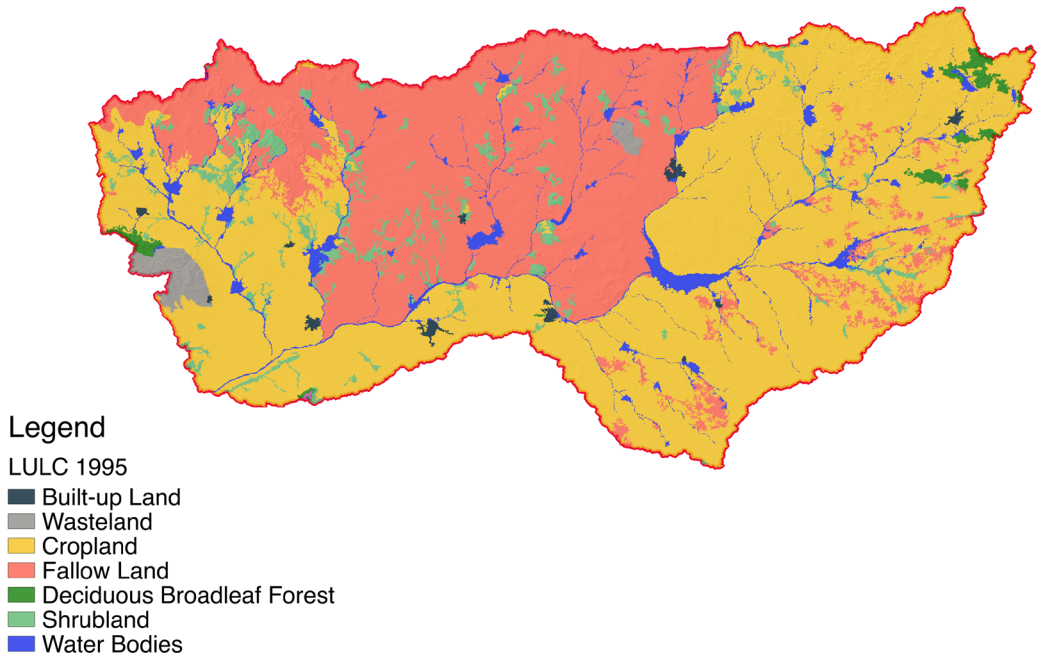

Figure 55: Land Use and Land Cover – 1995

Data from ORNL DAAC (Roy et al., 2016)

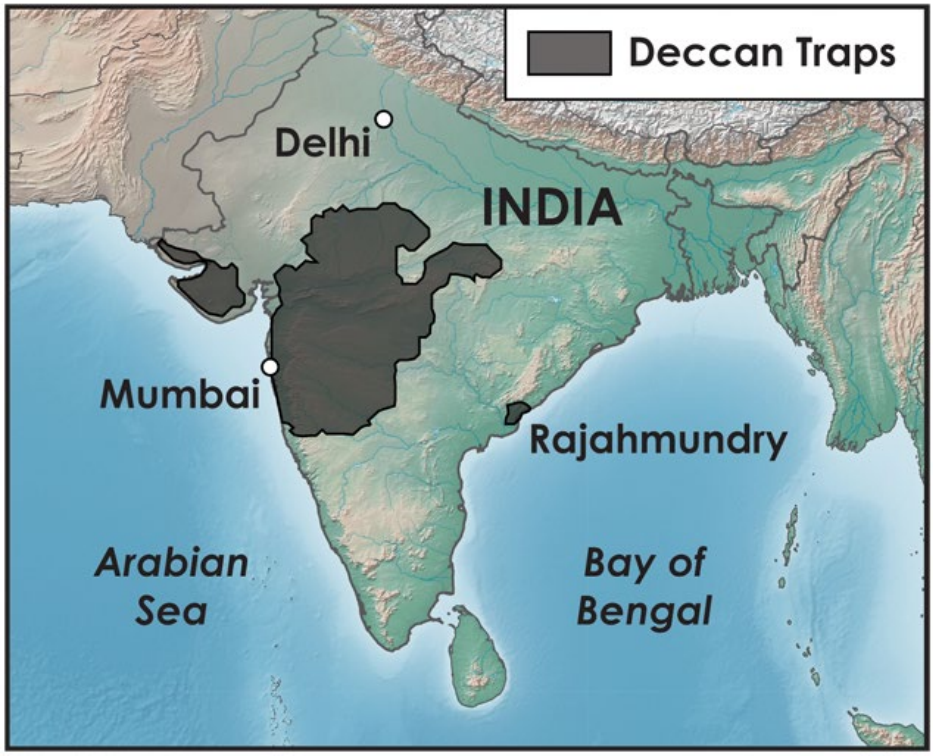

Figure 56: Deccan traps extension (Oleson, 2016)

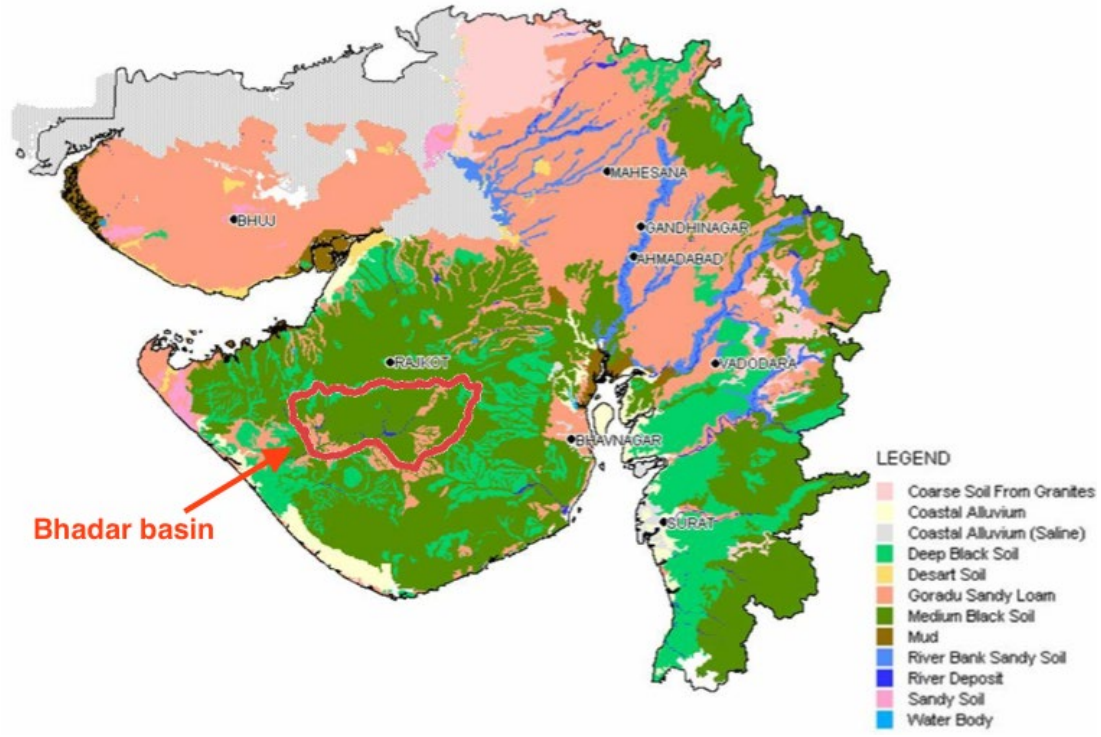

Figure 57: Map of soil deposits of Gujarat (Narmada, 2010)

Appendix B

Field visit questionnaire

Site (from observation well name):
Date:
Contact name and numbers of the people consulted:

Contact name:	Number:

Check dam characteristics

Check dam ID	
Maximum height	
Width	
Slope	
Soil type	
Year of construction	
Institution/Organization responsible for the design/construction and under which program	
Desilting practices (frequency, amount of silt removed, disposal)	

Check dam hydrology

How many times does it get full within a year (last year and on average)?	
Is there any eutriphication?	
How many days does it take to be empty from full capacity (on average)?	
Is the ponding water directly used? If so, how much?	
How much does the performance of the check dam vary between wet/normal/dry years? (In terms of storage and time interval before getting dry)	

Does abstraction from nearby wells affect notably the storage in the structure?	
N° of abstraction wells nearby (<2km)	
GPS coordinates of wells (with well ID)	

Well characteristics

Abstraction well ID	
Type of well	
Diameter	
Depth	
Depth to water table (at the time of visit)	
Depth to hard-rock	
Pump Installed (type, hp, year)	
Yield (m3/d) or (L/s)	

Water use

Who has access to the well?	
Up to which distance is water distributed after pumping?	
What is the main use (irrigation, domestic, profit)?	
Volumes of abstraction (not irrigation)	
How much time does it take the well to get empty (and at which pumping rate)?	
How much time does it take to be full again?	
Does the well fail? If so, in which period of the year?	
What dries first: the wells or the structures?	

Irrigation

Which crops are sown in the surrounding of the dam? With area	Kharif: Rabi:

	Summer:
Are there paddy crops?	
Total area of crops	
Cropping area irrigated by well?	
Which irrigation technique is implemented? (Sprinkler, flooded, drip)	
How many irrigation per season? For how many hours?	Kharif: Rabi: Summer:
Is there any other source of irrigation?	

Appendix C

Figure 58: Non-functioning old check dam in Arni

Figure 59: Broken check dam, Kamlapur 1

Figure 60: Check dam completely covered by silt, Kamlapur 2

Figure 61: Umrali 2 check dam

Figure 62: Material removal in Vrinagar

Figure 63: Columnar soil structure, Vrinagar

Figure 64: Silted check dam in Arni

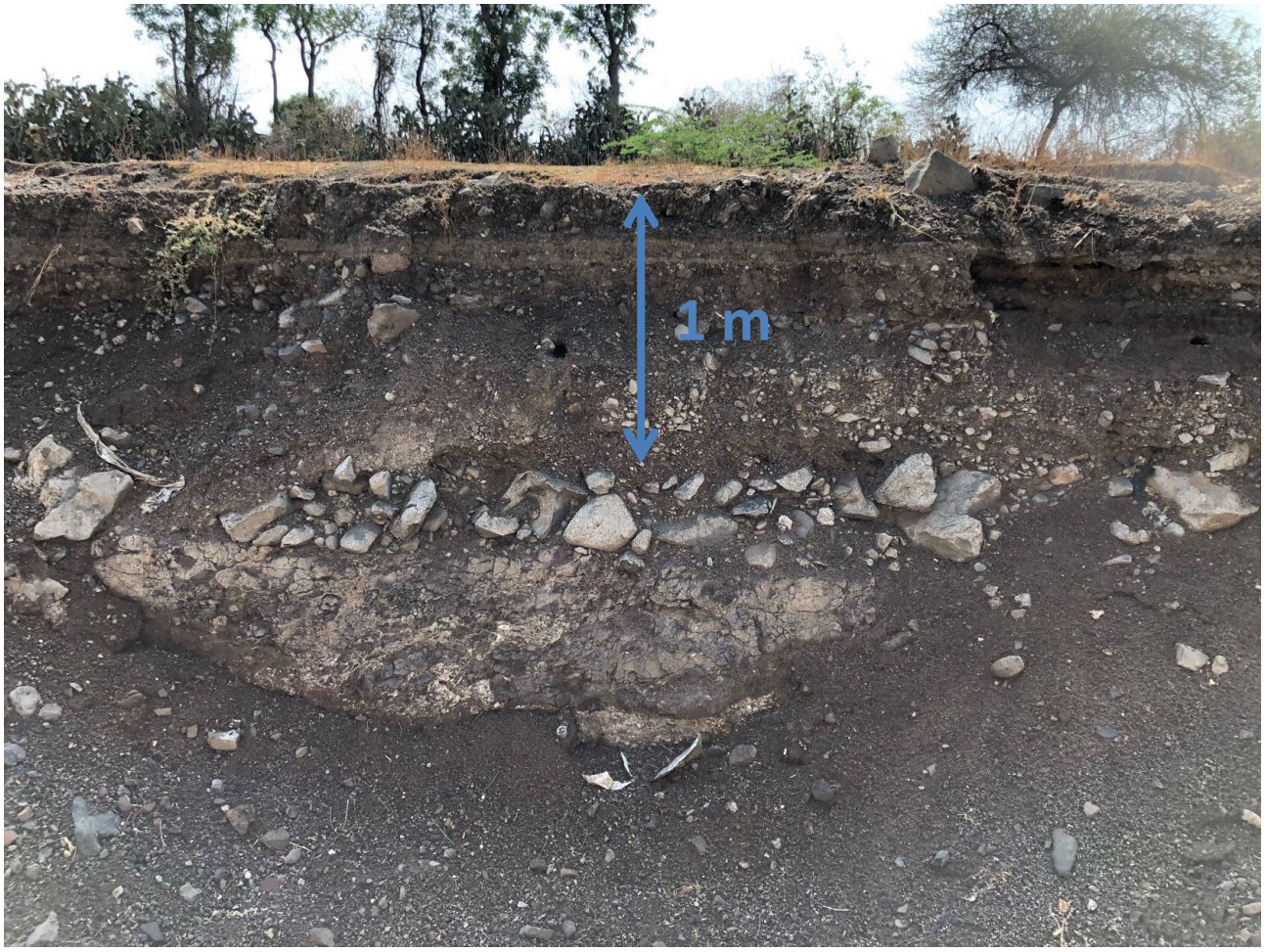

Figure 65: Outcrop at the river bed, Kamlapur

Figure 66: Hard-rock river bed, Umrali 1

Figure 67: Check dam on hard-rock river, Umrali 1

Figure 68: Refilling of a dug well from bore well – Umrali

Figure 69: Hole directly connecting dug wells with the check dam reservoir – well side

Figure 70:Hole directly connecting dug wells with the check dam reservoir – river bed side

Figure 71: Dug well full of biological activity, Arni

Appendix D

```
setwd("~/Documents/R")
rm(list = ls())
#data from 2000 to 2010
rounds=4018 #number of days

#AQUIFER PARAMETERS
K=0.1 #hydraulic conductivity of the weathered zone [m/day]
R_a=150#impendence of the clogging layer [day]
D_hr=5#depth to hard-rock [m]
T=200 #transmissivity of the aquifer [m2/d]

#CHECK DAM SITE PARAMETERS
W_s=30 #river with [m]
H_s=2 #structure depth [m]
A_catch=15 #catchment area of the check dam [km2]
alpha=0.1*pi/180 #slope of the area [radiants]
gamma=20*pi/180 #slope of the river bank [radiants]
a=4.3 #confition A parameter
F_a= 3 #condition A' parameter
P_cr=-0.5 #critic pressure for bouwer[m]

#IRRIGATION PARAMETERS
r_well=1.5 #radius of the well [m]
r_s=100 #distance between abstraction well and check dam [m]
V_abs=100 #maximum abstraction volume [m3/d]

#INPUT PARAMETERS
e=t(read.csv("Input.csv",header=TRUE,sep= ";", dec = ",")[1:rounds,3])/1000 #evaporation [mm/day]
p=t(read.csv("Input.csv", header=TRUE,sep=";",dec=",")[1:rounds,2])/1000 #precipitation [mm/day]
q=t(read.csv("Input.csv", header = TRUE, sep = ";", dec = ",")[1:rounds,4])/1000 #runoff [mm/day]
D_table=t(read.csv("Input.csv", header = TRUE, sep = ";", dec = ",")[1:rounds,5]) #water table [m]
time=as.Date(t(read.csv("Input.csv", header = TRUE, sep = ";", dec = ",")[1:rounds,1]),"%d/%m/%Y")

#irrigation events (0: no irrigation; 1: irrigation event):
irr_c=t(read.csv("Input.csv", header = TRUE, sep = ";", dec = ",")[1:rounds,6]) #cotton
irr_g=t(read.csv("Input.csv", header = TRUE, sep = ";", dec = ",")[1:rounds,7]) #groundnut
irr_w=t(read.csv("Input.csv", header = TRUE, sep = ";", dec = ",")[1:rounds,8]) #wheat


#Other factors and matrixes

V_max=W_s/(2*tan(alpha))*H_s^2 #maximum storage [m3]
W_b=W_s-2*H_s/(tan(gamma)) #width of the bottom [m]
k_a=(1+(1-sin(gamma))*2*H_s/(W_s*cos(gamma))) #coefficient between wet and surface area [-]
L_w=0.5*(H_s+W_s+D_hr) #Bouwer characteristic lenght
D_well=V_abs/(r_well^2*pi) #drawdown at the well
A=V_abs*3 #abstraction rate [m3/day]
D_abs=-A/(2*pi*T)*log(r_s/r_well)+D_well #THIEM equation
```

```
h=matrix(0,3,rounds) #water level in the check dam [m]
V=matrix(0,3,rounds) #volume stored [m3]
A_surf=matrix(0,3,rounds) #surface area [m2]
overflow=matrix(0,3,rounds) #overflow [m3/day]
i=matrix(0,3,rounds) #infiltration [m/day]
D_a=matrix(0,1,rounds) #drawdown from abstractions [m]
D_a=(0.5*irr_c+0.5*irr_g+irr_w)*D_abs
D_w=D_table#+D_a


#ROUTINE
for (t in 2:rounds){

#Saturated conditions
if(D_w[1,t]<=1 ){
i[,t]=0}

else{

#CONDITION A

if(V[1,t-1]>0){
#dry aquifer (CONDITION A')
if(D_w[1,t] >= D_hr+H_s ){
i[1,t]=K*(1+F_a*h[1,t-1]/W_s)}
else{
i[1,t]=K*pi*D_w[1,t]/(W_s*max(log(a*(D_hr+h[1,t-1])/(W_b+2*h[1,t-1]/cos(gamma))),1))}}


#CONDITION B

if(V[2,t-1]>0){

#Dry aquifer (CONDITION A')
if(D_w[1,t] >=D_hr+H_s ){
i[2,t]=K*(1+F_a*h[2,t-1]/W_s)}
else{

#Ernst's solution
if(D_hr>=3*W_b){
i[2,t]=K*D_w[1,t]/W_s/(max(log((D_hr+h[2,t-1])/(W_b+2*h[1,t-
1]/cos(gamma)))/pi+0.5*L_w/(D_hr+h[2,t-1]-0.5*D_w[1,t]),1))}
else{

#D-F assumption
i[2,t]=K*2*D_w[1,t]/W_s*(h[2,t-1]+D_hr-0.5*D_w[1,t])/(L_w-0.25*(W_b+W_s))}}}

#CONDITION C
```

```
 if(V[3,t-1]>0){

 i[3,t]=((h[3,t-1]-P_cr)*W_b+(h[3,t-1]-2*P_cr)*(h[3,t-1]/sin(gamma)))/(W_s*R_a)}}

#CHANGE IN STORAGES

 DeltaV1=A_surf[1,t-1]*(p[1,t-1]-e[1,t-1]-i[1,t-1]*k_a)+A_catch*q[1,t-1]*1000000
 overflow[1,t]= max(V[1,t-1]+DeltaV1-V_max,0)
 V[1,t]=max(min(V[1,t-1]+DeltaV1,V_max),0)
 h[1,t]=sqrt(V[1,t]/(W_s/(2*tan(alpha))))
 A_surf[1,t]=W_s*h[1,t]/tan(alpha)

 DeltaV2=A_surf[2,t-1]*(p[1,t-1]-e[1,t-1]-i[2,t-1]*k_a)+A_catch*q[1,t-1]*1000000
 overflow[2,t]= max(V[2,t-1]+DeltaV2-V_max,0)
 V[2,t]=max(min(V[2,t-1]+DeltaV2,V_max),0)
 h[2,t]=sqrt(V[2,t]/(W_s/(2*tan(alpha))))
 A_surf[2,t]=W_s*h[2,t]/tan(alpha)

 DeltaV3=A_surf[3,t-1]*(p[1,t-1]-e[1,t-1]-i[3,t-1]*k_a)+A_catch*q[1,t-1]*1000000
 overflow[3,t]= max(V[3,t-1]+DeltaV3-V_max,0)
 V[3,t]=max(min(V[3,t-1]+DeltaV3,V_max),0)
 h[3,t]=sqrt(V[3,t]/(W_s/(2*tan(alpha))))
 A_surf[3,t]=W_s*h[3,t]/tan(alpha)
 }
```

Appendix E

Table 13: Simulations input parameters

Symbol	Value	Unit	Description
H_s	2	m	Height of the check dam
W_s	30	m	Width of the check dam
V_{MAX}	34377	m^3	Storage capacity
alpha	0,1	°	Stream gradient
gamma	20	°	River bank slope
K	0,1	m/day	Hydraulic conductivity
R_s	200	day	Hydraulic impendence
A_{satch}	15	km^2	Check dam catchment area
D_{hr}	5	m	Depth to hard-rock
F_a	3	-	Geometry parameter condition A'
r_{well}	1,5	m	Radius of the well
r_s	100	m	Distance between check dam and abstraction well
V_{irr}	100	m^3/day	Abstracted volume for irrigation
T	200	m^2/day	Transmissivity of the aquifer

Table 14: Storage dates

Year	Condition A Permeable layer	Condition B Impermeable layer	Condition C Clogging layer
2000	July 4 - Sep 24	July 4 - Oct 20	July 4 - Nov 16
2001	June 15 - Nov 5	June 15 - Nov 20	June 15 - Dec 3
2002	June 21 – Sep 26	June 21 - Oct 21	June 21- Nov 11
2003	June 16 - Nov 22	June 16 - Dec 8	June 16 - Dec 13
2004	May 11 - Oct 31	May 11 - Nov 24	May 11 - Dec 14
2005	June 22 - Nov 21	June 22- Dec 11	June 22 - Jan 4
2006	June 2 - Dec 10	June 2- Dec 27	June 2- Jan 8
2007	June 20 - Dec 15	June 20 - Jan 3	June 20 – Jan 17
2008	June 10 – Dec 7	June 10 – Dec 23	June 10 – Jan 1
2009	June 24 – Nov 20	June 24 – Dec 5	June 24 – Dec 8
2010	June 7 – Dec 31	June 7 - Dec 31	June 7 - Dec 31

Table 15: Water budget for condition A (permeable layer), values in 1000m^3

Year	Runoff	Precipitation	Outflow	Infiltration	Evaporation
2000	2913	8	2772	133	15
2001	2148	11	1985	142	32
2002	3123	8	2991	123	17
2003	7065	26	6890	176	25
2004	6725	22	6557	161	29
2005	6550	24	6412	139	23
2006	6887	25	6686	190	35
2007	13680	44	13510	187	27
2008	7439	23	7272	163	27
2009	8353	23	8207	143	25
2010	12413	42	12224	200	31

Table 16: Water budget for condition B (impermeable layer), values in 1000m^3

Year	Runoff	Precipitation	Outflow	Infiltration	Evaporation
2000	2913	9	2795	101	26
2001	2148	12	2038	81	41
2002	3123	9	3009	98	25
2003	7065	27	6942	118	31
2004	6725	23	6606	105	37
2005	6550	25	6463	81	30
2006	6887	25	6741	132	40
2007	13680	44	13556	136	33
2008	7439	24	7312	118	33
2009	8353	25	8251	94	32
2010	12413	43	12292	121	34

Table 17: Water budget for condition C (clogging layer), values in 1000m^3

Year	Runoff	Precipitation	Outflow	Infiltration	Evaporation
2000	2913	9	2848	39	34
2001	2148	13	2060	56	44
2002	3123	10	3049	41	44
2003	7065	28	7002	58	32
2004	6725	24	6629	65	55
2005	6550	25	6478	63	34
2006	6887	26	6794	72	47
2007	13680	45	13624	69	32
2008	7439	25	7365	65	35
2009	8353	25	8296	50	31

2010	12413	44	12318	85	40

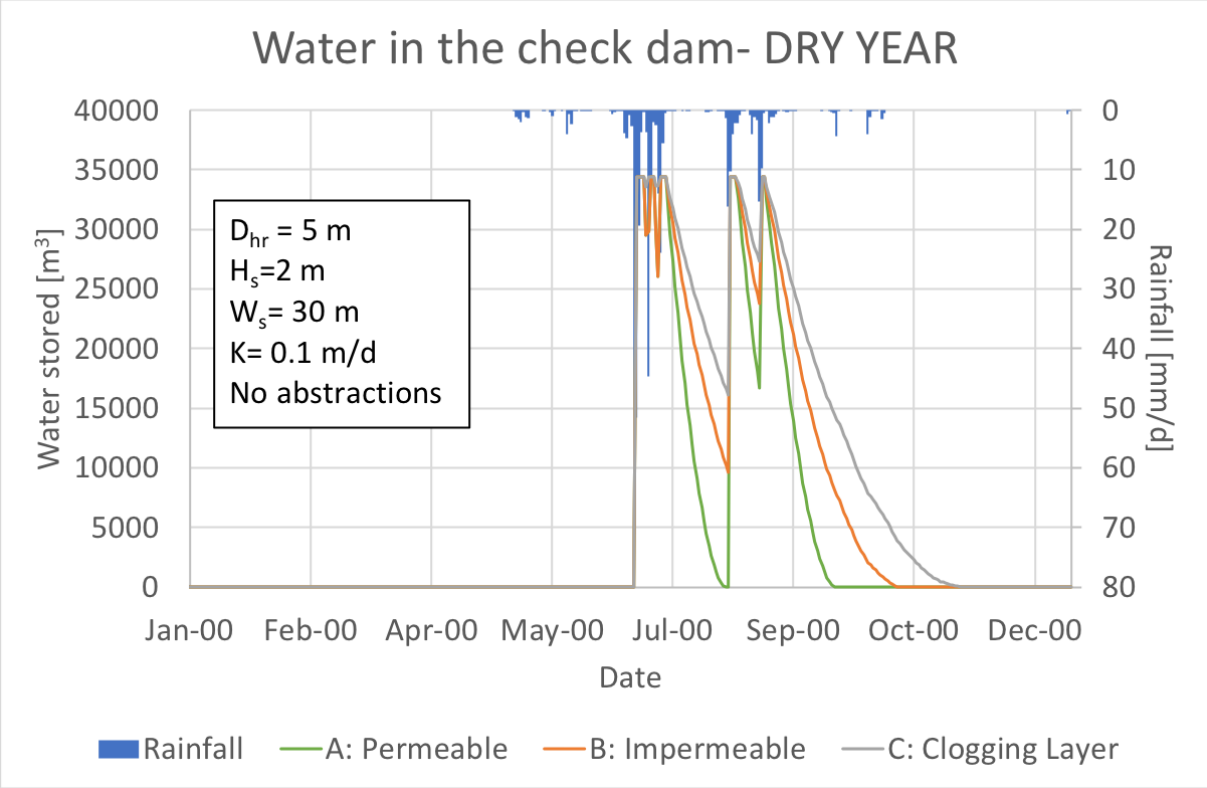

Figure 72: Water stored in the check dam – *dry* year (2000)

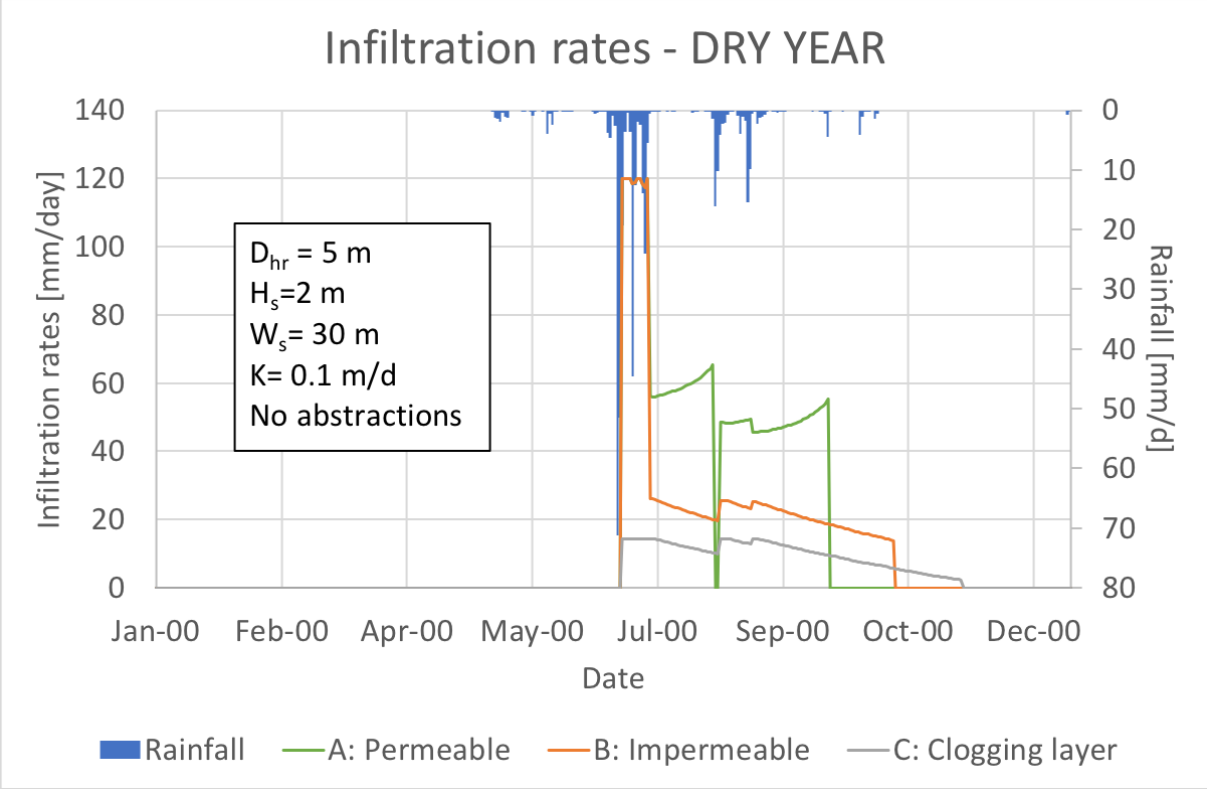

Figure 73: Infiltration rates from check dam - *dry* year (2000)

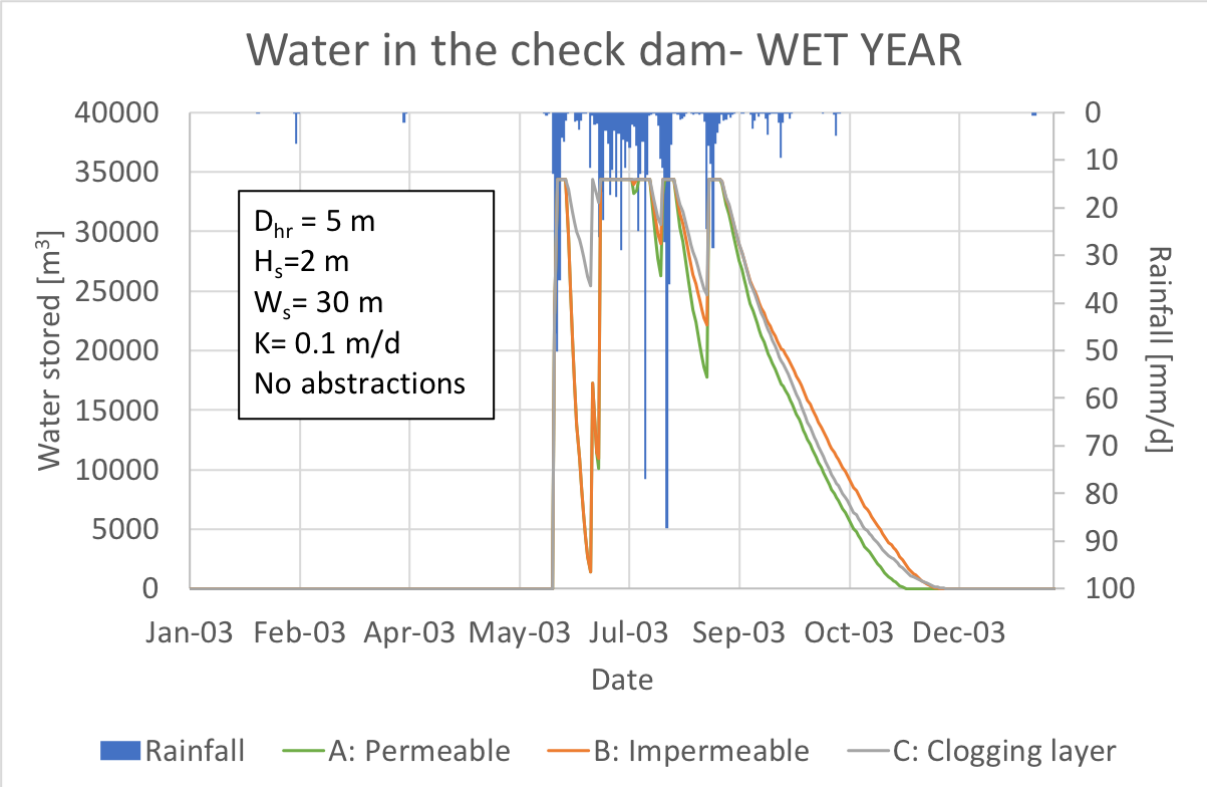

Figure 74: Water stored in the check dam – *wet* year (2003)

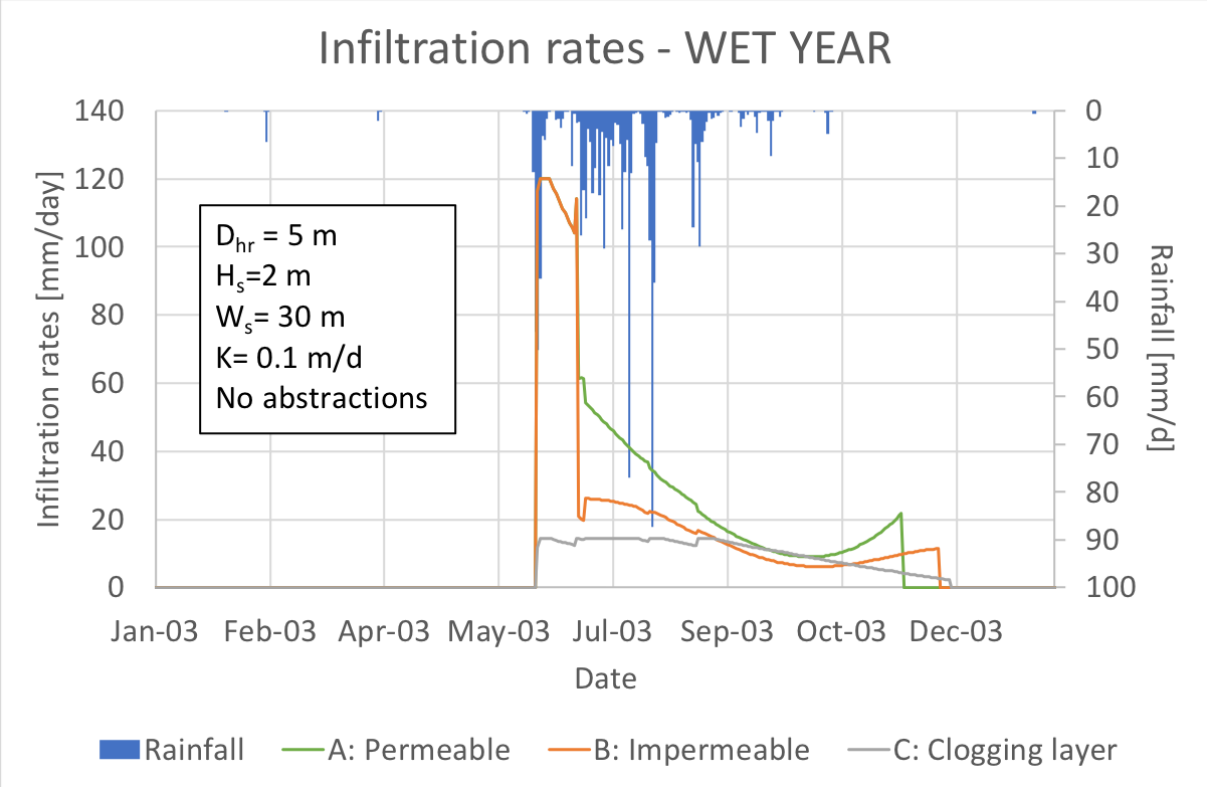

Figure 75: Infiltration rates from check dam – *wet* year (2003)

Table 18: Water budget for condition A (permeable layer) with abstractions, values in 1000m^3

Year	Runoff	Precipitation	Outflow	Infiltration	Evaporation
2000	2913	8	2777	128	16
2001	2148	11	1992	137	30
2002	3123	8	2995	119	18
2003	7065	26	6906	161	23
2004	6725	22	6566	153	28
2005	6550	24	6411	140	23
2006	6887	25	6698	180	34
2007	13680	44	13522	176	26
2008	7439	23	7276	160	26
2009	8353	23	8218	134	24
2010	12413	42	12236	189	30

Table 19: Water budget for condition B (impermeable layer) with abstractions, values in 1000m^3

Year	Runoff	Precipitation	Outflow	Infiltration	Evaporation
2000	2913	8	2787	114	20
2001	2148	12	2020	105	35
2002	3123	8	3005	106	21
2003	7065	27	6936	129	26
2004	6725	22	6595	122	31
2005	6550	24	6439	110	26
2006	6887	25	6729	148	36
2007	13680	44	13548	148	28
2008	7439	24	7301	134	28
2009	8353	24	8244	106	27
2010	12413	42	12272	149	31